Theoretical investigation into the origins of multicellularity.

A thesis presented in partial fulfilment of the requirements

for the degree of

PhD

in

Theoretical Biology

at Massey University, Albany, New Zealand.

Yuriy Pichugin

2015

Abstract

Evolution of multicellularity is a major event in the history of life. The first step is the emergence of collectives of cooperating cells. Cooperation is generally costly to cooperators, thus, non-cooperators have a selective advantage. I investigated the evolution of cooperation in a population in which cells may migrate between collectives. Four different modes of migration were considered and for each mode I identified the set of multiplayer games in which cooperation has a higher fixation probability than defection. I showed that weak altruism may evolve without coordination among cells. However, the evolution of strong altruism requires the coordination of actions among cells.

The second step in the emergence of multicellularity is the transition in Darwinian individuality. A likely hallmark of the transition is fitness decoupling. In the second part of my thesis, I present a method for characterizing fitness (de-)coupling which involves an analysis of the correlation between cell and collective fitnesses. In a population with coupled fitnesses, this correlation is close to one. As a population evolves towards multicellularity, collective fitness starts to rely more on the interactions between cells rather than the individual performance of cells, so the correlation between particle and collective fitnesses decreases. This metric makes it possible to detect fitness decoupling.

I used the suggested metric to investigate under which conditions fitness decoupling occurs. I constructed a model of a population defined by a linear traits-to-fitness function and used this to identify those functions that promote fitness decoupling. In this model, the fitness correlation is equal to the cosine of the angle between the gradients of fitnesses. Therefore, my results allow an estimation of the fitness (de-)coupling state before selection takes place.

In the third section of my thesis, the accuracy of this estimation was tested on available experimental data and using a model simulating an experimental selection regime, which featured non-linear traits-to-fitness functions. The results obtained from the estimation of fitness correlations showed a close approximation to the fitness correlation calculated from experimental data and from simulations in a range of selection regimes.

Acknowledgements

I would like to thank my supervisor, Distinguished Professor Paul B. Rainey for the opportunity to work on the exciting project concerning the fundamental questions of the biology; for his inspiration and for teaching me the high standards of science.

I am thankful for financial support from the Marsden Fund Council from government funding administered by the Royal Society of New Zealand and the New Zealand Institute for Advanced Study.

I thank my collaborators Dr. Katrin Hammerschmidt, Dr. Caroline Rose, Dr. Chaitanya S. Gokhale, Dr. Julian Garcia and my co-supervisors Dr. Eric Libby and Dr. Prof. Thomas Pfeiffer for sharing their scientific experience and the wisdom of life.

I thank Dr. Prof. Arne Traulsen and his group for fruitful collaboration during my stay in Max Planck Institute for Evolutionary Biology.

To these who read and commented drafts of this thesis: Dr. Saumya Agrawal, Dr. Benedikt Bauer, Dr. Prof. Cassandra Extavour, Dr. Weini Huang, and Dr. Jorge Peña, thank you for suggestions, which enormously helped me to improve the text.

I thank my colleagues in Rainey lab, especially my office-mates Yeserin Yildirim and Yunhao Liu for their support.

I thank David and Theresa Terry for their hospitality and help with settling down in New Zealand.

I also thank my friends Anton Potkalov, William Turner, Amber Milan, Alex Budny and Mark Caubo.

My teachers: Dr. Prof. Oliver Savchenko, Dr. Tatyana Baturina, Dr. Prof. Grigoriy

Dymshits and Dr. Vladimir Kharitonov, thank you for nurturing my passion for science.

Thank you, Dr. Prof. Sandra Rossie for encouraging me to pursue a PhD degree abroad.

To my parents and my grandmother, thank you for your support in my desire to travel to the other side of the world.

The most of all, I am thankful to my beloved wife Tatyana who followed me through the whole journey.

Contents

List of Figures

List of Tables

Chapter 1

Introduction

Multicellular organisms evolved from unicellular species. Such transitions to multicellular life happened independently in multiple taxa: red algae, land plants, animals, fungi and others (Buss 1987, Maynard Smith and Szathmáry 1995, Bonner 1998, 2000). More than 25 instances of the emergence of multicellularity are currently recognized (Grosberg and Strassmann 2007). The most ancient fossils of multicellular organisms are dated back to 2450–2100 million years ago (Mya) in cyanobacteria (Tomitani et al. 2006), while the most recent event of multicellularity emergence occurred just 200 Mya in the green alga *Volvox* (Herron et al. 2009). The repetitive occurrences of the evolution of multicellularity indicate that some common conditions exist that favour evolution of multicellular organisms. However, knowledge of what these conditions are is incomplete.

This introduction is divided into two parts: core concepts, knowledge of which is essential to the understanding of the evolution of multicellularity; and application of these concepts in experimental and theoretical studies. During this review I will emphasize recognized gaps in our understanding of the origins of multicellularity.

1.1 Core concepts of evolution and multicellularity

1.1.1 Definition of multicellularity

There is no consensus on the definition of multicellularity in the literature. Despite our intuitive understanding that a butterfly is a multicellular being and protist infusoria are not, multiple perspectives on the definition of multicellularity exist. Some authors require simply the physical cohesiveness of cells and the coordination of processes between cells (Kaiser 2001, Solari et al. 2007, Schirrmeister et al. 2011). Others consider multicellularity to be a combination of a set of traits: physical cohesiveness plus reproductive specialization (Michod and Roze 1999), and some also require a reproductive bottleneck (Godfrey-Smith 2009). The current study utilizes the ideas of Okasha (2006), who considers multicellularity as being a state that results from the evolution of collectives of cells by means of natural selection. This definition of multicellularity requires that collectives of cells participate in evolution by natural selection – although possibly only to a marginal extent – as a single unit.

1.1.2 Natural selection

The concept of natural selection, formulated by Darwin (Darwin 1859), is simple yet fascinating: if carriers of a certain trait leave more offspring than other members of the population, then in the next generation, the fraction of the population possessing this trait will increase. Natural selection is the source of evolutionary adaptations - changes in the response to the pressure of external factors. This process has been observed numerous times, both *in vitro* (Lenski et al. 1990, Ratcliff et al. 2012) and *in vivo* (Delwart et al. 1994, Smith and Eyre-Walker 2002, Mwangi et al. 2007, Huse et al. 2010).

The utility of the concept of natural selection resides in the fact that it is abstract, and not confined to populations of living organisms. For example, memes in human culture and behavioural patterns of humans and animals are also subjected to natural selection (Dawkins 1976, Boyd and Richerson 1985, Avital and Jablonka 2000). The abstract nature of natural selection allows its investigation using relatively simple mathematical concepts. However,

despite the widespread existence of natural selection, there are still some conditions that must be fulfilled before natural selection can operate in the population.

1.1.3 Darwinian individuality

To be able to evolve by means of natural selection, population members must be Darwinian individuals; that is, they must manifest Darwinian characteristics. In his classical paper, Lewontin (1970) provided a list of conditions that comprise Darwinian individuality. Usually these properties are listed as: reproduction, heredity and variation (Maynard Smith 1987). Reproduction is the ability of an individual to create other similar individuals. Heredity means that properties of offspring individuals are similar to progenitors' ones. Variation in reproductive output ensures that the composition of a population will change with time. If these three conditions are fulfilled in a population, then the population participates in evolution by natural selection.

While Lewontin conditions are fulfilled in the majority of existing populations, some populations express Darwinian properties in a marginal way only (Godfrey-Smith 2009). For instance, a slime mold slug is an aggregate of cells originating from different slugs in the previous generation (Strassmann et al. 2000). Therefore, a slug could have completely different properties from its progenitors. Under such circumstances, the condition of heredity is not easily met.

The evolution of multicellularity poses a unique problem in evolutionary theory. The multicellular organisms must be Darwinian individuals. The obtaining of Darwinian individuality by collectives is an adaptation, gained by natural selection. However, the evolution by natural selection is only possible in a population of Darwinian individuals. Thus, the question about evolution of multicellularity is similar to the problem of which came first, the chicken or the egg. This makes the investigation of the origins of multicellularity a challenging problem.

1.1.4 Multilevel selection

Life is organized hierarchically into multiple levels: cells are assembled in organisms, organisms constitute the social groups, which in turn are parts of the species. Natural selection may simultaneously operate on multiple levels of the hierarchy, and in such cases is referred to as *multilevel selection*.

To describe the evolution of populations under multilevel selection, lower-level units (particles) are considered in parallel with higher-level units (collectives) (Okasha 2006). Consequently, fitness, as a measure of evolutionary success, is measured independently at the particle and collective levels. Particle fitness is calculated as the number of offspring particles produced by a particular particle. Two definitions of collective-level fitness exist. These definitions are derived from two distinct approaches to the multilevel selection, known as MLS1 and MLS2 (Damuth and Heisler 1988).

Particles are the focus of attention in the MLS1 approach, while the role of collectives is merely to provide a structure to the population (Damuth and Heisler 1988, Okasha 2006). Thus, the MLS1 approach defines the fitness of collectives as the number of *offspring particles* originated from the collective[1].

Both particles and collectives are the focal units in the MLS2 approach (Damuth and Heisler 1988, Okasha 2006). Thus, the MLS2 approach defines the fitness of collectives as the number of *offspring collectives* produced by a particular collective.

In the scope of the current study, both approaches have their place, because they cover different stages in the evolution of multicellularity. The MLS1 approach is relevant in the investigation of the earlier stages of the evolution of multicellularity. Prior to the emergence of Darwinian individuality at the level of collective, groups were loose aggregates of particles. The evolution of the population at that stage was determined by the change of particle composition of these aggregates. Therefore, the number of particles produced characterized the evolutionary success of collectives at this stage. The MLS2 approach is relevant after the

[1]Collective fitness in MLS1 could be also defined as average particle fitness of members of collective. The conceptual difference between these definitions is not significant (Okasha 2006, p. 54).

Darwinian individuality has been gained by collectives. For example, the reproductive success of an elephant does not depend on how many cells it contains (MLS1 fitness), but it does depend on how many offspring elephants it produces (MLS2 fitness). Therefore, both MLS1 and MLS2 are able to adequately describe, respectively, the earliest, and the final stages in the evolution of multicellularity.

During the course of the evolution of multicellularity, the MLS1 framework is replaced with MLS2. The stage at which this transition takes place remains a "gray area". A theory connecting MLS1 and MLS2 approaches could provide tools to investigate the transition between them during the evolution of multicellularity, but such a theory has not yet been constructed.

1.1.5 Emergence of multicellularity as a major evolutionary transition

During the evolution of multicellularity, cells lost their ability to reproduce independently and started to reproduce as parts of a multicellular organism. Maynard Smith and Szathmary (Maynard Smith and Szathmáry 1995, Szathmáry and Maynard Smith 1995) identified several events when entities previously able to replicate individually, became capable of reproducing only as a part of a larger unit. These events are named major transitions, and a variety of them are extensively considered in Maynard-Smith and Szathmary (1995).

Examples of major transitions are: evolution of early replicators into chromosomes during early stages of the evolution of life (Szathmáry and Maynard Smith 1993, Maynard Smith and Szathmáry 1993), emergence of eukaryotes from prokaryotes (Margulis 1970, Gray 1989), and the evolution of multicellularity and eusociality (Nowak et al. 2010). The emergence of multicellularity holds a significant place on this list, because it includes a diverse collection of at least 25 independent events with similar outcomes, some of which are relatively recent (Herron et al. 2009).

The evolution of multicellularity as a major transition requires two major adaptations: collectivization of previously independent particles, and the acquisition of Darwinian properties by evolved collectives. The evolution of Darwinian individuality at the collective level

requires the existence of collectives, and therefore cannot evolve before the collectivization of particles. The simultaneous attainment of such major adaptations is unlikely to occur in nature because these evolutionary adaptations are essentially different; however, it has been observed to occur in evolutionary experiments (Ratcliff et al. 2012). Disregarding this exceptional case, the evolution of multicellularity can be divided into two distinct stages (see also Figure 3.1):

1. Emergence of collectives from independent cells. These collectives may not necessarily be Darwinian individuals.

2. Transition of Darwinian individuality from cells to collectives that manifest heritable variance in fitness and thus participate directly in the process of evolution by natural selection in their own right.

The first stage starts from a population containing only independent cells, and finishes with the cells themselves organized into collectives. Each cell, however, retains its Darwinian individuality, so this stage is an evolution of a complex trait (collectivization) occurring completely at a single level of life's hierarchy - the level of the cell.

The second stage, on the contrary, involves selection at both particle and collective levels. After the transition in individuality, the particles loose the capability of independent reproduction. Collectives, in contrast, gain the ability to reproduce.

1.2 Investigation of the origins of multicellularity

This section begins with a short discussion of the experimentally observable hallmarks of the evolution of multicellularity. The review the presents a selection of natural examples of life forms at different stages of transitioning towards multicellularity. Experimental attempts at artificially evolving multicellular beings are then discussed. Finally, various theoretical models of the evolution of multicellularity are considered.

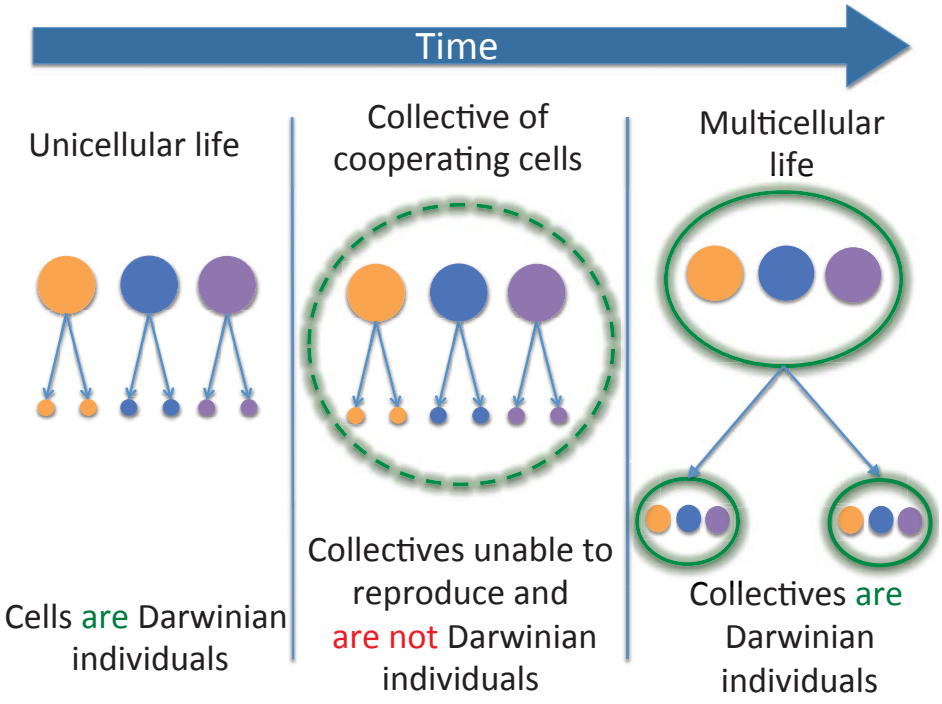

Figure 1.1: **The probable scenario of the evolution of multicellularity from single cells.** Independent ancestral cells are Darwinian individuals. Collectives of cooperating cells, may not be able to reproduce as a single entity, and thus, such collectives are not Darwinian individualities. Multicellular organisms can leave group-level offspring. During the evolution of multicellularity Darwinian individuality passes to the higher level.

1.2.1 Features of multicellularity

In the absence of a general approach to studying transitions in individuality, certain characteristics of multicellularity can be investigated in order to find a general pattern. Cooperation (Michod and Roze 2001), division of labour (Wahl 2002) and germ-soma differentiation (Gavrilets 2010) have been the focus of attention for a long time and are often associated with the evolution of multicellularity.

1.2.1.1 Cooperation

Collectives can evolve in MLS1 populations only if members of collectives have a selective advantage over independent cells. Such selective advantage of collectives may be gained through the evolution of cooperation among particles within collectives. Cooperation can be defined as a "joint action for mutual benefit" (Dugatkin et al. 1992, Mesterton-Gibbons and Dugatkin 1992, Clements and Stephens 1995, Stephens and Anderson 1997). The cooperative behaviour is generally costly to cooperators (Axelrod and Hamilton 1981, Clements and Stephens 1995). Thus, the cooperation provides selection conditions that favour the evolution of defecting (cheating) types. Defectors do not pay the cost of cooperation, but receive cooperative benefits from others. As a result, defectors have higher fitness than cooperators. Therefore, in a mixed population of cooperators and defectors, defectors can increase their presence in the population, and cooperators can be eradicated. This situation is known as a *tragedy of commons* (Hardin 1968) and is the major factor threatening the maintenance of cooperation.

The emergence of cooperation may be a major factor promoting the evolution from cells to collectives, which is the first stage in the evolution of multicellularity (Shapiro 1998). Some studies even consider the evolution of cooperation to be a determining process during the whole process of the evolution of multicellularity (Michod and Roze 2001), thus supposing that the development of cooperation might be the driving force also at the second stage - the transition in individuality.

However, cooperation is possible in populations, which did not undergo the transition in

individuality. For example, cooperation exists between the marine fish *Amphiprion ocellaris* and sea anemones, *Heteractis magnifica*, where the anemone protects the fish from predators and the fish cleans the anemone of parasites (Porat and Chadwick-Furman 2004). Collectives constructed from individual fish and anemones cannot express any properties of Darwinian individuality at the collective level. Even if cooperation takes place between representatives of the same species, the cooperating collective may not be a Darwinian individual. For example, members of a bacterial mat might cooperate with each other (Crespi 2001, Wingreen and Levin 2006), but the mat itself cannot reproduce as a group. Therefore, cooperation is not a synonym of multicellularity.

Conceptually, the inability of cooperation itself to explain the transition in individuality resides in the fact that the benefit of cooperation is completely formulated in terms of a particle's fitness (Nowak 2006b). The simple act of cooperation does not require, or promote, the existence of collective-level fitness.

1.2.1.2 Division of labour

Division of labour is a form of cooperation in which different tasks are distributed among different particles in a group. The division of labour between cells has been observed in some simple paradigm multicellular organisms such as *Trichoplax adhaerens* (Schierwater 2005). However, division of labour also exists in collectives that do not possess Darwinian properties. Examples of collectives exhibiting a division of labour but lacking Darwinian individuality are presented in Crespi (2001). These examples include: microbial biofilms, heterocysts in cyanobacteria, and the structured colonies of *Escherichia coli*. Despite the division of labour being an essential multicellular trait, requiring the existence of a group and increasing the group cohesiveness and viability, the evolution of this trait is not necessarily connected with a transition in individuality.

1.2.1.3 Germ-soma distinction

The germ-soma differentiation is a special case of division of labour, where some members of a collective are specialized in reproduction (germ), while other members are focused on the increase of collective viability and do not contribute to collective-level reproduction (soma). The germ-soma differentiation deserves special attention because the distributed functions are related to the nature of Darwinian individuality. Somatic cells in multicellular organisms reproduce only during the organism's life and, unlike germ cells, do not have any offspring that will outlive the organism. They are therefore only marginally Darwinian individuals. This is even more explicit in eusocial collectives where sterile workers do not reproduce and they are not Darwinian individuals at all. If Darwinian individuality does not exist at the level of cells, then it is expected that it will be present at the level of collectives.

However, the germ-soma differentiation in a collective is neither necessary nor a sufficient requirement for the presence of Darwinian individuality in that collective. Some modes of reproduction among multicellular Darwinian individuals do not require germ-soma differentiation: for example, simple Volvocine alga *Gonium pectorale* exists as collectives consisting of totipotent cells, which can beget collective-level offspring (Stein 1958). An example of a germ-soma distinction in a non-Darwinian collective is the modelled extreme case of division of labour in cyanobacteria (Rodrigues et al. 2012). Simulations have shown the evolution of effectively somatic cells in a collective that was unable to reproduce (Rodrigues et al. 2012). Since it is possible for the terminal somatic differentiation to evolve even in the complete absence of multilevel selection, then the presence of germ-soma differentiation is not the signature of the multicellularity.

Transitions in individuality remain an obscure process. The mechanisms causing Darwinian individuality to transition towards the level of collectives are unclear. In addition, clear hallmarks of an evolutionary transition in individuality are yet to be determined, so we may fail to observe this event even if it were to happen in front of our eyes. However, some transitions in individuality have been observed in nature, artificially constructed in the laboratory, and

many have been considered theoretically.

1.2.2 Examples of the emergence multicellularity observed in nature

1.2.2.1 Slime molds

Social amoebae, commonly known as slime molds (Baldauf and Doolittle 1997), are an example of an intermediate life form between unicellularity and multicellularity. They all share a complex life cycle, which exhibits both unicellular and multicellular forms of organization at different stages (Bonner 1959). When resources are abundant, slime mold cells live as independent organisms. Dispersed cells aggregate into multicellular slugs after resource depletion. These slugs behave as a single entity: for example, they travel significant distances (Inouye and Takeuchi 1979) and are even able to negotiate mazes (Nakagaki 2001). The real significance of the multicellular slugs in the life cycle of slime molds is their ability to transform from a mobile slug into a stationary vertical stalk with a fruiting body at its end, which is able to disperse spores throughout an area much larger than that available to independent cells. These spores form a new population of slime molds in new environments.

From one perspective, slime mold slugs are multicellular organisms because they are distinct collectives with reproductive division of labour. However, from the Darwinian perspective used in the current study, slime molds are only marginal forms of Darwinian individuality (Godfrey-Smith 2009), because they do not clearly satisfy to Lewontin's (1970) criteria: reproduction, variation, and heredity . Any slime mold is a combination of cells that originated from multiple slugs in the previous generation, and therefore it is not similar to any of them in particular (Kaushik and Nanjundiah 2003, Gilbert et al. 2009, Sathe et al. 2010). Hence, heredity is limited among slime molds, which renders them to be only marginal Darwinian individuals in terms of Godfrey-Smith's (2009) definition.

Despite possessing a mixture of unicellular and multicellular properties, the slime molds may not be considered as a general transitional state between uni- and multicellularity. The aggregation mode of slime mold collective formation (Bonner 1959) is different from the

formation mode shown by paradigm multicellular organisms, which originate from a single cell (Tarnita et al. 2013). Therefore, although slime molds contribute to the collection of collectives possessing Darwinian individuality in a marginal form, it is not parsimonious to hypothesize that progenitors of multicellular organisms had a life cycle similar to that of slime molds.

1.2.2.2 Volvocine algae

The volvocine algae are another important group of organisms. This monophyletic group contains species with different degrees of multicellular development (Rausch et al. 1989). The least developed volvocine alga is the unicellular *Chlamydomonas reinhardtii*. The most complex and famous member of this group is *Volvox carteri*, which is a multicellular organism existing as a spheroid colony of up to 10,000 cells. Collective-level reproduction in *V. carteri* occurs by the release of offspring colonies. This form of reproduction is heritable because all cells in the offspring colonies originate from a single cell from the parental colony. Therefore, colonies of *V. carteri* exhibit all the properties of Darwinian individuality, and this species can be viewed as a multicellular organism from all perspectives.

Additionally, volvocine algae contain several species exhibiting intermediary levels of complexity. This collection of species provides a unique opportunity to investigate the series of consecutive steps between unicellularity and multicellularity (Kirk 2005). The evolution of collective-level reproduction within volvocine algae is the most interesting of the three Lewontin conditions because variation is always present in natural populations and heredity is automatically provided by the mode of reproduction that has evolved in this collective. This collective-level reproduction is apparent even among the second simplest species in the Kirk's list (2005) – *Gonium pectorale*. The juvenile colony of *G. pectorale* consists of 16 cells, and each of them is potentially capable of performing a multiple fission and giving rise to a new colony (Stein 1958). The multiple fission occurs before the split of the mature colony into 16 juvenile ones, so the *G. pectorale* colonies directly give rise to new colonies. Each of the 16 newborn colonies are descendants of one of the 16 cells in the progenitor colony,

and therefore inherits its properties from the progenitor colony. Thus, *G. pectorale* exhibits the Darwinian individuality at the collective level, even if it does not exhibit a germ-soma distinction. Therefore, from the perspective that considers reproductive division of labour as a defining feature of multicellularity, *G. pectorale* is not a multicellular organism, but from a Darwinian perspective, it is multicellular in that it manifests heritable variation in fitness at the level of collectives.

Unfortunately, the absence of known intermediary species between unicellular *C. reinhardtii* and effectively multicellular *G. pectorale* diminishes the illustrative value of volvocine algae in understanding the emergence of Darwinian individuality. Nevertheless, this is still an important example in that it shows that Darwinian individuality can emerge in very simple colonies.

1.2.3 Experimental approaches in the artificial evolution of multicellularity

Experimental attempts to evolve multicellularity have been used in several studies. These evolution experiments shared a similar setup: populations of unicellular organisms were exposed to artificial selection, aimed at evolving various features of multicellularity. Resulting adaptations have shown that the mode of collective reproduction is the crucial factor for the evolution of Darwinian individuality.

1.2.3.1 Settling experiments

Experimental evolution of multicellularity in the budding yeast *Saccharomyces cerevisiae* has been performed by Ratcliff et al (2012, 2013b). This yeast generally exists as a unicellular species. However, as a result of incomplete cell division, the progenitor and offspring cells may remain stuck together. The following cell divisions result in clusters of cells with a tree-like structure. Such behaviour is abnormal for *S. cerevisiae* and is not part of its natural life cycle. Artificial selection in Ratcliff's experiment promoted the clustering trait and the evolution of clusters' ability to reproduce.

To select for larger clusters, the population of *S. cerevisiae* was competed for rapid settling in a static media. Only those cells that reached the bottom of the tube within a limited time were allowed to pass to the next experimental generation. Large clusters of cells settle faster, and therefore have an advantage over smaller clusters and independent cells.

In this experiment, *S. cerevisiae* evolved to persist as clusters of cells. Remarkably, the ability of clusters to produce collective-level offspring clusters emerged at the same time as an ability of cells to form clusters. These clusters reproduced by asymmetric fission, where the large cluster released smaller ones. This asymmetric division was maintained by the apoptosis of cells within the cluster, so the tree-like structure of the yeast colony fragmented into clusters of unequal size. After apoptosis, the connection of the "branch" originated from the apoptotic cell with the main cluster becomes weak, so this "branch" may split from the main tree and become a new cluster.

Cell clusters evolved in this experiment possess Darwinian properties to some extent. Collective-level reproduction is maintained by the fragmentation of collectives. The evolved mode of collective reproduction ensures some collective-level heredity. Cells in the cluster are descendants of a single cell, so they share similar traits, and will pass them to offspring clusters. Thus, all three Lewontin conditions are fulfilled by *S. cerevisiae* clusters evolved in this experiment.

The importance of Ratcliff's study is limited by the fact that all traits and mechanisms evolved in the population are tightly bound to the tree-like structure of collectives specific to the yeast. The very process of collective reproduction is based on the presence of the connection only between parent and offspring cells. It makes possible fragmentation of clusters by apoptosis of a single cell. The evolved life cycle is different from ones observed in *C. reinhardtii*, *V. carteri* or slime molds, and contributes to the collection of possible ways to express the Darwinian individuality at the level of collectives.

A similar evolutionary experiment has been performed with the unicellular algae *C. reinhardtii* (Ratcliff et al. 2013a). The artificial selection was the same: cells or cell clusters were required to reach the bottom of the tube within a limited time in order to pass to the next

generation. Like the experimental population of *S. cerevisiae* in the previous example, *C. reinhardtii* was able to form cell clusters to speed up the sedimentation process and win the competition against rivals. Unlike *S. cerevisiae*, however, reproduction of the *C. reinhardtii* clusters was achieved by the release of motile cells, which could subsequently grow into new clusters. This mode of reproduction explicitly exhibits a single-cell bottleneck, which is the most robust way to ensure heredity of the reproduction. Therefore, clusters of *C. reinhardtii* are Darwinian individuals. Interestingly, none of the multicellular volvocine algae expressed such explicit single-cell bottlenecks in the life cycle. So, the life cycle observed in this experiment is another addition to the collection of transitional states towards multicellularity.

1.2.3.2 Life cycle experiments

The evolution of reproduction at the level of collectives has been experimentally investigated by Hammerschmidt et al (2014) using the bacteria *Pseudomonas fluorescens* as a model organism. The experiment was designed to assess whether a single-cell phase could act to promote reproduction of collectives. The bacterial collectives, which were initially unable to reproduce as a whole, were subjected to multilevel selection. The presence of a single-cell bottleneck in the selection regime allowed the experimental population to evolve at the collective level independently from the level of particles (see also Libby and Rainey (2013)).

This investigation also highlighted the importance of cheats for the transition in individuality. The bacterial population in the experiment evolved under either a *cheat-embracing* selection regime or a *cheat-purging* regime. The analysis of the difference in evolutionary outcomes of cheat-purging and cheat-embracing regimes has shown that only the cheat-embracing regime promoted the emergence of Darwinian individuality at the level of collectives.

The opportunity to cooperate (or to defect) in this experiment stemmed from the interesting ability of *P. fluorescens* to switch between two distinct morphotypes with different properties: the so-called smooth (S) and wrinkly spreader (W) (Rainey and Travisano 1998). S-morphotype cells can easily separate from each other after division, and therefore populate

the broth of the media as a collection of independent cells. The W morphotype overproduces cellulose on its surface, which acts as a glue (Spiers et al. 2003), so W-morphotype cells remain stuck together after division. Thus, W-morphotype cells are able to rapidly colonize the air-liquid interface and form a bacterial mat on the surface of liquid media (Rainey and Travisano 1998, Rainey and Rainey 2003). Cells in this mat have an exclusive access to both air oxygen and medium nutrients, which provide them with a selective advantage over cells persisting in the broth. W-morphotype cells expend part of their resources in producing a cellulose, which supports the integrity of the mat and provides benefit to all cells in it. Therefore, the W-morphotype cells in the mat can be considered as cooperators (Rainey and Rainey 2003). S-morphotype cells do not produce the glue, so S-morphotype cells in a mat have a selective advantage over W-morphotype cells. However, the presence of S-morphotype cells in the mat compromises the mat's stability and can even lead to the its collapse (Rainey and Rainey 2003). Therefore, S-morphotype cells in the mat pose as cheaters.

Cheat-purging and cheat-embracing selection regimes used by Hammerschmidt et al (2014) involved a sequence of growth phases, with transfers of small samples between them. The cheat-embracing regime forced the switch between S and W morphotypes. The growth phase started with inoculation of W-morphotype cells and was followed by a transfer of only S-morphotype cells to the next phase. The next phase started with a sample of S-morphotype cells, but only W-morphotype cells were allowed to pass the bottleneck before the next phase. Two morphotype switches: S$\rightarrow$W and W$\rightarrow$S constituted a single life cycle in the cheat-embracing regime. The cheat-purging regime promoted the maintenance of the W morphotype. Under this selection regime, W-morphotype cells were always transferred to the next phase, see Figure 1.2, panel A.

Selection at the particle level occurred between cells with different characteristics who competed for being sampled at the end of the growth phase. Since the chance of being sampled was proportional to the number of cells, the particle-level selection mostly favoured the increase in the growth rate. However, since in the cheat-embracing regime the S$\rightarrow$W phase started with a population containing multiple cell lines, cell lines able to produce the

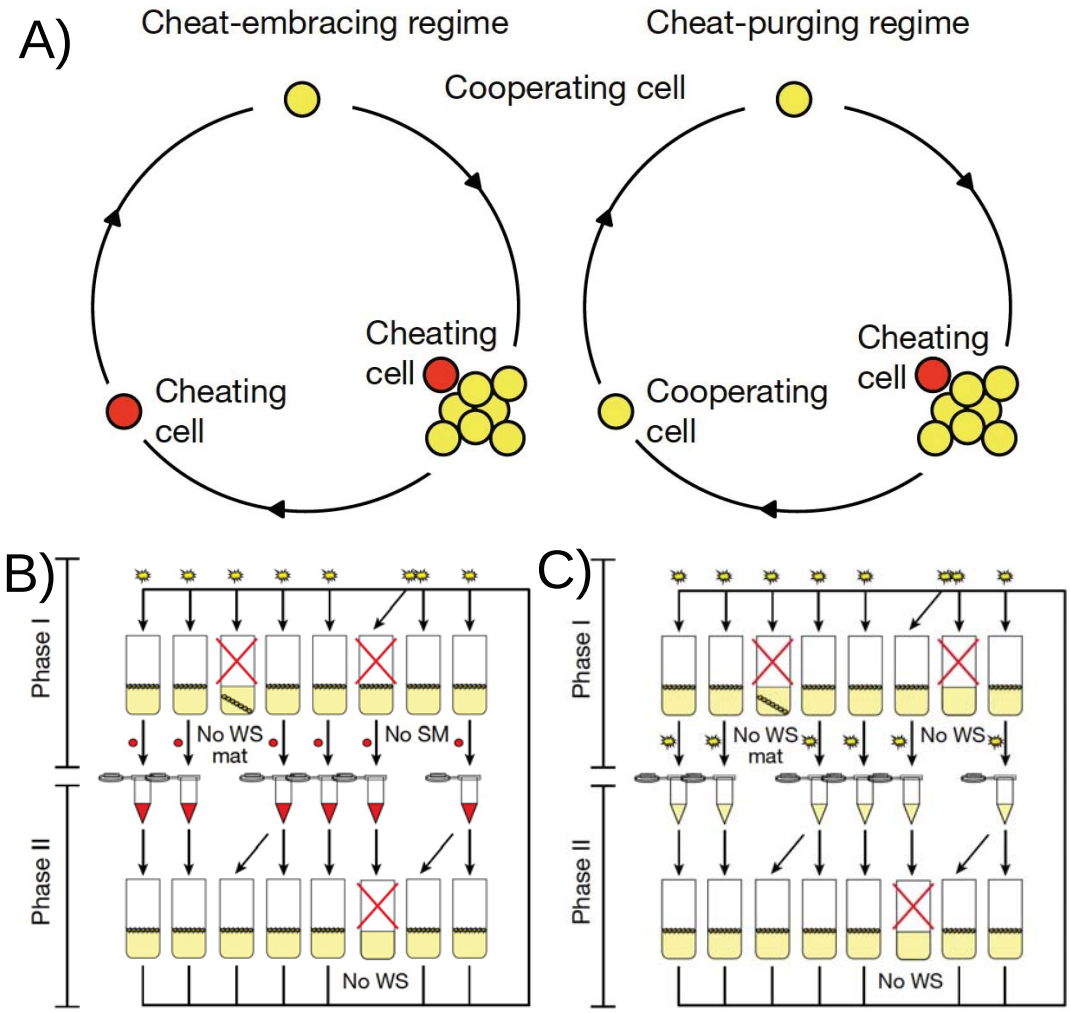

Figure 1.2: **Scheme of evolutionary experiment used in Hammerschmidt et al (2014).** A) Ideas of cheat-embracing and cheat-purging regimes. In the cheat-embracing regime, the controlled production of cheating cells is an essential part of the life cycle. In the cheat-purging regime, the production of cheating cells is suppressed. B) Selection scheme of cheat-embracing regime. Phase I (W→S) started with cooperating W-morphotype cells and ended with sampling of cheating S-morphotype cells. Collectives who did not produce S-morphotype cells or with collapsed mats were replaced. Phase II (S→W) started with S-morphotype cells and ended with a sampling of W-morphotype cells. Collectives who did not produce W-morphotype cells were replaced. C) Selection scheme of cheat-purging regime. Each started with cooperating W-morphotype cells and ended with sampling of cooperating W-morphotype cells. Collectives who did not produce W-morphotype cells or with collapsed mats were replaced. Figure adapted from Hammerschmidt et al (2014).

W morphotype quickly gained an advantage. Therefore, the increase in the transition rate between S and W morphotypes might also be favoured by the particle-level selection in the cheat-embracing regime.

The selection at the collective level was driven by the requirement of the imposed life cycle. In the cheat-purging regime, microcosms with mats that collapsed under the load of cheating S-morphotype cells were considered extinct and were replaced by the samples from successful collectives. Collectives that did not produce a detectable amount of W-morphotype cells were also considered extinct (see Figure 1.2, panel C). So, in the cheat-purging regime, the selection at the collective level favoured the viability of collectives expressed by the production of cooperators, while production of cheaters was suppressed.

In the cheat-embracing regime, collectives that did not produce S-morphotype cells at the end of the W→S phase were considered extinct. Similarly, collectives that did not produce W-morphotype cells at the end of S→W phase were also considered extinct as were collectives in which the mat collapsed under the load of S-morphotype cells (see Figure 1.2, panel B). Thus, the selection at the collective level in the cheat-embracing regime favoured viability and fertility of collectives. The viability of collectives was expressed by the production of cooperating W-morphotype cells in S→W phase, and by keeping the mat intact. The fertility of collectives was expressed by the production of cheating S-morphotype cells during the W→S phase.

The particle- and collective-level fitnesses of bacterial populations evolved under cheat-embracing and cheat-purging regimes were analyzed (Hammerschmidt et al. 2014). During the course of evolution under the cheat-embracing regime, the collective-level fitness improved, while the particle-level fitness decreased. Hence, under the cheat-embracing regime, the collective-level fitness becomes independent of the particle-level fitness. This independence of fitnesses indicates that the collectives were able to evolve as a unit of selection (see discussion of fitness decoupling in section 1.2.4.2.2 below). Therefore, collectives evolved under the cheat-embracing regime expressed Darwinian characteristics.

Evolution under the cheat-purging regime led to similar increases in the particle and col-

lective fitnesses. Thus, the change in the collective-level fitness could be explained by the change in the particle-level fitness. There is no reason to consider collectives evolved under cheat-purging regime as Darwinian individuals.

The experiment of Hammerschmidt et al (2014) shows that the presence of cheating types might provide the opportunity for the transition in individuality. Also, these findings underline the particular importance of the life cycle in the evolution of multicellularity.

1.2.4 Theoretical studies of the evolution of multicellularity

The evolution of multicellularity has been intensively studied theoretically (Maynard Smith and Szathmáry 1995, Michod and Roze 2001, Pfeiffer and Bonhoeffer 2003, Rainey and Kerr 2010, Libby and Rainey 2013, Shelton and Michod 2014, De Monte and Rainey 2014). Investigation into the origins of multicellularity requires more than gathering a collection of examples of its emergence, it also involves explanation of this process. The explanations comprise a verbal or mathematical proof that some factors are driving forces behind the evolution of multicellularity. The construction of such proof is impossible without models – abstract constructs that take a hypothesis and make a logical prediction about the behaviour of the modelled system that arise from that hypothesis. Comparison of the model prediction with experimental observations lead to confirmation or rejection of tested hypotheses. Thus, a theoretical approach is not a replacement of experimental studies but an essential part of modern science.

Evolutionary game theory is widely used in the modelling of evolution of cooperation (Weibull 1997, Vincent and Brown 2005). In evolutionary game theory, members of a studied population are considered as *players*, participating in a formally defined interaction called the *game*. As a result of the game, each participant receives a *payoff*, which determines the fitness of the player. Players obtaining higher payoffs become more abundant in the population by means of natural selection. The direct application of evolutionary game theory is a test as to which strategy is the most evolutionarily successful under given conditions (the game). The solution of such a direct problem by simulation, or analytical means, allows

investigation of the inverse problem: under which conditions is a given behaviour able to evolve. Multiple types of ecological interactions between players have been interpreted as strategies in certain games and their evolution has been investigated using the game theory approach. These include cooperation (Boyd and Richerson 1992), predation (Brown and Vincent 1992), eusociality (Nowak et al. 2010) and parasitism (Renaud and De Meeus 1991).

In this section I review theoretical findings that shed light on the evolution of multicellularity. Studies relevant to the two stages of this process, emergence of groups and transition in individuality from cells to collectives, are considered separately.

1.2.4.1 Stage 1: Evolution of groups from the unicellular state

The first step of evolution from independent cells to multicellular organisms is an emergence of cell collectives in a population of initially free-floating cells. The main advantage to the cell of being part of a collective is an opportunity to participate in cooperative interactions. Thus, the evolution of groups from independent cells can be considered as a part of a more general phenomenon: the evolution of cooperation.

1.2.4.1.1 Evolution of cooperation

Mechanisms that promote the evolution of cooperation were reviewed by Nowak (2006b). He listed five biologically relevant processed involved in the evolution of cooperation: kin selection, direct reciprocity, indirect reciprocity, network reciprocity and group selection. Under kin selection, a player tends to interact with its relatives, who most likely share the same strategy. A player using direct and indirect reciprocities gains access to the information of past actions of its co-player, so the strategy of a player can be adjusted. In direct reciprocity, games are repeated multiple times with the same pair of players, so a player can remember the past actions of its counterpart. In indirect reciprocity, a reputation system is established, so each player knows its counterpart's behaviour in previous encounters with others. In network reciprocity, players are arranged on a lattice, and the number of co-players is limited to ones located on the connected lattice nodes. Finally, in group selection, players are partitioned into

Table 1.1: **Payoff matrix for the prisoner's dilemma game.** b is the benefit provided by cooperation, c is the cost of cooperation, and $b > c$.

	Cooperate	Defect
Cooperate	$b - c$	$-c$
Defect	b	0

distinct groups, and groups containing higher numbers of cooperators are more successful than are groups containing a lot of defectors.

In the evolutionary game theory, cooperation is formally described by the social dilemmas. The social dilemmas are a broad class of games where the strategy maximizing the total payoff to the whole group of players (cooperation) is different from the strategy maximizing the player's payoff (defection). Among all social dilemmas, the prisoner's dilemma (PD) game is the most often used in the investigation of the evolution of cooperation (Axelrod and Hamilton 1981, Milinski 1987, Dugatkin 1997). This is a two-player game, where each player adopts one of two strategies: to cooperate or to defect. A cooperator pays cost c to provide benefit $b > c$ to its co-player. A defector neither pays cost, nor produces a benefit. If both players cooperate, then each will gain a payoff of $b - c$, and the total payoff $2(b - c)$ is the highest possible in this game. If one of players is a defector and another one is cooperator, then defector's payoff will be equal to b, which is the highest possible player payoff, while the cooperating co-player will gain payoff $-c$, which is the lowest possible payoff. If both players defect, then both will receive zero payoff. The payoff matrix for the PD game is presented in Table 1.1 [2].

To defect in the PD game is always better, than to cooperate. If the opponent cooperates, then the defecting player will gain a higher payoff than a cooperating one $(b > b - c)$. If the opponent defects, then the payoff to the defecting player will be still higher than the payoff to the cooperating player $(0 > -c)$. Independently of the strategy of the opponent, the defecting player in the PD game gains a higher payoff than a cooperating player in the same situation.

[2] In general case the Prisoner's dilemma is any two player game, which payoff matrix satisfy condition $P_{D|C} > P_{C|C} > P_{D|D} > P_{C|D}$, where $P_{X|Y}$ is a payoff to player with strategy X in game against player with strategy Y.

In evolutionary game theory, the simplest model for a population participating in cooperative interactions is a group of individuals playing the PD game with a randomly chosen opponent. In this well-mixed model, the average payoff to the defector is higher than the average payoff to the cooperator. Under evolutionary game theory, the fitness of players depends on the obtained payoff. So, in a well mixed population, defectors reproduce better than cooperators, which leads to the tragedy of commons situation.

The main factor preventing the evolution of cooperation in a well mixed population is a random pairing of players, so in this model cooperators have to interact with defectors and lose to them in the PD game. Models with non-random pairing of players are able to promote the evolution of cooperation. When cooperators could preferentially play with other cooperators, then they gain higher payoff than defectors playing with defectors. The effect of the influence of player assortment on the evolutionary success of cooperators has been studied by van Veelen (2009). He found that assortment of players, i.e. the chance of cooperators to interact with other cooperators, determines the evolutionary success of cooperation.

The efficiency of player assortment is affected by the group formation mode. Two principal modes are known: "coming together" and "staying together" (Tarnita et al. 2013). Under the "coming together" mode, groups are formed from multiple, previously independent particles. Under the "staying together" mode, groups are formed from particles who refuse to separate from each other after division. Models incorporating either formation mode have been constructed in order to study the evolution of cooperation (Maynard Smith and Szathmáry 1995, Michod 2007).

1.2.4.1.2 Evolution of "coming together" groups

The "coming together" mode is prone to the invasion of defectors. The group assembled from multiple players allows defectors to infiltrate into groups of cooperators. Defectors then reap the benefits of cooperation, without paying associated costs. This situation has been modelled as well as having been observed in nature, for example among slime molds (Buss 1982). Defectors in slime molds are cell lines that do not participate in stalk formation and

always go into the fruiting body. The benefit comes from the possibility for defectors' spores to be dispersed and the payment, in the form of sacrificing some cells to stalk formation, is not paid. The defecting cell lines of slime molds are able to successfully invade the population (Buss 1982). This drawback significantly limits the opportunities of cooperation to evolve in the "coming together" group formation mode.

Several models of group selection use the "coming together" formation mode (Bardele and Margulis 1981, Bonner 1998, Krebs and Davies 2009). The trait-groups model (Wilson 1975, 1977) was one of the earliest of them and was focused on the evolution of cooperation in groups with this mode of formation. In the trait-groups model, each player can be either cooperator or defector. The reproduction of players occurs within the groups, so groups containing more cooperators produce more offspring than groups containing less cooperators; however, within each group, defectors produce more offspring than cooperators. After reproduction is complete, groups are disassembled and then players reassemble again. The trait-groups model is able to promote cooperation even if there is no assortment of cooperators during trait-groups formation. So, if the "coming together" group formation is established, then cooperation may evolve.

However, an inverse problem has particular interest in the context of this thesis: How may the group structure emerge in a unicellular population? The evolution of "coming together" groups from a population of independent cells has been modelled (Avilés 2002, Garcia and De Monte 2013, Powers et al. 2011). Garcia and De Monte consider the population of cells able to aggregate in groups. The group aggregation is only possible in this model, but is not necessary, so collectives coexist with lonely particles. Cooperators pay a cost to produce a glue used to assemble other cells into groups. All cells within a group gain same benefit, so cells that do not produce the glue act as defectors in this model because they do not pay the cost of group aggregation but receive benefits if they are included in the group. Garcia and De Monte have shown that the proportion of glue-producing players, the average size of groups and the proportion of players living in the groups increases with time in this model. Other models (Avilés 2002, Powers et al. 2011) show similar results. Therefore, even in the

"coming together" group formation mode cooperation may promote independent players to gather into collectives.

1.2.4.1.3 Evolution of "staying together" groups

The "staying together" mode is also able to promote cooperation (Traulsen and Nowak 2006). In this model, the group-structured population evolved under multilevel selection. At the particle level each player was either cooperator, or defector, playing the multiplayer variant of PD game within a collective. Defectors have higher fitness than cooperators within the collective of mixed composition, so they reproduce faster. When collectives reach a certain size, they split in two and one of them dies, so the total number of collectives remains constant. Collectives containing more cooperators have a higher average fitness, so they reproduce faster. Simulations and analytical results showed that the cooperators can have a higher fixation rate than defectors if the benefit to cost ratio is high enough. This shows that cooperation can evolve in a population of groups reproducing by the "staying together" mode.

The co-evolution of cooperation and ability to form clusters was considered in Pfeiffer and Bonhoeffer (2003). In this model, each player is characterized by two traits: its role in the interaction and its stickiness. The interaction role was either defector or cooperator. The stickiness was either positive, so the player was attached to its parent after division, or negative, so the player could freely drift in 2D space. If all players were free-floaters, then the defection was the successful strategy in the majority of environmental conditions. However, if players able to "stay together" were introduced in the population, then these players became dominant in the range of conditions previously favouring defectors. These results have two important implications: first, that cooperation can evolve in "staying together" groups; second, "staying together" groups can evolve in a population of initially independent cells.

Notably, groups formed by the mechanism of the "staying together" mode are more resistant to invasion of defectors. "Staying together" groups are composed of genetically close particles, so in the absence of mutations they will share the same strategy. Defection may

invade the "staying together" group only by the mutation of its members. This robust mode of group formation is widely used by the majority of existing multicellular organisms: fungi, plants and animals.

1.2.4.1.4 Hybrid modes of collective reproduction

Simon et al (2013) derived an equation describing the multilevel selection in a population, where groups may fuse and break apart. Such a population contains groups formed by the "staying together" mode (by group fission) and the "coming together" mode (by group fusion). The developed equation has been tested on the model of evolution of early collectives from a population of independent particles. Two types of particles were presented in the model: sticky and normal. Sticky particles had a lower growth rate than normal ones. Sticky particles were able to assemble other particles around them, and collectives containing more sticky particles were more likely to fuse and were less likely to split. Additionally, smaller collectives were more likely to be consumed by predators. The combination of all factors led to the increase of the fraction of sticky particles in a population, which can be considered as an evolution of cooperation. However, this model did not show which of the multiple factors was the driving force in the evolution of collectives.

1.2.4.1.5 Influence of group structure on the evolution of cooperation

Multiple models show how cooperation evolves in a population subdivided into groups (Wilson 1975, Charnov and Krebs 1975, Tarnita et al. 2013). However, the group structure is not the only factor that affects the evolution of cooperation in these models. For instance, the life cycle used by "coming together" models (Wilson 1975, Garcia and De Monte 2013), particles simultaneously assemble into groups and these groups then simultaneously disassemble. Such a life cycle is impossible without the coordination of players' actions. Another example is the "staying together" model, where reproduction of collectives occurs via fragmentation of collectives (Traulsen and Nowak 2006, Rodrigues et al. 2012, Tarnita et al. 2013). This process can be performed either by breaking of a linearly arranged collective, like cyanobacteria filaments, or by coordinated actions of multiple cells in a collective dur-

ing fragmentation. Both these mechanisms require something more than just existence of groups: internal group organization and coordination of the cells' actions respectively. Thus, the influence of the group structure itself on the evolution of cooperation is unclear.

The evolution of groups is a major step towards multicellularity. However, the group of cooperating Darwinian individuals may not itself be a Darwinian individual. For example, bacterial cell mats might exhibit such a complex form of cooperation as division of labour (Crespi 2001, Wingreen and Levin 2006), but the mat itself cannot reproduce as a group. The ability of groups to reproduce was taken for granted in most models that described the evolution of cooperation (Wilson 1975, Traulsen and Nowak 2006, Rodrigues et al. 2012, Garcia and De Monte 2013). However, the evolution of group reproduction is an essential step in the emergence of Darwinian individuality at the level of groups.

1.2.4.2 Stage 2: Transition in individuality

Darwinian individuality does not necessarily appear at the collective level as soon as particles become member of collectives. For instance, slime mold slugs possess Darwinian individuality only in marginal form (see section 1.2.2). During the transition in individuality, Darwinian properties are obtained by the collectives, so they start to participate in natural selection in their own rights. Slime molds illustrate that the Darwinian individuality may evolve at the collective level only under some specific selection conditions. These conditions are not yet well known.

Evolution of Darwinian individuality at the collective level is influenced by the life cycle of collectives (Bonner 1959, Kirk 2005, Ratcliff et al. 2012, 2013a, Hammerschmidt et al. 2014). Experimental studies have shown that the choice of life cycle has a strong effect on the possibility of the transition in individuality. Under some life cycles, the transition in individuality can occur within several weeks (Ratcliff et al. 2012, Hammerschmidt et al. 2014), but under others it does not happen (Hammerschmidt et al. 2014). What makes the life cycle promote the transition in individuality is still unknown.

To examine what class of life cycles promote transition in individuality, Libby and Rainey

(2013) constructed a classification of life cycles based on the mechanisms of collective recurrence. As a result, three classes of life cycles have been recognized. The first class is where a collective is an offspring of a previously existing collective, i.e. collectives reoccurring by fragmentation. The second class is where a collective is a descendant of an independent cell, which is in turn a descendant of another collective, i.e. slime molds and trait-groups model. The third class is where a collective is a descendant of an independent cell from a continuous line of independent cells. Organisms with germ-soma differentiation belong to the third class because any progenitor of a germ cell is another germ cell. However, the authors indicated that Darwinian individuality at the collective level may potentially emerge under any class of life cycles. So, no universal criteria for making a life cycle promote or prevent the transition in individuality is known.

Nevertheless, some specific subsets of life cycles favouring the transition in individuality are known. A plausible route toward emergence of Darwinian individuality at the collective level has been proposed by Rainey and Kerr (2010). They noted that defector cells may serve as proto-germ for early collectives. Cooperation and defection in the early collectives are linked to the sustaining of the collective together. For example, if cells are bound together by some glue-like substance, then the production of such a substance is a cooperative trait. So, cells that do not produce the glue can be considered as a defectors because they save some resources for own reproduction and their presence makes the collective less stable. Due to the absence of glue production, defecting cells can easily detach from the collective. If detached cells are able to reverse back to cooperative type, they will reform a collective in another place. The proposed mechanism turns the conflict between defectors and cooperators into the mechanism of the collective reproduction.

The establishing of reproduction at the collectives' level is one of the three Lewontin conditions of Darwinian individuality (the other two being variation and heredity). Therefore, the mechanism proposed by Rainey and Kerr could be responsible for the transition in individuality.

The presence of defectors is a necessary condition for the transition in individuality in this

mechanism. This is consistent with the findings of Hammerschmidt et al (2014): experimental evolution under the cheat-embracing regime led to the emergence of Darwinian properties among *P. fluorescens* collectives, while evolution under the cheat-purging regime did not.

Another way to investigate the transition in individuality is to extend the application of natural selection beyond the classical definition of Darwinian individuality. De Monte and Rainey (2014) proposed an alternative to Lewontin's conditions for natural selection (reproduction, variation and heredity) (Lewontin 1970). The De Monte and Rainey conditions are: an ability to *identify* the collective, *recurrence* of collectives in time, and tractable *genealogy* of collectives. Recurrence is a broader concept than reproduction used by Lewontin (1970). Recurrence addresses for cases, where the link between collectives existing at different time points lacks causal connection and is established through actions of external factors. Genealogy is a broader concept than heredity because genealogy of the entity can be traced back even if the properties of "parent" and "offspring" are dissimilar. Any population satisfying Lewontin's conditions (1970) also satisfies conditions of De Monte and Rainey (2014) because the reproduction ensures recurrence of population members, heredity requires the genealogy, and variation is generally present in populations. The opposite does not hold true because De Monte and Rainey's conditions cover marginal cases of Darwinian individuality as well as paradigm ones.

An example of one such marginal case is the population considered in the model of Garcia and De Monte (2013) (see section 1.2.4.1.2). Collectives in this population were able to evolve even if they were not paradigm Darwinian individuals. This result indicates that the paradigm Darwinian individuality at the collective level may later evolve from its marginal form by means of natural selection acting at the collective level.

To investigate the evolution of the Darwinian individuality from marginal to paradigm form, a means of characterizing this transition is necessary. Two different techniques can be used to characterize the transition in individuality: decomposition methods (Price 1972, Heisler and Damuth 1987, Okasha 2006) and fitness decoupling (Michod and Roze 1999, Okasha 2006). Decomposition methods formally divide the evolutionary changes occurring

in population into the particle-level and collective-level selection contributions. The non-zero contribution of the collective-level selection is generally interpreted as an existence of Darwinian individuality at the collective level. The fitness decoupling concept detects the emergence of Darwinian individuality at the collective level by the fact that in this case the collective fitness becomes independent from the particle fitness. Therefore, populations with paradigm Darwinian individuality at the collective level can be distinguished from marginal cases. The strengths and weaknesses of both approaches are reviewed below.

1.2.4.2.1 Decomposition methods

The Price method (1972) is widely used in the investigation of multilevel selection (Frank 1998, Queller 1992, Rice 2004). The Price equation decomposes the selective change of the trait into particle-level and collective-level components (Okasha 2006, p. 65):

$$\bar{w}\Delta\bar{z} = Cov(W_k, Z_k) + \mathbb{E}(Cov_k(w_i, z_i)) \tag{1.1}$$

Here $\bar{w}$ is an average fitness of population members, $\Delta\bar{z}$ is the total change in average value of the trait due to the selection. W_k and Z_k are respectively average fitness and average trait value in k-th collective. w_i and z_i are respectively fitness and trait value of i-th particle. Index k in $Cov_k(w_i, z_i)$ means that the covariation is calculated for members of k-th collective.

The first term in Eq. 1.1 is a covariation between average trait in collectives and average fitness in collectives. This term is interpreted as a collective-level component of selection. Thus, the non-zero value of the collective-level term can be read as a presence of selection at the collective level.

However, in some cases, the Price equation incorrectly decomposes the selection to particle and collective-level components (Sober 1993). For example, consider the population of particles nested within collectives, where the fitness of any particle depends only on its own character (Sober 1993). In this population, collectives containing fitter particles are fitter as collectives as well. The collective level term in the Price decomposition $Cov(W_k, Z_k)$ is not

equal to zero in this case. However, the selection does not act on the collective level because the group structure does not affect the fitness of particles. The reason why the Price equation works incorrectly in some cases is because this method provides *statistical* decomposition of selective change, but this is not always the same as a *causal* decomposition (Okasha 2006). Thus, the Price decomposition is incorrect in situations, where correlation between collective-level traits and collective-level fitness is a byproduct of the selection at the particle level. The Price method is therefore not a robust indicator of the presence of Darwinian individuality at the collective level.

The contextual approach is an alternative algorithm to decompose the selection to particle-level and collective-level components (Heisler and Damuth 1987). In this method, the particle fitness is considered as a linear function of two parameters: the particle's trait and the average collective trait (see Eq. 1.2). Observed particle fitnesses are fitted with a linear regression model, and the two resulting regression components are considered as impacts of the corresponding level on the selection, see Eq. 1.3.

$$w_i = \beta_1 z_i + \beta_2 Z_k + \epsilon \tag{1.2}$$

$$\bar{w}\Delta\bar{z} = \beta_2 Var(Z) + \beta_1 Var(z) \tag{1.3}$$

Here w_i and z_i are fitness and trait value of the i-th particle. Z_k is an average trait value in k-th collective. ϵ is a discrepancy of the fitting. $\bar{w}$ is an average fitness of population members, $\Delta\bar{z}$ is the total change in average value of the trait due to the selection. $Var(Z)$ is a variation of average trait values among collectives, $Var(z)$ is a variation of particle trait values. β_1 and β_2 are regression coefficients from the linear model, representing selection at collective and particle levels respectively.

The decomposition of selection using the contextual method is incorrect in some cases. Consider a population where each collective contributes the same number of offspring particles to the next generation but particles within collectives produce different number of off-

726 spring. This situation is known as soft selection. Using the contextual decomposition ap-
727 proach both components of selection β_1 and β_2 are non-zero. However, no selection at the
728 collective level is present in this example because there is no variation among the fitnesses of
729 the collectives. Thus, the contextual approach is not as robust a detector of the presence of
730 collective-level selection as is the Price approach.

731 Decomposition methods may indicate the presence of collective-level selection while
732 Darwinian individuality is not present at the collective level. For instance, consider the
733 mixed population of cooperators and defectors inhabiting a fragmented environment, such
734 as an archipelago. Each island can be considered as a collective. Selection at the particle
735 level favours defectors because they have higher fitness than cooperators. However, selec-
736 tion at the collective level favours cooperators because islands with higher proportions of
737 cooperators produce more offspring, so that if offspring can migrate between islands, then
738 cooperation may fixate in the population. Both the Price equation and the contextual ap-
739 proach detect the presence of selection at the collective level in this scenario, but the island
740 within the archipelago is just a boundary dividing the population into compartments and,
741 therefore, does not possess a Darwinian individuality. So, decomposition methods are not
742 robust indicators of Darwinian individuality at the collective level.

743 **1.2.4.2.2 Fitness decoupling**

744 The fitness decoupling concept proposed by Michod and Roze (Michod and Roze 1999,
745 2001, Michod 2007) can be used to detect Darwinian individuality at the collective level.
746 Michod and Roze noted that among collectives "on the threshold of multicellular life" the
747 MLS2 collective fitness most likely depends on the size of collectives, and, therefore, is
748 correlated with particle fitness. In contrast, for species possessing developed multicellularity
749 the fitness of an organism depends on cell functionality, but not on the cell number. So,
750 during the transition in individuality, the fitness of collectives becomes decoupled from the
751 fitness of cells. There is much merit in this idea, which can be used to distinguish collectives
752 before and after transition in individuality.

A formal method to characterize fitness decoupling was previously proposed by Michod, Viossat, Solari, Hurand, and Nedelcu (2006) and is discussed by Bossert et al (2013), named by the authors' initials – the MVSHN index. The MVSHN index is defined as a product of collective viability and collective fertility, which in turn are sums of particle viabilities and fertilities respectively. This index has been developed to be used in models with a division of labour between members of a collective. The fitness in these models is a product of two components: fertility and viability, which can be measured for each particle in the collective.

The MVSHN index can be used to determine whether fitness decoupling has occurred. The difference between average particle fitness and the MVSHN index is equal to the covariance between particle viability and fertility within the collective. The value of this difference changes with the development of division of labour within the collective and therefore can be used as an indicator of the fitness decoupling in the model.

The application of the MVSHN index to detect fitness decoupling is limited to systems where transitions in individuality occur via development of a division of labour between germ and soma. However, in the general case, Darwinian individuality may, in principle, be obtained by collectives using other mechanisms. One can imagine a species reproducing by fragmentation, without sexual reproduction. Such an organism is a multicellular one, but with no germ-soma differentiation. This makes the MVSHN index impossible to apply in such cases. Therefore, a more general method for detecting fitness decoupling would be useful in this field of study.

1.3 Research objectives

The focus of this thesis is a theoretical investigation of the origins of multicellularity. The evolution of multicellularity can be divided into two stages, as outlined in section 1.1.5: the evolution of collectives from independent cells, and the transition of Darwinian individuality from cells to collectives. The objectives of this thesis are:

- To investigate the conditions under which cooperation may emerge in early collectives without established collective-level reproduction.

- To develop a formal method of numerical characterization of the fitness decoupling applicable to any population under multilevel selection. To apply the developed method to the derivation of the set of selective conditions favouring the fitness decoupling.

- To validate the utility of the proposed set of conditions favouring the fitness decoupling using experimental populations and theoretical models. To investigate how the life cycle affects the emergence of the fitness decoupling.

1.3.1 Thesis structure

An investigation of the effect of population group structure on the evolution of cooperation is presented in Chapter 2. I show that if the role of cell collectives is just to be boundaries compartmentalizing the population, then it will be possible for only weak altruism to emerge. More complex scenarios are also considered; they illustrate how strong altruism can fixate in a group-structured population if cells can coordinate their activity within collectives.

In the Chapter 3 a formal measure of fitness decoupling is proposed. This measure is illustrated using several examples intermediary between uni- and multicellularity. A simple linear model of multilevel selection is then considered, and selective conditions for the fitness decoupling are found.

In Chapter 4 the developed method of the fitness decoupling is verified on the system used by Hammerschmidt et al (2014). The fitness decorrelation value predicted by the developed method is compared against experimental data and results of a simulation model. Two different life cycles are considered. One selection regime from each life cycle is tested using experimental data and simulations. 64 selection regimes from each life cycle are tested with simulations. The robustness of the developed method is shown and the influence of the life cycle on the fitness decoupling is investigated.

Chapter 2

Modes of migration and multilevel selection in evolutionary multiplayer games

Chapter two is based on work that is currently in revision for publication as an article in *Journal of Theoretical Biology*: **Yuriy Pichugin, Chaitanya S. Gokhale, Julián Garcia, Arne Traulsen and Paul B. Rainey. Modes of migration and multilevel selection in evolutionary multiplayer games.** *Journal of Theoretical Biology*, in press.

Alterations have been made for continuity in the context of this thesis.

812

MASSEY UNIVERSITY
GRADUATE RESEARCH SCHOOL

STATEMENT OF CONTRIBUTION TO DOCTORAL THESIS CONTAINING PUBLICATIONS

(To appear at the end of each thesis chapter/section/appendix submitted as an article/paper or collected as an appendix at the end of the thesis)

We, the candidate and the candidate's Principal Supervisor, certify that all co-authors have consented to their work being included in the thesis and they have accepted the candidate's contribution as indicated below in the *Statement of Originality*.

Name of Candidate: Yuriy Pichugin

Name/Title of Principal Supervisor: Dist. Prof. Dr. Paul B. Rainey

Name of Published Research Output and full reference:

Yuriy Pichugin, Chaitanya S. Gokhale, Julian Garcia, Arne Traulsen and Paul B. Rainey. Modes of migration and multilevel selection in evolutionary multiplayer games. Journal of Theoretical Biology, in press.

In which Chapter is the Published Work: chapter 2

Please indicate either:

- The percentage of the Published Work that was contributed by the candidate:90%

  and / or

- Describe the contribution that the candidate has made to the Published Work:

  Yuriy participated in the design of investigation, performed all calculations, analyzed data and wrote most of the text.

Yuriy Pichugin Digitally signed by Yuriy Pichugin DN: cn=Yuriy Pichugin, o, ou, email=y.g.pichugin@gmail.com, c=DE Date: 2015.09.29 14:16:14 +02'00'

Candidate's Signature

29.09.2015

Date

Principal Supervisor's signature

6.10.2015

Date

2.1 Introduction

Cooperation can be defined as "a joint action for mutual benefit" (Dugatkin et al. 1992, Mesterton-Gibbons and Dugatkin 1992, Clements and Stephens 1995, Stephens and Anderson 1997). Participation in a cooperative act is generally costly to cooperators (Hamilton 1963, Axelrod and Hamilton 1981, Clements and Stephens 1995). Therefore, cooperators have lower fitness than non-cooperators (defectors) and, thus, should be eliminated by natural selection. Nevertheless, cooperation is widespread in nature (Crespi 2001, Porat and Chadwick-Furman 2004, Wingreen and Levin 2006). How cooperation evolves and is maintained in the face of selfishness has been the subject of intensive investigation (Hamilton 1963, Wilson 1975, Axelrod and Hamilton 1981, Nowak 2006b, van Veelen 2009).

In a group-structured population, members of cooperative groups have a selective advantage over the members of non-cooperative groups. This advantage can make the evolution of cooperation possible (Hamilton 1964, Wilson 1975, Traulsen and Nowak 2006, Nowak 2006b). The essential idea is that population structure channels cooperation preferentially to other cooperators (Doebeli et al. 2006, Fletcher and Doebeli 2009). Wilson and Wilson (Wilson and Wilson 2007) formulated this as: "Selfishness beats altruism within groups. Altruistic groups beat selfish groups. Everything else is commentary." However, the interplay between these effects is important because it determines whether cooperation will evolve.

Group structure by itself does not provide an advantage to cooperation (Godfrey-Smith 2009) - indeed within groups, selfish types have an advantage over cooperating types (Wilson 1975). For cooperating types to be maintained, groups must participate in some kind of birth and death process. For this to happen, individuals arising within one group must have opportunity to become a member of another group. There are many ways by which this may occur. For instance, in standard trait group models (Wilson 1975, Avilés 2002, Garcia and De Monte 2013), individuals within groups are released into a global pool and then randomly form new groups. Alternatively groups may fragment (Traulsen and Nowak 2006). A further possibility is that individuals from one group may migrate to another (Christiansen 1975, Kelly 1992, Hauert and Imhof 2012, Hauert et al. 2014). Via the process of migration,

groups themselves do not reproduce in a conventional sense, but the effects are parallel.

In this study I consider models where an individual may become a member of another group by migration between groups. Individuals migrating from one group to another may fixate in the new group, or be eradicated as a consequence of individual-level selection. A defecting individual has a higher probability of fixation in a group of cooperators than does a cooperating individual in a group of defectors, thus individual-level selection favours defectors. However, individuals in groups of cooperators are more productive than in groups of defectors, and therefore groups of cooperators release more migrants than do groups of defectors. Thus, while previous studies have shown that migration makes cooperation more difficult to evolve (because it brings about the mixing of groups (Traulsen and Nowak 2006)), recent work shows that rare migration can favor cooperation (Hauert et al. 2014). Here, I consider a range of modes by which migration might occur and describe ensuing effects on the evolution of cooperation.

Migration can be implemented in multiple ways: individuals may migrate individually, or in clumps; subsequent migrations may or may not be influenced by previous ones; migration may be triggered by signals perceived by individuals, or may be influenced by the group. In this study I compare different modes of migration. For each mode, I identify the games in which cooperation is evolutionarily successful, i.e., where selection at the group level is strong enough to overcome selection at the individual level. The comparison between modes of migration shows that the set of games in which cooperation evolves generally expands with increasing degrees of coordination surrounding the migration process.

2.2 Evolutionary dynamics within a single group

I make the assumption that individuals live in a population with a fixed number of groups. The interactions between all individuals within a group are determined by a multiplayer game. The payoff of each individual depends on its strategy and the composition of the group. Each individual can be either a cooperator (C) or a defector (D). The size of the game is equal to

group size. Thus, all players sharing the same strategy within a group have the same payoff. More specifically, the payoff of a cooperator in a group with i cooperators and $n-i$ defectors is a_i, and the payoff of a defector in a group with i cooperators and $n-i$ defectors is b_i. Thus, a game is completely determined by two sequences, $a_1, ..., a_n$, and $b_0, ..., b_{n-1}$ (Kerr et al. 2004, Gokhale and Traulsen 2010).

I use an exponential function to map payoff to fitness. The fitnesses of cooperators and defectors in a group with i cooperators are therefore e^{wa_i} and e^{wb_i}, respectively (Traulsen et al. 2008). Here, w measures the intensity of selection. For $w = 0$, selection is neutral. For $w \ll 1$, the fitness is approximately linear in payoffs. For large w, small differences in payoffs lead to large fitness differences.

The evolutionary dynamics are governed by a Moran process. At each time step a single individual in the population is chosen for reproduction with probability proportional to fitness (Moran 1953, Nowak et al. 2004). This chosen individual produces identical offspring, replacing a randomly chosen individual. Thus, population size is kept constant. For such a process, the probability for a single cooperator to take over the whole population, ϕ_C, can be calculated exactly, as well as the probability of a single defector taking over the whole population, ϕ_D (Goel and Richter-Dyn 1974, Traulsen and Hauert 2009). These fixation probabilities form the basis of the measure of success for each strategy.

In order to compare the evolutionary success of the two strategies C and D, I examine whether $\phi_C > \phi_D$. Thus, the value of ϕ_C/ϕ_D determines which strategy is more common. For a ratio greater than 1, cooperation is favoured over defection. If the ratio is less than 1, defection is favoured. The fixation probabilities of cooperators and defectors in the Moran process with exponential mapping are (Karlin and Taylor 1975, Nowak et al. 2004, Traulsen et al. 2008)

$$\phi_C = \frac{1}{1 + \sum_{j=1}^{n-1} \prod_{i=1}^{j} e^{w(b_i - a_i)}} \tag{2.1}$$

$$\phi_D = \frac{1}{1 + \sum_{j=1}^{n-1} \prod_{i=1}^{j} e^{w(a_i - b_i)}}. \tag{2.2}$$

The ratio of the fixation probabilities is given by (Nowak 2006a)

$$\frac{\phi_C}{\phi_D} = \prod_{i=1}^{n-1} \frac{e^{wa_i}}{e^{wb_i}} = e^{w \sum_{i=1}^{n-1} (a_i - b_i)}. \tag{2.3}$$

Whether the ratio in Eq. 2.3 is greater than 1 (i.e. cooperators are favoured) depends solely on the sign of

$$\Lambda_0 = \sum_{i=1}^{n-1} (a_i - b_i). \tag{2.4}$$

This is a generalization of the classic result of risk dominance to multiplayer games (Kandori et al. 1993, Nowak et al. 2004, Fudenberg et al. 2006, Antal et al. 2009, Kurokawa and Ihara 2009, Gokhale and Traulsen 2014). For a positive Λ_0, cooperation is favoured in terms of the fixation probability, while a negative Λ_0 means that defectors are selected. I will use these Λ values for comparing the different migration modes.

2.3 Migration modes

I now extend this analysis to multiple groups, and include migration between groups (see Fig. 2.1). Consider m different groups, each with a fixed group size of n. I discuss several different modes of migration that individuals can use to move between groups.

The rate of migration between groups is assumed to be very small compared to the rate of fixation of a strategy within a group. This implies that migration events typically occur only when groups are homogeneous (Traulsen and Nowak 2006, Traulsen et al. 2008). Under this time-scale separation, fixation events in the whole population occur in two stages: first a strategy fixes inside a group – with probability ϕ_C (ϕ_D) for cooperators (defectors) – and then in the whole population – with probability Φ_C (Φ_D) for groups of cooperators (defectors).

I use Eqs. (2.1) and (2.2) to compute ϕ_C and ϕ_D at the individual level. At the group

level, the fixation probabilities Φ_C and Φ_D depend on the mode of migration. Expressions for these probabilities are generally simpler than for the probabilities at the individual level due to the fact that all individuals within a group have the same fitness when migration occurs (see 2.6.1.2-2.6.1.5 for details).

The ratio of fixation probabilities in the structured population (analogous to Eq. (2.3)) is then given by $\frac{\phi_c \Phi_c}{\phi_d \Phi_d}$ (Traulsen and Nowak 2006).

Here I present a brief derivation of fixation probabilities and corresponding "sign sums" Λ. A different Λ will be calculated for each migration mode (See 2.6.1.1 – 2.6.1.5 for details).

2.3.1 Single individual migration

As in Traulsen and Nowak (Traulsen and Nowak 2006), I assume that offspring are added to the parent group with probability $1-\lambda$, or to a randomly chosen group with probability λ. This is the simplest migration process, with λ being the migration probability. Due to $\lambda \ll 1$, I consider the probability that a group where the mutant has fixated will send out a migrant that will become a member another group. This probability is equal to $ne^{wa_n}\lambda$ for groups of cooperators, and $ne^{wb_0}\lambda$ for groups of defectors. For the fixation probabilities at the group level, I obtain the ratio

$$\frac{\Phi_C}{\Phi_D} = \prod_{j=1}^{m-1} \frac{ne^{wa_n}\lambda\phi_C}{ne^{wb_0}\lambda\phi_D} = e^{w(m-1)(a_n-b_0+\sum_{i=1}^{n-1}(a_i-b_i))}. \tag{2.5}$$

Combining Eqs. (2.3) and (2.5) I obtain

$$\frac{\phi_C\Phi_C}{\phi_D\Phi_D} = e^{w((m-1)(a_n-b_0)+m\sum_{i=1}^{n-1}(a_i-b_i))}. \tag{2.6}$$

Here, the outcome of evolution is determined by the sign of Λ_1, given by

$$\Lambda_1 = (m-1)(a_n-b_0) + m\sum_{i=1}^{n-1}(a_i-b_i) = (m-1)(a_n-b_0) + m\Lambda_0 \tag{2.7}$$

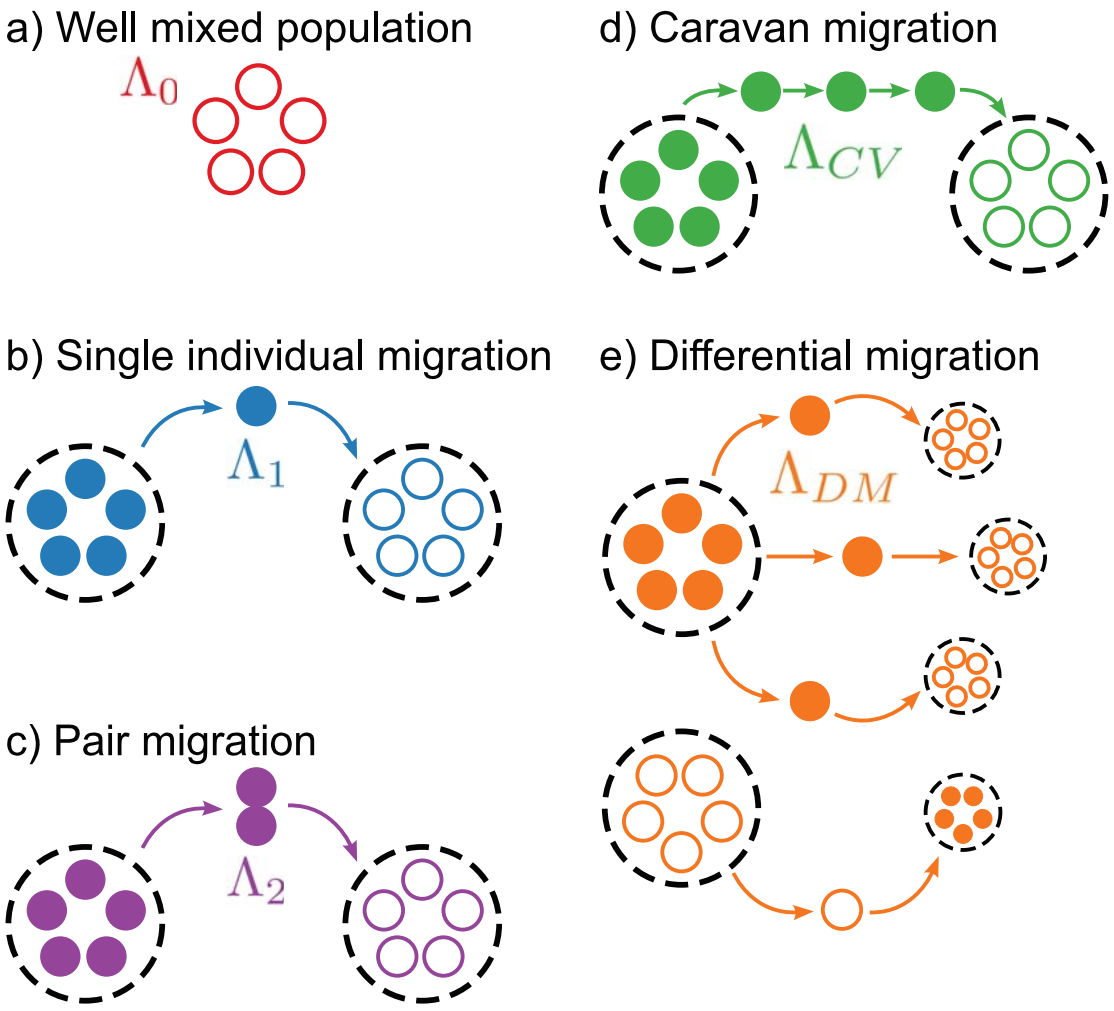

Figure 2.1: **Different modes of migration.** Closed circles represent cooperators, open circles represent defectors, dotted line circles represent groups. (a) *Well mixed population,* where no migration is possible. (b) *Single individual migration mode*, where each individual migrates independently. (c) *Pair migration mode*, where individuals migrate in pairs. (d) *Caravan migration mode*, where multiple migrants go to the same group. (e) *Differential migration mode*, where cooperators have higher chances to migrate than defectors. In each case, the quantity Λ determines whether cooperation evolves or not, cf. Fig. 2.2.

The equation for the sign sum Λ_1 contains the sign sum of the single group mode, Λ_0, as the second term. The first term $(m-1)(a_n - b_0)$ is proportional to the fitness difference of the purely cooperative group and the purely defecting group, and describes the effect of group migration. Eq. 2.7 explicitly expresses conditions for selection to favor cooperation in the single individual migration mode (Hauert and Imhof 2012) through payoffs from a multiplayer game that is played within groups.

Groups of cooperators send out more migrants than groups containing high frequencies of defecting types, which means that cooperative strategies gain an advantage in the face of migration. The effect of migration depends on the number of groups m in a population. The relative weight of the new term in comparison with the lower-level selection term $\sum_{i=1}^{n-1}(a_i - b_i)$ depends only weakly on the number of groups m. With decreasing number of the groups, Λ_1 approaches Λ_0, and for $m = 1$ both are identical.

2.3.2 Pair migration

Another mode of migration is one where migrants leave simultaneously. For this mode I assume that every migration event carries propagules of a finite number. For illustrative purposes, I discuss propagules of size 2 or 'pair migration'. In this case, I consider the probability that two deviating individuals take over the population. The sign sum is

$$\Lambda_2 = \Lambda_1 + \frac{m-1}{w} \ln \left[\frac{1 + e^{-w(a_1 - b_1)}}{1 + e^{w(a_{n-1} - b_{n-1})}} \right] \tag{2.8}$$

The additional term, now including the selection coefficient, may be positive or negative, depending on the payoff comparison in groups with 1 and $n-1$ individuals of each type. For a game where cooperators receive a lower payoff than defectors in the same group, this additional term is always positive. Therefore the increase of invading propagule size from 1 to 2 benefits cooperators. The sign sums can be calculated for propagules of arbitrary size in a similar fashion.

2.3.3 Caravan migration

Next, I assume that a new migrant might follow a previous migrant with a probability p. This causes a caravan effect, whereby migrants invade the same group with a probability greater than random. Due to the time scale separation assumption, a migrant is fixed or eliminated from the group before the next migrant arrives. Therefore, the caravan migration mode considers multiple migrations of single individuals, whereas the propagule mode of migration considers simultaneous migration of multiple individuals. For simplicity I introduce an additional time scale separation to the caravan migration model: all follow-up migrants arrive at recipient groups earlier than migrants from any other group. The caravan migration mode represents biological systems in which migrants may leave some record of their migration that stimulates the production of further individuals within the group to follow the first departed migrant. This approximates a situation where, for example, an ant leaves a chemical trail that other follow (Hölldobler and Wilson 1990). This contributes the simplest example of the model in which all players in the group coordinate their actions.

The probability that the number of migrants entering the same group is equal to k is given by

$$P(k) = p^{k-1}(1-p). \tag{2.9}$$

The probability that at least one migrant is successful is equal to

$$\phi_C^{\text{Caravan}} = 1 - \sum_{k=1}^{\infty} P(k)(1-\phi_C)^k = \frac{\phi_C}{1-p(1-\phi_C)} \tag{2.10}$$

Here ϕ_C^{Caravan} is the probability of a successful invasion of a group of defectors by a cooperative group.

Similarly, the expected probability of the opposite event is $\frac{\phi_D}{1-p(1-\phi_D)}$. Thus, the ratio of fixation probabilities at the group level is

$$\frac{\Phi_C}{\Phi_D} = \prod_{j=1}^{m-1} \frac{ne^{wa_n}\lambda\phi_C(1-p(1-\phi_D))}{ne^{wb_0}\lambda\phi_D(1-p(1-\phi_C))}. \tag{2.11}$$

If $p \gg 1-\phi$, the probability that the group invaded by the first migrant is eventually taken over approaches 1, such that the result becomes independent of ϕ_C and ϕ_D. The group that receives the first migrant will be invaded with a probability equal to 1. The flow of migrants from one group to another means that the invaded group will be converted with a probability equal to 1. The ratio of fixation probabilities at the group level in this limit is

$$\frac{\Phi_C}{\Phi_D} = \prod_{j=1}^{m-1} \frac{ne^{wa_n}\lambda}{ne^{wb_0}\lambda} = e^{w(m-1)(a_n-b_0)}. \tag{2.12}$$

The sign sum (see Eq. (2.7)) for this mode is then

$$\Lambda_{CV} = (m-1)(a_n-b_0) + \sum_{j=1}^{n-1}(a_j-b_j) = \Lambda_1 - (m-1)\Lambda_0. \tag{2.13}$$

This is larger than in the migration mode for a single individual Λ_1, as $\Lambda_0 < 0$ for traits that are disadvantageous at the individual level ($a_i < b_i$). An increase in the number of groups in a population significantly increases the advantage to cooperators caused by this migration process. Since the caravan mode effectively displaces the accepting group with a copy of the donor group, the result obtained here is mathematically equivalent to those of Traulsen and Nowak (Traulsen and Nowak 2006), where it was assumed that a group splits and displaces a randomly selected group.

2.3.4 Differential migration

In the earlier migration modes I have assumed that the migration rate is independent of the type of emigrant. Here I relax this assumption. For example, a group of cooperators may

increase the migration rate of its members, therefore increasing the fitness of the group as a whole. Biologically, this could be envisioned to occur via secretion of a chemical signal promoting newly emerged individuals to leave the parent group.

In this mode, let λ_C be the migration rate of C types, and λ_D be the migration rate of D types. Assuming that the time scale separation is not violated by increased migration rates, I calculate the ratio of fixation probabilities on the group level as

$$\frac{\Phi_c}{\Phi_d} = \prod_{j=1}^{m-1} \frac{ne^{wa_n}\lambda_C}{ne^{wb_0}\lambda_D} = e^{w(m-1)(a_n - b_0 + \frac{\ln(\lambda_C/\lambda_D)}{w})}. \tag{2.14}$$

Therefore, the sign sum in this mode is

$$\Lambda_{DM} = \Lambda_1 + \frac{m-1}{w} \ln\left(\frac{\lambda_C}{\lambda_D}\right). \tag{2.15}$$

The difference in migration rates ($\lambda_C > \lambda_D$) provides an advantage to cooperating groups, which emits proportionally more migrants in this mode. This is reflected in an additional term $\ln\left(\frac{\lambda_C}{\lambda_D}\right)$, which can shift the balance of selection in favour of cooperators. Interestingly, the overall sign sum Λ_{DM} may still be negative, despite the fact that groups of cooperators produce more migrant offspring than groups of defectors. This can be explained by the fact that the raw number of migrant offspring is not a determinant of evolutionary success, instead the number of successfully invaded migrants is a defining characteristic of evolution in my model. As such, even if the number of migrants emitted by the cooperating group might be high, the fixation process occurring by means of selection at the individual level favours defectors. The interplay of these two factors does not necessarily promote cooperation even in the differential migration mode, where cooperators are considered to have an advantage.

2.4 Social dilemmas

To be more concrete, I now apply the results of the previous sections to different social dilemma games (Dawes 1980, Axelrod and Hamilton 1981, Kerr et al. 2004, Nowak 2006b).

In social dilemma games, the average payoff to players increases with the number of cooperators, but defectors gain higher payoff than cooperators. An example of a pairwise social dilemma is the prisoner's dilemma, which is extensively used for the study of the evolution of cooperation (Axelrod and Hamilton 1981, Milinski 1987, Dugatkin 1997). For my purposes, it is useful to differentiate between weak and strong altruism.

2.4.1 Weak and strong altruism

Weak altruism is a situation where cooperators provide an advantage to the group, but regardless of the group composition, cooperators have lower payoff than defectors (Wilson 1980, Kerr et al. 2004). Therefore, the payoffs under weakly altruistic interactions have two properties,

1. If the number of cooperative players increases, the payoffs of all players increase. That is $a_i < a_{i+1}$ and $b_i < b_{i+1}$.

2. Cooperators have lower payoff than defectors. That is $a_i < b_i$.

Since $a_i < b_i$, then, consequently, $\Lambda_0 < 0$. Unsurprisingly, weak altruism does not arise in the absence of selection at the group level.

In the case of single migrants, the migration-related term in the sign sum Λ_1 (Eq. (2.7)) can balance, and even overcome, the term that represents lower level selection. Thus, weak altruism can be favoured in simple migration settings. Similar arguments hold for the pair migration, caravan migration and differential migration modes.

Strong altruism (Wilson 1980), also termed as focal complement altruism (Kerr et al. 2004), are interactions where switching to cooperation always entails a loss of reproductive success. A well-known example of strong altruism is the prisoner's dilemma where strongly altruistic interactions are characterized by two properties:

1. If the number of cooperative players increases, the payoffs of all players increase. That is $a_i < a_{i+1}$ and $b_i < b_{i+1}$.

2. If a player switches from defection to cooperation, their payoff decreases. That is $a_i < b_{i-1}$.

Strong altruism is always disadvantageous in populations without structure, i.e. $\Lambda_0 < 0$. In addition, I find that

$$\Lambda_1 = (m-1)(a_n - b_0) + m\sum_{i=1}^{n-1}(a_i - b_i) = \underbrace{-(a_n - b_0)}_{<0} + m\sum_{i=1}^{n}\underbrace{a_i - b_{i-1}}_{<0} < 0, \qquad (2.16)$$

which means that strong altruism is also disfavoured with simple individual-based migration. This result generalizes previous findings that cooperation in the Prisoner's dilemma game cannot evolve when migration involves just a single individual (Hauert and Imhof 2012).

For pair migration, Λ_2 can become positive due to the additional term that is present in Λ_2 (see Eq. 2.8). Also for caravan migration, cooperation can be favored due to the additional positive term $-(m-1)\Lambda_0$.

Next, I discuss more specific examples of social dilemmas.

2.4.2 Public goods games

Pairwise games, such as the prisoner's dilemma, where only two players participate in each game round, cannot represent cooperation with synergistic interactions. With synergistic interactions, multiple cooperators amplify each other's contributions, thus providing higher benefit than they would produce independently. To encompass these kinds of interactions, I utilize *multiplayer games*, where multiple players are taken into account in the payoff calculation (Hauert et al. 2006, Kurokawa and Ihara 2009, Gokhale and Traulsen 2014).

Public goods games are a type of multiplayer game where each player can make a donation to a public pool. The collected amount is then multiplied, and evenly shared amongst all players, including those that decided not to make a donation. Weak and strong altruism can be naturally represented by self-returning benefit and self-excluding benefit games, respectively (Sigmund 2010, De Silva et al. 2010). In self-returning benefit games, the public

goods are shared among all participants; therefore, a proportional part of a donation returns to contributors as a part of their payoff. In this case, all players receive the same share of a public good, but defectors save the cost of donation. Therefore self-returning benefit games represent weak altruism. In self-excluding benefit games, a donation by a focal individual is only shared among other participants; therefore, the payoff of this focal player depends only on the donation of others. In self-excluding benefit games, switching from cooperation to defection does not change the received amount of the public goods, but saves the cost of cooperation. This makes cooperation in self-excluding benefit games strongly altruistic.

I start with the simplest public goods game. Here, the reward to cooperators increases linearly with the number of cooperators. Cooperative individuals pay a cost γ, in order to provide a benefit β. This benefit is either split amongst the rest of the group, in the linear self-excluding game (LSE game); or split among the whole group, in the linear self-returning game (LSR game). A defecting individual does not pay the cost, but reaps the benefits from other cooperators. The LSR game is weakly altruistic, see Table 2.1. The LSE game is strongly altruistic, and can be viewed as a multiplayer generalization of the standard prisoner's dilemma.

In addition, I consider non-linear public goods games. If there are synergies in the production of the public goods, each additional donation can provide more benefits than the previous one. Likewise, if the marginal benefit decreases with the number of donations, the benefits are discounted and become saturated as the number of cooperators increase. These so-called non-linear public goods games have been extensively analyzed (Eshel and Motro 1988, Bach et al. 2006, Hauert et al. 2006, Wakano et al. 2009, Pacheco et al. 2009, Gokhale and Traulsen 2010, Wakano and Hauert 2011, Archetti and Scheuring 2012, Peña 2012, Purcell et al. 2012, Abou Chakra and Traulsen 2014).

In the simplest version of the game incorporating synergy and discounting, the first cooperator in the group pays a cost γ to generate β units of a public good. Each additional cooperator present in the group provides ζ times the public good than the previous one. If $\zeta > 1$, then cooperators act synergistically. If $\zeta < 1$, benefits are discounted. Again, donations can

Table 2.1: **Payoffs and their differences for the linear self-returning (LSR), the linear self-excluding (LSE), the synergy/discounting self-returning (SDSR), and the synergy/discounting self-excluding (SDSE) public goods games.** a_i is the payoff to a cooperator in a group of size n with i cooperators, and b_i is the payoff for a defector. The sum of the payoff difference $a_i - b_i$ determines the value of Λ_0 (see Eq. 2.4). Switching from defection to cooperation leads to a payoff difference $a_i - b_{i-1}$. Switching always decreases payoffs for the self-excluding benefit games (LSE and SDSE); however, the change in payoff for the self-returning benefit games (LSR and SDSR) can be positive and therefore cooperators could have a higher fixation rate than defectors in these games.

	LSR	LSE	SDSR	SDSE
a_i	$\frac{i}{n}\beta - \gamma$	$\frac{i-1}{n-1}\beta - \gamma$	$\frac{\beta}{n}\frac{1-\zeta^i}{1-\zeta} - \gamma$	$\frac{\beta}{n-1}\frac{1-\zeta^{i-1}}{1-\zeta} - \gamma$
b_i	$\frac{i}{n}\beta$	$\frac{i}{n-1}\beta$	$\frac{\beta}{n}\frac{1-\zeta^i}{1-\zeta}$	$\frac{\beta}{n-1}\frac{1-\zeta^i}{1-\zeta}$
$a_i - b_i$	$-\gamma < 0$	$-\frac{\beta}{n-1} - \gamma < 0$	$-\gamma < 0$	$-\frac{\beta}{n-1}\zeta^{i-1} - \gamma < 0$
$a_i - b_{i-1}$	$\frac{\beta}{n} - \gamma$	$-\gamma < 0$	$\frac{\beta}{n}\zeta^{i-1} - \gamma$	$-\gamma < 0$
Altruism	Weak	Strong	Weak	Strong

be either shared among all players (synergy/discounting game with self-returning benefit, or SDSR game), or only among other players and excluding the donor (synergy/discounting game with self-excluding benefit, or SDSE game).

The payoffs a_i and b_i to players in these games (LSR, LSE, SDSR and SDSE) and their differences are presented in Table 2.1. For each of these games I derive the conditions for the evolution of cooperation under different migration schemes (see Section 2.3). The sign sums for each combination of game and migration mode are presented in Tables 2.2 (for self-returning games) and 2.3 (for self-excluding games).

Sign sums as functions of benefit β for different games and modes of migration are presented in Fig. 2.2. In the well mixed model, cooperation is evolutionary unsuccessful in all games ($\Lambda_0 < 0$).

For the games representing weak altruism (LSR and SDSR), cooperation may be successful in all migration modes, provided that the benefit to cost ratio is large enough. Clearly, increasing synergy in self-returning games favours cooperation.

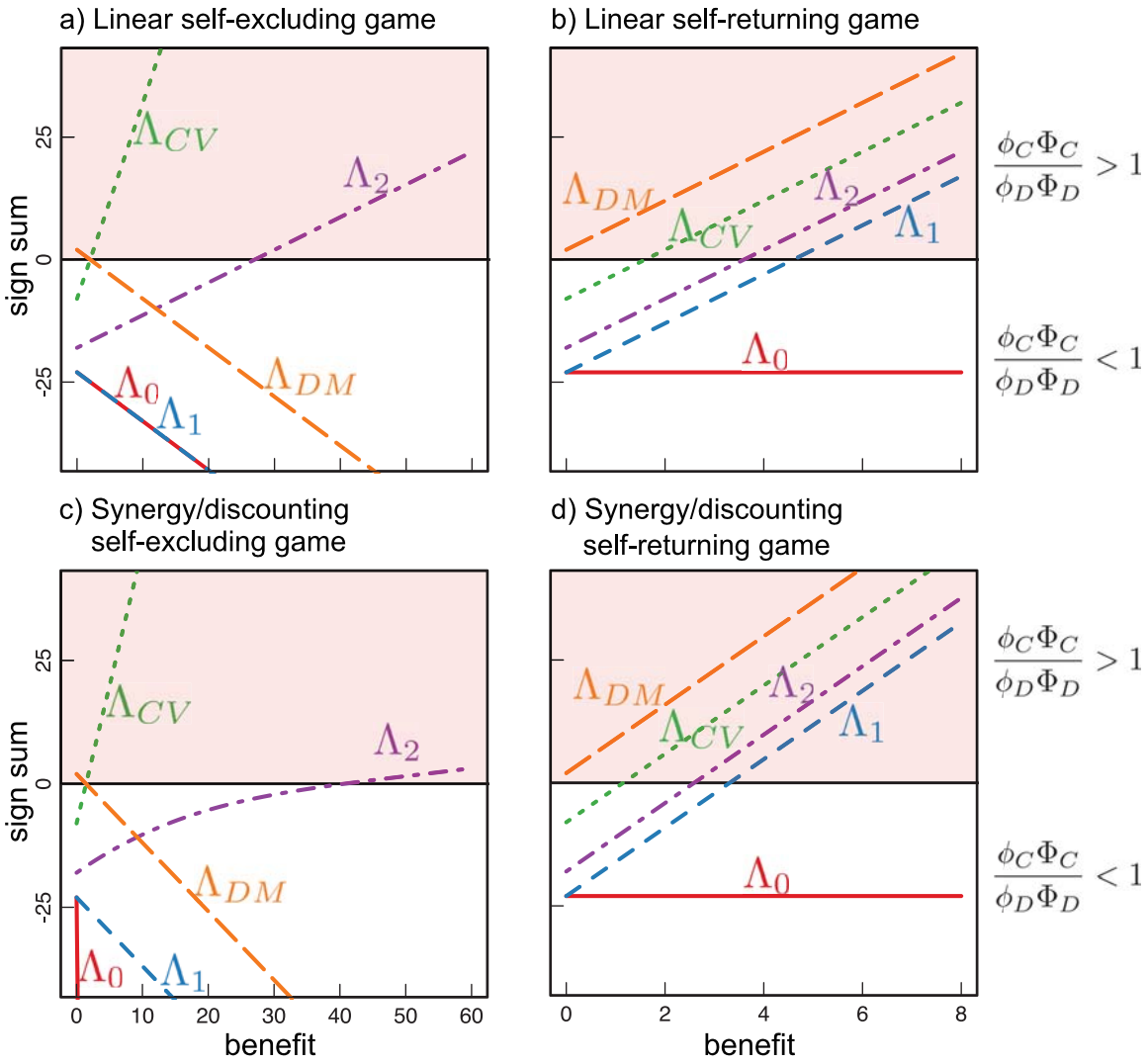

Figure 2.2: **The evolution of cooperation does not always become easier with increasing benefit β.** Cooperation is advantageous in terms of fixation probabilities if the sign sum Λ calculated for migration modes (lines) is positive (shaded region). In the well mixed case, Λ_0 decreases in self-excluding games and stays constant for self-returning games. In the single individual migration mode and the differential migration mode, cooperation becomes easier with increasing benefit in the self-returning case, but harder in the self-excluding case. In the pair migration mode and in caravan migration, cooperation becomes easier with increasing benefit for all games with the current parameter set. ($n = 24$ for the well mixed population, $m = 6$ and $n = 4$ in migration models, $\zeta = 1.35$, intensity of selection $w = 0.1$, cost of cooperation $\gamma = 1$, group migration bonus factor in differential migration mode $w^{-1}\ln(\lambda_C/\lambda_D) = 5$, colors as in Fig. 2.1).

Table 2.2: Sign sums for self-returning games (weak altruism) in a well mixed population and under different modes of migration.

	LSR	SDSR
Λ_0	$-(n-1)\gamma$	$-(n-1)\gamma$
Λ_1	$(m-1)\beta-(mn-1)\gamma$	$(m-1)\frac{\beta}{n}\frac{1-\zeta^n}{1-\zeta}-(mn-1)\gamma$
Λ_2	$(m-1)\beta-m(n-1)\gamma$	$(m-1)\frac{\beta}{n}\frac{1-\zeta^n}{1-\zeta}-m(n-1)\gamma$
Λ_{CV}	$(m-1)\beta-(m+n-2)\gamma$	$(m-1)\frac{\beta}{n}\frac{1-\zeta^n}{1-\zeta}-(m+n-2)\gamma$
Λ_{DM}	$(m-1)\left(\beta+\frac{\ln(\lambda_C/\lambda_D)}{w}\right)-(mn-1)\gamma$	$(m-1)\left(\frac{\beta}{n}\frac{1-\zeta^n}{1-\zeta}+\frac{\ln(\lambda_C/\lambda_D)}{w}\right)-(mn-1)\gamma$

Table 2.3: Sign sums for self-excluding public good games (strong altruism) in a well mixed population and under different modes of migration.

	LSE	SDSE
Λ_0	$-\beta-(n-1)\gamma$	$-\frac{\beta}{n-1}\frac{1-\zeta^{n-1}}{1-\zeta}-(n-1)\gamma$
Λ_1	$-\beta-(mn-1)\gamma$	$-\frac{\beta}{n-1}\frac{1-\zeta^{n-1}}{1-\zeta}-(mn-1)\gamma$
Λ_2	$\beta\frac{m-n}{n-1}-m(n-1)\gamma$	$-\frac{\beta}{n-1}\frac{1-\zeta^{n-1}}{1-\zeta}-(mn-1)\gamma+\frac{m-1}{w}\ln\left[\frac{1+e^{w\left(\frac{\beta}{n-1}+\gamma\right)}}{1+e^{-w\left(\frac{\beta}{n-1}\zeta^{n-2}+\gamma\right)}}\right]$
Λ_{CV}	$(m-2)\beta-(m+n-2)\gamma$	$(m-2)\frac{\beta}{n-1}\frac{1-\zeta^{n-1}}{1-\zeta}-(m+n-2)\gamma$
Λ_{DM}	$(m-1)\frac{\ln(\lambda_C/\lambda_D)}{w}-\beta-(mn-1)\gamma$	$(m-1)\frac{\ln(\lambda_C/\lambda_D)}{w}-\frac{\beta}{n-1}\frac{1-\zeta^{n-1}}{1-\zeta}-(mn-1)\gamma$

For the games representing strong altruism (LSE and SDSE), even for the individual migration mode, cooperators have no selective advantage ($\Lambda_1 < 0$). For the pair migration and caravan migration modes, strong altruism may have a selective advantage over defection and in LSE game this is possible if the benefit to cost ratio is high enough. Under differential migration strong altruism also can have a selective advantage in the LSE game. However, the prerequisites for this are restrictive: the group migration bonus factor $w^{-1}\ln(\lambda_C/\lambda_D)$ must be high enough to ensure a strong implicit advantage to cooperators. Interestingly, an increase in the benefit to cost ratio works against cooperation under this mode of migration.

At the qualitative level, the difference between linear and non-linear games from the same migration scheme are minor, with a few notable exceptions. Strongly altruistic, non-linear SDSE games, can promote cooperation in the pair migration mode at high values of benefit

β (the sign sum in this case cannot be reduced to benefit to cost ratio) only if the number of groups m is high enough (2.6.1.6). The minimal number of groups necessary for the success of cooperation for this game increases with the increase of the synergy. Therefore synergistic interactions work against cooperation success in the pair migration mode.

In the caravan migration mode, the SDSE game, similar to the linear LSE game, promotes cooperation if the benefit to cost ratio (β/γ) is high enough. However, synergy of cooperators makes cooperation successful at lower values of benefit to cost ratio than in the LSE game. Finally, in the SDSE game with differential migration, as well as in the LSE game, the advantage of cooperation depends on the group migration bonus factor, while both high benefit to cost ratio and synergy work against cooperation.

Synergy always favours cooperation in weakly altruistic self-returning games (LSR and SDSR); however, it may work against cooperation in strongly altruistic LSE and SDSE games under certain modes of migration. Intuitively, cooperation will be enhanced if the benefit provided by a cooperator is large or if there is more synergy between cooperators (larger β, larger or increasing ζ). Counterintuitively, in self-excluding games this works against cooperation (Ohtsuki 2012). Consider the prisoner's dilemma game, played by one cooperator and one defector. An increase in the amount of benefit produced by cooperator β leads only to an increase in the payoff to the defector; thereby harming cooperation. Furthermore, in a multiplayer game, an increasing ζ just provides more benefit for defectors to exploit, as it does not return benefit to the contributor. This shows that cheaper cooperation can benefit defectors.

In all four games, for all values of the benefit to cost ratio, defection is favoured (negative sign sums) in well mixed populations. This illustrates that even weak altruism is less successful than defection in the absence of population structure. The standard migration mode allows LSR and SDSR games to have a positive sign sum if the benefit to cost ratio is large enough. However, cooperators in LSE and SDSE games, being strongly altruistic are always disadvantageous, independent of the benefit to cost ratio.

2.5 Discussion

I have shown that migration, even in the absence of coordination between individuals, promotes the evolution of weakly altruistic cooperation. The single individual migration mode presented here is not based on processes that involve an entire group (Traulsen and Nowak 2006), or specific structure of groups (Libby et al. 2014). My results indicate that cooperation may emerge by means of group-level selection even if selection is conducted by the non-coordinated actions of individuals. In other words, selection on the group level can be mediated by population structure alone.

In modes where migration involves the coordinated actions of multiple individuals, cooperation can evolve in a much wider range of games than in the single individual migration mode. In the pair, caravan and differential migration modes, strong altruism can be favored. Also, in weakly altruistic games the range of parameters promoting the evolution of cooperation is extended: the domain of benefit to cost ratio with positive sign sums becomes wider than in the single individual migration mode (see Figure 2.2 panels b and d). Thus, introduction of coordination between individuals' actions substantially extends the set of conditions under which cooperation may evolve.

Throughout this manuscript, I have concentrated on the exponential payoff to fitness mapping, which allows a very compact representation of the sign sums. However, many of my results hold for more general payoff to fitness mappings (Wu et al. 2010, 2015). For example, for any mapping in which the number of emitted migrants is proportional to the reproductive output of the players within the group the single individual migration mode can favor weak altruism, but not strong altruism, see 2.6.2. This is in contrast to a scenario of a pairwise comparison process (Hauert and Imhof 2012, Hauert et al. 2014), where production of migrants moving between groups depends directly on payoffs, but the competition between types within the group depends on differences between individual payoffs.

The evolution of cooperation under the limited coordination of individuals' actions may have particular importance for understanding early stages of the evolution of multicellularity. While details remain unclear, there is general agreement that the earliest stages involved

the evolution of simple, undifferentiated groups of cooperating cells (Velicer and Yuen-tsu 2003, Rainey and Rainey 2003, Pfeiffer and Bonhoeffer 2003, Aledo 2008, Koschwanez et al. 2013, Hammerschmidt et al. 2014). In theoretical models of the evolution of cooperation, the mechanistic details surrounding the re-distribution of individuals among groups are often overlooked. Two broad kinds of group formation are generally considered: groups originating from growth of a single individual, referred to as "staying together", and groups formed by aggregation of individuals, referred to as "coming together" (Tarnita et al. 2013). An example of the "staying together" mode is fragmentation (Traulsen and Nowak 2006), as found in the algae *Gonium pectorale* (Stein 1958). The "coming together" mode is utilized by slime molds (Bonner 1959) and in trait group models (Wilson 1975). Multiple individual modes of group formation can be constructed within these two kinds (Wilson 1975, Avilés 2002, Pfeiffer and Bonhoeffer 2003, Traulsen and Nowak 2006, Powers et al. 2011, Garcia and De Monte 2013, Libby and Rainey 2013, Simon et al. 2013, Tarnita et al. 2013), including those in which 'staying together' is combined with migration events that establish new groups (Rainey and Kerr 2010, Libby and Rainey 2013, Ratcliff et al. 2013a, Hammerschmidt et al. 2014). From a mechanistic point of view, modes of individual assignment, considered in the previous paragraph, are typically assumed to arise by the coordinated actions of multiple individuals in the group. However, early cellular groups were most likely unable to act as a single coordinated unit, and as such recurrence of these groups was presumably conducted by unregulated actions of individual cells (De Monte and Rainey 2014).

Based on my results, one can perform a classification of multilevel selection models based on the level of complexity of the interactions between groups. The first class consists of models in which processes between groups are mediated by a single individual, such as the single individual migration mode and metapopulation models (Eshel 1972, Hui and McGeoch 2007). As shown here, these kinds of models can promote weak altruism, but not strong altruism. The second class of models are those in which between-group processes involve several individuals, or even whole groups. Examples include the pair, caravan and differential migration modes, and also the splitting of whole groups (Traulsen and Nowak 2006). In

the context of the early stages of the evolution of multicellularity, the first class of models likely have particular importance, as the multi-individual actions of the second class generally require coordinated activity, which might not be available for early groups.

2.6 Appendix

2.6.1 Derivation of sign sums

2.6.1.1 Derivation of Λ_0

The fixation probability for one individual of the two strategies in a well mixed population is equal to (Nowak 2006a, Traulsen and Hauert 2009)

$$\begin{aligned} \phi_C &= \frac{1}{1+\sum_{j=1}^{n-1}\prod_{i=1}^{j}\frac{e^{wb_i}}{e^{wa_i}}} \\ \phi_D &= \frac{1}{1+\sum_{j=1}^{n-1}\prod_{i=1}^{j}\frac{e^{wa_{n-i}}}{e^{wb_{n-i}}}}. \end{aligned} \tag{2.17}$$

The ratio of these fixation probabilities is

$$\frac{\phi_C}{\phi_D} = \prod_{i=1}^{n-1}\frac{e^{wa_i}}{e^{wb_i}} = e^{w\sum_{i=1}^{n-1}(a_i-b_i)} = e^{w\Lambda_0}. \tag{2.18}$$

Here, $\Lambda_0 = \sum_{i=1}^{n-1}(a_i - b_i)$ is the sign sum for a well mixed population, as stated previously, for example by Kurokawa and Ihara (2009) and Gokhale and Traulsen (2010).

2.6.1.2 Derivation of Λ_1

For group structure and small migration rates, the trait of interest first needs to fix in a group (ϕ_C) and then that group needs to fix in the population (Φ_C). The total fixation probability ratio is thus equal to $\frac{\Phi_C}{\Phi_D}\frac{\phi_C}{\phi_D}$ (Traulsen and Nowak 2006). Here $\frac{\phi_C}{\phi_D}$ is calculated according to

Eq. (2.18). The ratio $\frac{\Phi_C}{\Phi_D}$ is calculated as

$$\frac{\Phi_C}{\Phi_D} = \prod_{j=1}^{m-1} \frac{ne^{wa_n}\lambda\phi_C}{ne^{wb_0}\lambda\phi_D} = \prod_{j=1}^{m-1} \left(\frac{e^{wa_n}}{e^{wb_0}} e^{w\Lambda_0} \right) = e^{w(m-1)(a_n - b_0 + \Lambda_0)}. \tag{2.19}$$

Therefore the total fixation probability ratio is

$$\frac{\phi_C}{\phi_D}\frac{\Phi_C}{\Phi_D} = e^{w\Lambda_0} e^{w(m-1)(a_n - b_0 + \Lambda_0)} = e^{w((a_n - b_0)(m-1) + m\sum_{i=1}^{n-1}(a_i - b_i))}. \tag{2.20}$$

Thus, the sign sum for the single individual migration mode is

$$\Lambda_1 = (a_n - b_0)(m-1) + m\sum_{i=1}^{n-1}(a_i - b_i). \tag{2.21}$$

2.6.1.3 Derivation of Λ_2

In the pair migration mode, the individual-level fixation probabilities are different from the single individual migration mode because the initial state of the group with mixed composition after accepting a migrant is $n-2$ players of the base type and two players of the invading type. Therefore, the fixation probabilities are not equal to the ones presented in Eq. (2.17). According to Nowak (2006a), the fixation probabilities ϕ^i for an initial number of i individuals solves the recurrence equation

$$\phi^i = \phi^i(1 - T^{i+} - T^{i-}) + \phi^{i-1}T^{i-} + \phi^{i+1}T^{i+}. \tag{2.22}$$

Here $T^{i+} = ...$ and $T^{i-} = ...$ are probabilities to increase or decrease the number of players with a chosen strategy if there are currently i players. Because $\phi^0 = 0$, ϕ^2 is

$$\phi_C^2 = \phi_C^1 \left(1 + \frac{T^{1-}}{T^{1+}}\right) = \phi_C^1 \left(1 + e^{-w(a_1 - b_1)}\right) \tag{2.23}$$

$$\phi_D^2 = \phi_D^1 \left(1 + \frac{T^{(n-1)+}}{T^{(n-1)-}}\right) = \phi_D^1 \left(1 + e^{w(a_{n-1} - b_{n-1})}\right). \tag{2.24}$$

Therefore, the ratio of individual-level fixation probabilities in the pair migration mode is

$$\frac{\phi_C^2}{\phi_D^2} = \frac{\phi_C^1}{\phi_D^1}\frac{1+e^{-w(a_1-b_1)}}{1+e^{w(a_{n-1}-b_{n-1})}} = \exp\left[w\Lambda_0 + \ln\left[\frac{1+e^{-w(a_1-b_1)}}{1+e^{w(a_{n-1}-b_{n-1})}}\right]\right]. \tag{2.25}$$

The total ratio of fixation probabilities (taking into account that the invading strategy starts with one player in the first group, and with two players in all following migration invasions) is

$$\frac{\phi_C^1}{\phi_D^1}\frac{\Phi_c}{\Phi_d} = e^{w\left((a_n-b_0)(m-1)+m\sum_{i=1}^{n-1}(a_i-b_i)+(m-1)\frac{1}{w}\ln\left[\frac{1+e^{-w(a_1-b_1)}}{1+e^{w(a_{n-1}-b_{n-1})}}\right]\right)} \tag{2.26}$$

and the sign sum is

$$\Lambda_2 = (a_n-b_0)(m-1) + m\sum_{i=1}^{n-1}(a_i-b_i) + (m-1)\frac{1}{w}\ln\left(\frac{1+e^{-w(a_1-b_1)}}{1+e^{w(a_{n-1}-b_{n-1})}}\right). \tag{2.27}$$

2.6.1.4 Derivation of Λ_{CV}

In the caravan migration mode with large p, the probability of successful invasion of one group into another is equal to 1. Therefore, the ratio of group-level fixation probabilities is

$$\frac{\Phi_C}{\Phi_D} = \prod_{j=1}^{m-1}\frac{ne^{wa_n}\lambda}{ne^{wb_0}\lambda} = e^{w(a_n-b_0)(m-1)}. \tag{2.28}$$

This way the total fixation probabilities ratio is

$$\frac{\phi_C}{\phi_D}\frac{\Phi_C}{\Phi_D} = e^{w\Lambda_0}e^{w(a_n-b_0)(m-1)} = e^{w((a_n-b_0)(m-1)+\sum_{i=1}^{n-1}(a_i-b_i))} \tag{2.29}$$

and the sign sum in the caravan migration mode is

$$\Lambda_{CV} = (a_n-b_0)(m-1) + \sum_{i=1}^{n-1}(a_i-b_i). \tag{2.30}$$

2.6.1.5 Derivation of Λ_{DM}

In the differential migration mode, the groups have control over the migration probabilities of the players. This affects the fixation probabilities at the group level. The migration probabilities no longer cancel,

$$\frac{\Phi_C}{\Phi_D} = \prod_{j=1}^{m-1} \frac{ne^{wa_n}\lambda_C\phi_C}{ne^{wb_0}\lambda_D\phi_D} = \prod_{j=1}^{m-1} \left(\frac{e^{wa_n}}{e^{wb_0}} e^{w\Lambda_0 + \ln\left(\frac{\lambda_C}{\lambda_D}\right)} \right) = \exp\left[w(m-1)\left(a_n - b_0 + \Lambda_0 + \frac{1}{w}\ln\left(\frac{\lambda_C}{\lambda_D}\right)\right)\right. \tag{2.31}$$

Therefore, the total fixation probability ratio is

$$\frac{\phi_C}{\phi_D}\frac{\Phi_C}{\Phi_D} = e^{w(m-1)\left(a_n - b_0 + \Lambda_0 + \frac{1}{w}\ln\left(\frac{\lambda_C}{\lambda_D}\right)\right) + w\Lambda_0} \tag{2.32}$$

and the sign sum becomes

$$\Lambda_{DM} = \left(a_n - b_0 + \frac{\ln\left(\frac{\lambda_C}{\lambda_D}\right)}{w} \right)(m-1) + m\sum_{i=1}^{n-1}(a_i - b_i). \tag{2.33}$$

2.6.1.6 The SDSE game in the pair migration mode

The sign sum for the SDSE game in the pair migration mode is:

$$\Lambda_2^{SDSE} = -\frac{\beta}{n-1}\frac{1-\zeta^{n-1}}{1-\zeta} - \gamma(mn-1) + \frac{m-1}{w}\ln\left[\frac{1+e^{w\left(\frac{\beta}{n-1}+\gamma\right)}}{1+e^{-w\left(\frac{\beta}{n-1}\zeta^{n-2}+\gamma\right)}}\right]. \tag{2.34}$$

If benefit β is high enough $\left(\beta \gg n-1, \beta \gg \frac{n-1}{\zeta^{n-1}}\right)$, then the sign sum approaches

$$\Lambda_2^{SDSE} \approx \frac{\beta}{n-1}\left(m - 1 - \frac{1-\zeta^{n-1}}{1-\zeta}\right) - \gamma m(n-1). \tag{2.35}$$

Therefore, the sign sum is positive at high benefit values, if the number of groups m is high enough: $m > 1 + \frac{1-\zeta^{n-1}}{1-\zeta}$. In the case of the discounting game ($\zeta < 1$), this condition is more restrictive than $m \geq 2$, which is always required in multilevel selection models.

2.6.2 Other payoff to fitness mappings

Strong altruism is at a disadvantage in the single individual migration mode, when I use the exponential payoff to fitness mapping (Traulsen et al. 2008). Here I show that this result holds true with any mapping.

In terms of fitness, strong altruism is characterized by two properties:

1. If the number of cooperative players increases, the payoffs of all players increase. That is $f_a(i) < f_a(i+1)$ and $f_b(i) < f_b(i+1)$, where $f_a(i)$ ($f_b(i)$) is the fitness of cooperators (defectors) in a group with i cooperators.

2. If a player switches from defection to cooperation, their payoff decreases. That is $f_a(i) < f_b(i-1)$.

The ratio of fixation probabilities in the structured population is given by $\frac{\phi_c}{\phi_d} \cdot \frac{\Phi_c}{\Phi_d}$ (Traulsen and Nowak 2006). I calculate each term separately.

The ratio of fixation probabilities of a single cell in a group of opposite composition (Karlin and Taylor 1975, Nowak 2006a) is

$$\frac{\phi_C}{\phi_D} = \prod_{i=1}^{n-1} \frac{f_a(i)}{f_b(i)}. \tag{2.36}$$

The ratio of fixation probabilities of a single group in a population of opposite composition is

$$\frac{\Phi_C}{\Phi_D} = \prod_{j=1}^{m-1} \frac{n f_a(n) \lambda \phi_C}{n f_b(0) \lambda \phi_D} = \left(\frac{f_a(n)}{f_b(0)} \prod_{i=1}^{n-1} \frac{f_a(i)}{f_b(i)} \right)^{m-1}. \tag{2.37}$$

Combining Eqs. (2.36) and (2.37) I get the ratio of fixation probabilities of a single cell in a population of opposite composition:

$$\frac{\phi_C \Phi_C}{\phi_D \Phi_D} = \prod_{i=1}^{n-1} \frac{f_a(i)}{f_b(i)} \cdot \left(\frac{f_a(n)}{f_b(0)} \prod_{i=1}^{n-1} \frac{f_a(i)}{f_b(i)} \right)^{m-1} = \frac{f_b(0)}{f_a(n)} \cdot \left(\frac{f_a(n)}{f_b(0)} \prod_{i=1}^{n-1} \frac{f_a(i)}{f_b(i)} \right)^{m}. \tag{2.38}$$

Expression in parenthesis can be rewritten:

$$\frac{f_a(n)}{f_b(0)}\prod_{i=1}^{n-1}\frac{f_a(i)}{f_b(i)} = \frac{f_a(n)\prod_{i=1}^{n-1} f_a(i)}{f_b(0)\prod_{i=1}^{n-1} f_b(i)} = \frac{\prod_{i=1}^{n} f_a(i)}{\prod_{i=0}^{n-1} f_b(i)} = \prod_{i=1}^{n}\frac{f_a(i)}{f_b(i-1)}. \tag{2.39}$$

Thus, the fixation probabilities ratio is equal to

$$\frac{\phi_C\Phi_C}{\phi_D\Phi_D} = \underbrace{\frac{f_b(0)}{f_a(n)}}_{<1}\cdot\left(\prod_{i=1}^{n}\underbrace{\frac{f_a(i)}{f_b(i-1)}}_{<1}\right)^m < 1. \tag{2.40}$$

So, the inability of the strong altruism to emerge in a single individual migration mode holds true for all possible payoff to fitness mappings.

Chapter 3

Fitness correlation as a new indicative metric of Darwinian individuality

3.1 Introduction

The emergence of multicellularity from unicellular forms is a significant event in the evolution of life. From the outset unicellular ancestors participated in the process of evolution by natural selection. This was possible because each cell was a Darwinian individual, that is, it exhibited the following characteristics: variation in phenotype, differential reproduction of individual units and heredity of their properties (Lewontin 1970). In some instances single cells formed collectives. On a number of occasions, in about 20 cases (Bonner 1998), these collectives become Darwinian individuals in their own right, i.e. they become multicellular organisms (Figure 3.1). Although the precise transition events are unclear, mechanisms details and selective processes are currently the subject of experimental (Rainey and Rainey 2003, Ratcliff et al. 2012, Hammerschmidt et al. 2014) and theoretical analysis (Libby and Rainey 2013, Shelton and Michod 2014).

Transitions in Darwinian individuality – from cells to collectives – are central to the evolution of multicellular organisms. A population prior to a transition consists of unicellular life forms that by virtue of Darwinian properties (variation, reproduction and heredity) par-

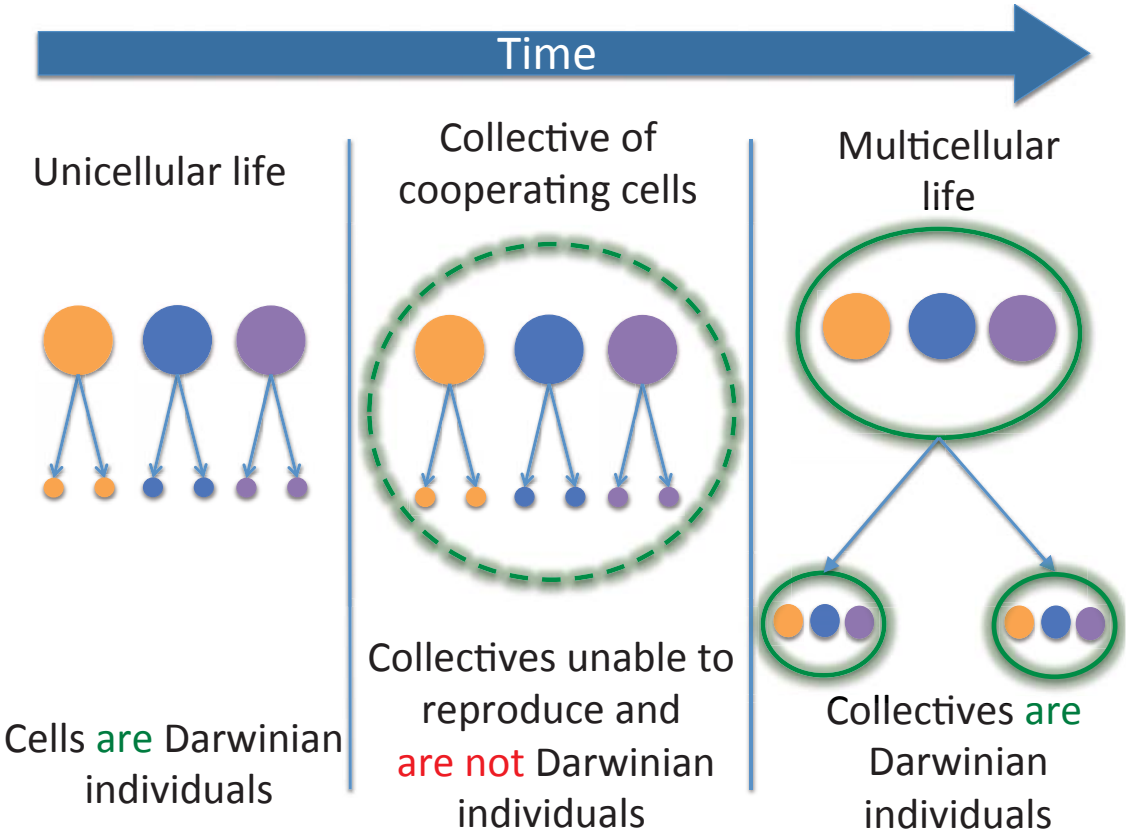

Figure 3.1: **The evolution of multicellularity from the single cells.** Left hand panel: ancestral cells are Darwinian individuals. Cells within the population vary, reproduce, and, with the exception of the occasional mutation, offspring resemble parental types. Such cells are Darwinian individuals and members of Darwinian populations. Middle panel: collectives are formed from individual cooperating cells but newly formed collectives have no inherent capacity for collective-level reproduction the collective thus lacks a crucial Darwinian property. Right hand panel: collectives are replete with the same Darwinian properties as evident in the single cells shown in the left hand panel and are thus Darwinian individuals and members of Darwinian populations.

ticipate in the process of evolution by natural selection. The final stage, after the transition, is a multicellular life form that participates directly in its own right – in the process of evolution by natural selection[1]. However, the intermediary stages – during which collective level Darwinian properties emerge – are not well understood: neither the properties of the intermediate forms, nor the ecological and evolutionary conditions that promote transitions in individuality.

Before it is possible to investigate the causes of a given transition in individuality, a method for detecting Darwinian individuality at the collective level is necessary. Existing approaches for detection of Darwinian individuality are either unreliable or operate only on a limited range of populations.

A number of approaches (Okasha 2006) attempt to identify signatures of selection operating at the level of collectives and then use them to infer whether collectives posses Darwinian properties. The Price equation approach (Price 1970, 1972, 1995) calculates the collective-level component of selection as the covariance between collective level fitness and particle level traits (see equation 1.1 in chapter 1). Contextual analysis (Heisler and Damuth 1987) performs a linear regression of particle fitnesses with respect to two variables: the particle's trait and the average trait in the collective (see equation 1.2 in chapter 1). The latter component shows the impact of collective-level characters on particle fitness and, consequently, on change in the trait due to natural selection at the collective level (see equation 1.3 in chapter 1). Each of these approaches shows how change in the value of a given trait can be decomposed into particle-level and collective-level selection terms.

However, evidence of collective-level selection is not a reliable indicator of transitions in individuality. For example, a group-structured population, evolving with limited migration between groups (e.g., the single individual migration mode considered in Ch 2), experiences selection at the collective level but does not manifest collective-level Darwinian properties. In this mode, each newborn particle has a small chance to migrate to a new randomly cho-

[1]Some species may be considered as a multicellular organisms but do not exhibit Darwinian properties in the full extent. As such, these organisms are only marginal Darwinian individuals (reviewed in (Godfrey-Smith 2009)).

sen collective. Collectives consisting of cooperators produce more migrants and, therefore, are more successful than collectives of defectors. With this migration mode, collective level selection exists; however, collectives themselves do not participate directly in the process of evolution by natural selection: they are nothing more than compartments containing reproducing particles. Therefore, the existence of selection at the collective level, detected by covariance and contextual approaches, need have nothing to do with the emergence of Darwinian properties at the level of collectives.

Another approach to detect the emergence of Darwinian properties was proposed by Michod and Roze (1999). As a collective evolves to become an evolutionary unit, its success relies more on the interactions between parts of the collective rather than the individual performance of the parts. Therefore, at final stages of evolutionary transitions to multicellularity, collective fitness is likely to be affected by functions of particles other than those that contribute to the particle fitness. When this happens, particle and collective fitnesses become independent characteristics of collective; in other words, fitnesses begin to decouple. If this assumption is true, then fitness decoupling may be a useful hallmark of the transition of individuality from cells to multicellular organisms[2].

To assess the degree to which a given transition in individuality has proceeded, a formal measure of fitness decoupling is required. For populations in which a transition in individuality is achieved by the development of reproductive division of labour, Michod et al (2006) proposed MVSHN[3] index as a method to measure fitness decoupling. In such populations, fitness decoupling can be characterized by the level of the development of reproductive division of labour. MVSHN is equal to the difference between collective fitness and average particle fitness in this collective. This difference is equal to zero in a population without germ-soma distinction but increases with the development of reproductive division of labour (Michod et al. 2006). Thus, if the transition in individuality occurs via development of a reproductive division of labour, then the MVSHN index can be used as an indicator of fitness

[2]In principle, Darwinian individuality at the collective-level may not exhibit fitness decoupling. However, the evolution of such a population would be indistinguishable from the evolution of a population where selection acts exclusively at the particle level. See discussion section for details.

[3]MVSHN is an acronym for original authors names: Michod, Viossat, Solari, Hurand and Nedelcu.

decoupling.

However, in the general case, Darwinian individuality may, in principle, be obtained by collectives that reproduce by different mechanisms. One can imagine a species reproducing by budding, without sexual reproduction. Such an organism is multicellular but lacks a germ-soma differentiation. In this case the MVSHN index is unable to detect fitness decoupling were in fact it to have occurred. Therefore, a more general method for detecting fitness decoupling would be useful.

In this chapter I consider fitness decoupling as a possible hallmark of the transition in individuality. I propose a formal method for the measurement of fitness coupling based on the shape of the co-distribution of particle and collective level fitnesses. This I refer to as the fitness correlation metric (FCM) and is described in section 3.2. This makes it possible to distinguish between populations at different stages of a transition in individuality where the presence/absence of fitness decoupling is not intuitively clear. I test the FCM and then apply it to outline selective conditions promoting fitness decoupling in section 4.3. In the Discussion (section 4.4) I return to the topic of reliability of the proposed method, consider possible applications of it and review several examples of models, which provide counter intuitive results when treated with other methods.

3.2 Method for detecting fitness decoupling

Fitness decoupling can be detected by the co-distribution of particle and collective[4] fitnesses. In a population with coupled fitnesses, high particle fitness of a collective means high collective fitness because evolutionary success of the collective, prior to the transition in individuality, is determined by the number of particles produced. Thus, coupled particle and collective fitnesses are highly correlated. By contrast when fitnesses become decoupled, collective fitness is no longer dependent on the fitness of particles but instead depends of the capability of particles to perform tasks needed for the reproduction of a collective as a whole. In this

[4]The measurement of collective fitness for primitive collectives is discussed in the section 3.4.1

case, high average particle fitness does not determine high collective fitness, therefore, the correlation between particle and collective fitness is low. The fitness co-distribution can be characterized and thus used to detect fitness decoupling.

To detect fitness decoupling, I propose the fitness correlation metric (FCM) as a covariation coefficient between collective and particle fitnesses in the population[5]:

$$\text{FCM} = \frac{\text{Cov}(F_P, F_C)}{\sigma(F_P)\sigma(F_C)} = \frac{\langle\, (F_P - \langle F_P \rangle)(F_C - \langle F_C \rangle)\,\rangle}{\sqrt{\langle\, (F_P - \langle F_P \rangle)^2\,\rangle}\sqrt{\langle\, (F_C - \langle F_C \rangle)^2\,\rangle}} \tag{3.1}$$

Here F_P is a particle fitness averaged within collectives, F_C is a collective fitness, $\text{Cov}(F_P, F_C)$ is a covariation of particle and collective level fitnesses in the population, $\sigma(F)$ is a variation of fitness in the population and $\langle x \rangle$ is the mean value of x where averaging is performed over all collectives in the population.

To illustrate that populations with different degrees of the fitness decoupling may have different FCM, I provide a set of examples. These examples are designed to explain the idea of FCM, so they present my method in the best light. Less apparent and more problematic scenarios are considered in the Discussion (section 3.4.2).

The first example illustrates a case where fitness of collectives and particles are directly coupled. Consider a population where particles are nested into distinct collectives but the fitness of each particle depends only on the internal characteristics of the particle. When collectives accumulate a critical number of particles, they split into two smaller collectives. These collectives can be considered as collective-level offspring, and thus, the fitness of a collective in this example is determined by the frequency of splitting. Collectives containing rapidly reproducing particles split often, i.e., they have high collective fitness. In this example, any increase in the fitness of the particle also increases the fitness of the collective. The resulting co-distribution of fitnesses is presented in the left panel on of Fig. 3.2. Here particle and collective fitnesses are highly correlated, and therefore, express FCM close to 1.

The second example illustrates a scenario in which fitnesses of particles and collectives

[5]Alternatively, the Spearman rank coefficient may be used instead of the Pearson covariation coefficient. However, the Pearson correlation provides nice analytical properties to FCM, so I use Pearson coefficient in this thesis.

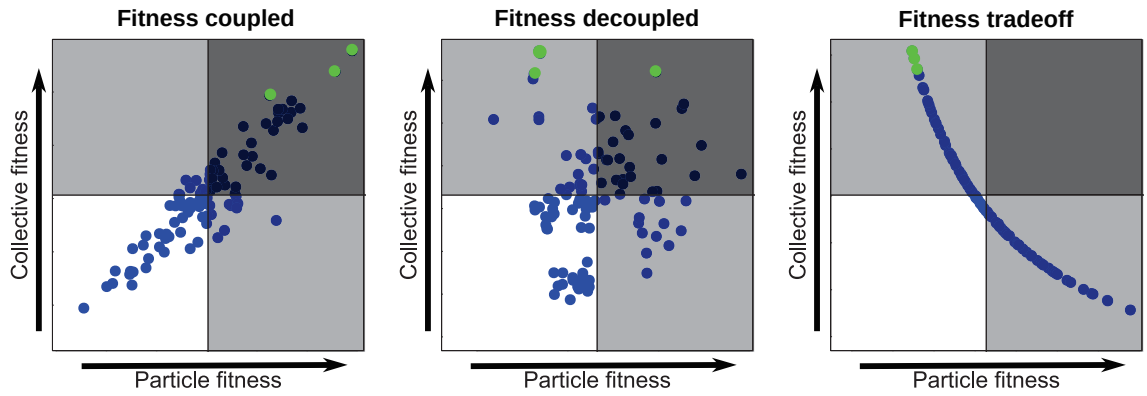

Figure 3.2: **Distributions of particle and collective fitnesses in populations with different degrees of fitness decoupling.** Each point represents one collective in a population. Left panel: fitnesses are coupled. The top right quadrant (both fitnesses are high) and bottom left quadrant (both fitnesses are low) contain the majority of collectives. Middle panel: fitnesses are decoupled. All quadrants are approximately equally abundant. Right panel: fitness tradeoff. The top left and bottom right quadrants (one fitness is high and another is low) gather most of the collectives. Presented distributions were obtained from simulations by models presented in Appendix 3.5.1. To illustrate that the MVSHN index is subjected to the sample noise, three collectives with the highest collective fitness are highlighted (see main text).

are independent of each other. Consider a population where a collective of particles divides on some internal signal, which does not correlate with the size of the collective. In this case, collective level fitness is determined by the frequency of the signal and is independent of particle level fitness. The fitnesses co-distribution is presented in the middle panel on of Fig. 3.2. Here particle and collective fitnesses are non-correlated, and therefore, express FCM close to 0.

The third example illustrates the case of the fitnesses tradeoff. Consider a population where a collective divides in two only after a certain level of resource is accumulated in a commonly accessible pool. At the same time, this resource can be used by particles for their own reproduction. Each particle within this collective has a choice either to invest its resource into the collective pool or to spend this resource on its own reproduction. The higher the number of investing particles the greater the number of collective-level offspring but this decreases the number of particles in the organism. Therefore, an increase in fitness at one level results in a reduction in fitness at another. The fitnesses co-distribution is presented in the right panel on of Fig. 3.2. Here particle and collective fitnesses are anti-correlated, and therefore, express FCM close to -1.

These examples represent populations with different degrees of fitness decoupling. The different degrees of fitness decoupling correspond to different shapes of the co-distribution of fitnesses. The FCM characterizes particle and collective fitness co-distributions and therefore, the FCM can be used to detect fitness decoupling.

The proposed FCM metric deals with two of Lewontin's (1970) properties: reproduction and variation, leaving heredity aside. The ability to reproduce is accounted for by consideration of fitness – the numerical characteristic of reproduction. Variation among members of the population plays a role in calculation of the (co-)variations of fitnesses in Eq. 3.1. The FCM value says nothing about the similarity between progenitor and offspring groups. Other methods, including Price equation, contextual approach and MVSHN index, also fail to account for heredity.

The MVSHN index (Eq. 3.2) can be calculated for these examples as well. However,

MVSHN index takes into account only one collective in a population – one with the highest collective fitness, and as such its value is subjected to sampling noise, especially in the case of decoupled fitnesses. To illustrate this, the three collectives with the highest collective fitness are highlighted in Fig. 3.2. On the middle panel, representing decoupled fitnesses, the collective with the highest collective fitness is located at the top left quadrant, and has collective fitness much larger than particle fitness. However, if this collective were not detected, or had a lower collective fitness, then the MVSHN index would have been calculated using the second-best group in the top right quadrant. In this case, the particle and collective fitness would be much closer to each other and MVSHN index would be much lower. In order to ensure the accuracy of the MVSHN index, it is necessary to know that the collective used for the calculation of MVSHN index has the highest collective fitness possible in this population. The FCM takes into account the whole population and therefore, is much less susceptible to the sampling noise.

3.3 Results

In section 3.3.1, I test the ability of FCM to correctly detect fitness decoupling in a population where another method of detection has been already developed. To do so, I calculated FCM in a model population with a reproductive division of labour and compared obtained FCM values with the MVSHN index. I show that in the model population, both metrics provide similar assessment of the fitness (de-)coupling state. These results indicate that FCM is a reasonably accurate representation of the transition in individuality for a population in which such a transition occurs by means of a reproductive division of labour.

In the section 3.3.2 I applied FCM to the more general case of a population subjected to multilevel selection but which does not necessarily possess a reproductive division of labour and thus cannot be characterized by MVSHN index. To find the conditions that promote the fitness decoupling, I constructed a phenomenological model of a population under weak multilevel selection. I found the combinations of the selective conditions and distribution of

traits that promote fitness decoupling.

Since the distribution of traits may change in the course of evolution, I investigated how this change may alter the fitness (de-)coupling state. In the section 3.3.3, I performed a simulation of multilevel selection and measured the dynamics of the FCM in populations with different distributions of traits. I found that over a sufficiently long time period, the initial distribution of traits does not affect the resulting FCM. Therefore, the fitness (de-)coupling state, achieved by the population in the long run, is determined by the selective conditions alone.

3.3.1 Comparison of FCM and MVSHN indices in a model population with reproductive division of labour.

FCM is able to detect fitness decoupling in a wide range of populations, including populations with reproductive division of labour. In such populations, the MVSHN index is applicable to detect fitness decoupling (Michod et al. 2006, Bossert et al. 2013). In this section I found that values of both metrics are highly correlated with each other in a wide range of populations. Therefore, the FCM and MVSHN index similarly identify the fitness (de-)coupling state in a population with reproductive division of labour.

The MVSHN index was developed for populations with reproductive division of labour between cells: some cells specialize in viability (soma) and some cells specialize in fertility (germ) (Michod et al. 2006). The MVSHN index is defined as the difference between collective fitness (F_C) and average particle fitness (F_P), calculated in a collective with the highest collective fitness:

$$\text{MVSHN} = \max_{F_C}(F_C - F_P) \tag{3.2}$$

A positive value of MVSHN index indicates fitness decoupling, while a value of zero indicates the absence of it.

To test the agreement between the FCM and MVSHN, I constructed a model population

based on that used previously by Michod et al. (2006). I used the constructed model to generate a set of populations with various degrees of division of labour and under various selective conditions. For each population, I measured values of both metrics and analysed their correlation.

3.3.1.1 Model of population with reproductive division of labour

I consider a population of particles nested in collectives. Following the original work of Michod et al (2006), particles possess two traits: fertility b and viability v. The population contains particles of three types: completely specialized germ, completely specialized soma and non-specialized particles. Soma particles have zero fertility and a unit viability: $b = 0$, $v = 1$, germ particles have a unit fertility and zero viability: $b = 1$, $v = 0$, non-specialized particles have both at the intermediary level: $b = b_N$, $v = v_N$, $0 < b_N < 1$, $0 < v_N < 1$.

Michod et al (2006) considered collectives with equal number of germ and soma particles, however, in a given arbitrary case, the fraction of particles assigned to soma and germ may be different. Thus, collective composition is characterized by the level of specialization $L = G + S$ and asymmetry of specialization $A = \frac{G-S}{G+S}$, here G, S and N are the fractions of germ, soma and non-specialized particles, respectively. The level of specialization (L) indicates the total fraction of specialized particles and asymmetry of specialization (A) indicates the prevalence of germ particles over soma particles.

Particle fitness (F_P) is equal to the product of particle fertility and viability. The collective fitness (F_C) is a product of collective fertility and viability. Following (Michod et al. 2006), collective fertility is the average particle fertility in the collective and collective viability is the average particle viability. Thus, the collective fitness and average particle fitness in a given collective are:

$$\begin{aligned} F_P &= \langle vb \rangle = (1 - L)v_N b_N \\ F_C &= \langle v \rangle \langle b \rangle = \left((1 - L)b_N + \frac{L + LA}{2}\right)\left((1 - L)v_N + \frac{L - LA}{2}\right) \end{aligned} \tag{3.3}$$

Here F_P and F_C are particle and collective fitness respectively, v_S and v_N are viabilities

of somatic and non-specialized particles, b_G and b_N are fertilities of germ and non-specialized particles, L is level of specialization in a collective and A is asymmetry of specialization in a collective. The averaging is performed across all particles in a collective.

Unlike the original model of Michod et al (2006), I considered a population, which contains collectives of various particle composition. Thus, the population as a set of collectives is characterized by the distribution of collective parameters: level of specialization (L) and asymmetry of specialization (A). In my model, the level of specialization belongs to a normal distribution with mean μ_L and variance σ_L, truncated at 0 and 1. The asymmetry of specialization belongs to a normal distribution with mean μ_A and variance σ_A, truncated at -1 and 1. Therefore, the arbitrary population is characterized by six parameters: average level and asymmetry of specialization within collectives (μ_L and μ_A), variance of level and asymmetry of specialization between collectives (σ_L and σ_A), and fertility and viability of non-specialized particles (b_N and v_N).

The population set used to test the performance of the FCM contained $10,000$ populations possessing different values of six parameters $(\mu_L, \mu_A, \sigma_L, \sigma_A, b_N, v_N)$. The values of these parameters was randomly and independently chosen from uniform distributions: $\mu_L \in U(0,1)$, $\mu_A \in U(-1,1)$, $\sigma_L \in U(0,1)$, $\sigma_A \in U(0,1)$, $b_N \in U(0,1)$ and $v_N \in U(0,1)$ where $U(x,y)$ is a uniform distribution between x and y. The limits of distributions was chosen to cover biologically meaningful parameter values. Each population contained 100 collectives. The FCM and MVSHN index were calculated for each population according to Eq. 3.1 and Eq. 3.2, respectively.

3.3.1.2 Comparison of FCM and MVSHN indices

The obtained MVSHN and FCM values are highly correlated $\mathrm{Cov}(\mathrm{FCM}, \mathrm{MVSHN}) = 0.83$, as presented in the Fig. 3.3. High correlation between two metrics indicates that under this model the FCM provides a similar numerical characterization of the population as the MVSHN index.

Michod et al (2006) indicated the criterion of the transition in individuality in this model

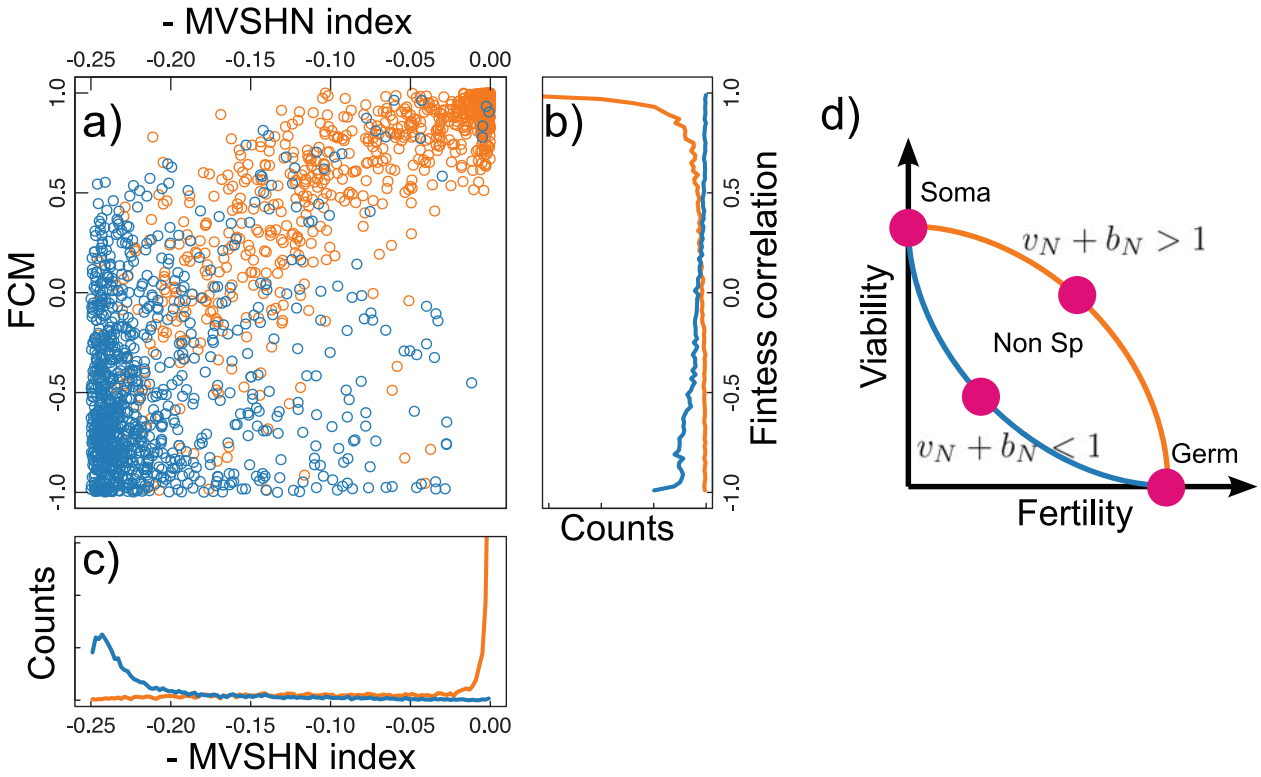

Figure 3.3: **Relation between the MVSHN index and the FCM in a model where a transition in individuality is achieved by a division of reproductive labour.** a) Co-distribution of the negative MVSHN index and the FCM among populations with various parameters (see details in the text). Values of the MVSHN index and the FCM are significantly correlated Cov(FCM, MVSHN)$= 0.83$. Blue circles represent populations with convex tradeoffs between fertility and viability ($v_N + b_N < 1$) that promote transition in individuality by means of division of labour. Orange circles represent populations with concave tradeoffs between fertility and viability ($v_N + b_N > 1$) that limit the possibility of a transition in individuality. 2000 populations out of 10000 are shown. b) The distribution of the FCM among populations with convex (blue) and concave (orange) tradeoffs. Populations under selective conditions preventing transition in individuality are mainly clustered near the point FCM $= 1$. Populations under selective conditions promoting transition in individuality have predominantly negative FCM. c) Distribution of MVSHN index among populations with convex (blue) and concave (orange) tradeoffs. Populations evolving under selective conditions that limits the chance of a transition in individuality are mainly clustered near the point MVSHN$= 0$. Populations under selective conditions promoting transitions in individuality have significant non-zero MVSHN indices. d) Viability v and fertility b of specialized and non-specialized particles (purple dots) under convex (blue) and concave (orange) tradeoffs.

– the nature of the tradeoff between fertility b and viability v. With a convex tradeoff, collectives containing specialized particles have higher collective fitness than collectives composed of non-specialized particles. In this case, a division of labour will evolve and underpin the transition in individuality. With a concave tradeoff, collectives containing non-specialized particles have higher collective fitness than collectives composed of specialized particles. In this case, a division of labour may not evolve, so the transition in individuality does not happen. The nature of the tradeoff is determined by the sign of the expression $v_N + b_N - 1$ (see Fig. 3.3 d). Therefore, $v_N + b_N - 1 < 0$ results in a convex tradeoff. Similarly, $v_N + b_N - 1 > 0$ results in a concave tradeoff. To outline the influence of the nature of the tradeoff on the metric values, I indicated populations with different tradeoff characters in Fig. 3.3 by different colours. Notably, despite the continuous distributions of all parameters of populations (μ_L, μ_A, σ_L, σ_A, b_N and v_N), the FCM and the MVSHN index are clustered into two groups: one with convex and one with concave tradeoffs.

To investigate how well the MVSHN index and the FCM represent the tradeoff character $v_N + b_N - 1$, their co-distributions are shown in the Fig. 3.4. Both measures (MVSHN index and FCM) show a high correlation with the tradeoff character: $\text{Cov}(v_N + b_N - 1, \text{MVSHN}) = 0.73$ and $\text{Cov}(v_N + b_N - 1, \text{FCM}) = 0.84$, respectively.

The primary use of the metric is to assess fitness decoupling when a direct measure of the tradeoff character is impossible to achieve. Based on the results presented in Fig. 3.4, particle and collective fitnesses are likely to be decoupled if FCM < 0 or MVSHN > 0.125[6]. However, both methods of fitness decoupling assessment are not always correct. The quality of the metrics can be also characterized by the percentage of incorrect fitness decoupling determination. The fail rate for the MVSHN index is equal to 15.5% and the fail rate for the FCM is equal to 12%. The FCM shows slightly better performance over the MVSHN index in the assessment of a tradeoff character.

These results show that the MVSHN index and FCM are both reasonably accurate representations of the transition in individuality for the model of a population under multilevel

[6]This is the half of the maximal value of the MVSHN index in this model – 0.25.

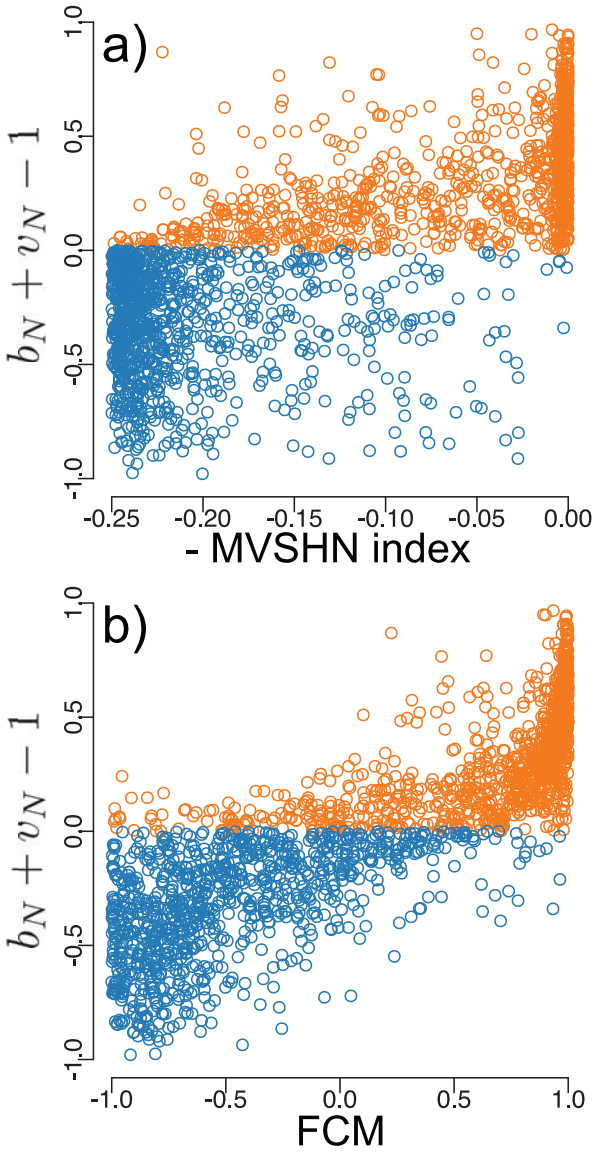

Figure 3.4: **Relation between the MVSHN index, FCM and character of tradeoff $b_N + v_N - 1$.** a) Co-distribution of the negative MVSHN index and tradeoff character, Cov(MVSHN, $b_N + v_N - 1$) = 0.73. b) Co-distribution of the FCM and the tradeoff character, Cov(FCM, $b_N + v_N - 1$) = 0.84. Blue circles represent populations with convex tradeoff between fertility and viability ($v_N + b_N < 1$) that promotes transition in individuality by means of division of labour. Orange circles represent populations with concave tradeoffs between fertility and viability ($v_N + b_N > 1$) that prevents transition in individuality.

selection where such transition occurs by means of the division of reproductive labour.

3.3.2 Application of the FCM to identify selective conditions providing fitness decoupling under weak selection.

Transition in individuality may occur by a variety of mechanisms, each requires an individual set of selective conditions to be successful. For instance, the convex tradeoff between fertility and viability promotes a reproductive division of labour (Michod et al. 2006). Alternatively, collective reproduction with single cell bottlenecks establishes heredity of reproduction at the collective level, and therefore, may also facilitate a transition in individuality. However, if selection promotes simply cooperation of particles, the transition in individuality does not happen (Hammerschmidt et al. 2014). Transitions in individuality can also be achieved by means of two phase life cycles (Hammerschmidt et al. 2014). However, the investigated examples of two phase life cycles require an external switch between two environments (Libby and Rainey 2013, Hammerschmidt et al. 2014). The diversity of mechanisms and corresponding selective conditions makes understanding the origins of transitions in individuality difficult.

Instead of analysis of various mechanisms and corresponding selective conditions, I searched for general features shared by populations undergoing a transition in individuality. I focused on the analysis of traits-to-fitness functions that can be constructed for any population. To investigate a range of traits-to-fitness functions, I developed a phenomenological model of a population under weak multilevel selection. I found that the FCM in this model is determined by the traits-to-fitness functions and the parameters of the trait distribution. Analysis of the FCM values shows that in a population with uncorrelated traits the fitnesses are decoupled if the gradients of selection at the particle and collective levels are orthogonal to each other in traits space.

3.3.2.1 Phenomenological model of a population under weak multilevel selection

I consider a population in which particles are nested into collectives. Collectives are unstructured: any two identical particles inside a collective have the same particle-level fitness. The population of collectives is unstructured as well: any two collectives with identical composition have the same collective-level fitness.

Each particle in a population has a set of numerical traits $(x_1, x_2, ...)$. For example, these traits could be the size of the particle at birth, or the average concentration of particular enzymes, or the presence of certain genes in the genome (in this case the value can be only 0 or 1).

The fitness of a particle in a collective is a function of the particle's traits. The actual form of the traits-to-fitness function may be very complex and is generally unknown for real-world examples. To construct this function, I utilize the weak selection assumption that implies a linear relationship between trait values and particle-level fitnesses. So, the average particle fitness in a collective is $F_P = \sum_{i \in \text{traits}} \alpha_{P,i} X_i$. Here F_P is average particle fitness in a collective, $\alpha_{P,i}$ is an effect of i-th trait on the particle fitness and X_i is an average value of the trait x_i in a collective. The weak selection assumption does not restrict the interplay between particle and collective level fitnesses, which are the main concern in my model. Therefore, the assumption of weak selection can be used for my purposes without any loss in the generality of results.

The collective fitness depends on all the particles in a collective. Under weak selection collective fitness is a linear combination of all trait values in all particles in the collective: $F_C = \sum_{j \in \text{particles}} \sum_{i \in \text{traits}} \alpha_{C,ij} x_{ij}$. Here F_C is a collective fitness of a collective, x_{ij} is the value of the i-th trait in the j-th particle in the collective, and $\alpha_{C,ij}$ is an effect of the i-th trait in the j-th particle on the collective fitness. Taking into account the absence of structure inside the collective, the influence of any trait on the collective fitness is the same for all particles: $\alpha_{C,ij} = \alpha_{C,ik} = \alpha_{C,i}$. This way the sum over particles can be replaced by averaging trait values over all particles in a collective: $F_C = \sum_{i \in \text{traits}} \alpha_{C,i} X_i$.

I considered a population with two traits because it is the minimal number that allows

fitness decoupling. If only one trait controls values of both fitnesses, then fitnesses are always correlated by the very nature of system. The case with a larger number of traits is presented in the appendix 3.5.2.

In a population with two traits, the collective with average trait values X_1 and X_2 has collective and average particle fitnesses equal to:

$$\begin{aligned} F_P(X_1, X_2) &= \alpha_{P1} X_1 + \alpha_{P2} X_2 \\ F_C(X_1, X_2) &= \alpha_{C1} X_1 + \alpha_{C2} X_2 \end{aligned} \tag{3.4}$$

3.3.2.2 Investigation of selective conditions that cause fitness decoupling

The traits-to-fitness functions represent the relationship between selective conditions, traits and fitnesses. This relationship can be used to analytically calculate the FCM in a population. This creates a link between the selective conditions imposed over a population and the fitness (de-)coupling state achieved in it. In this section I explicitly derive the FCM as a function of selective conditions α and the parameters of the traits distribution.

The combination of 3.1 and 3.4 gives:

$$\text{FCM} = \frac{\alpha_{P1}\alpha_{C1}\sigma_1^2 + \alpha_{P2}\alpha_{C2}\sigma_2^2 + \rho_T\sigma_1\sigma_2(\alpha_{P1}\alpha_{C2} + \alpha_{P2}\alpha_{C1})}{\sqrt{\alpha_{P1}^2\sigma_1^2 + \alpha_{P2}^2\sigma_2^2 + 2\rho_T\sigma_1\sigma_2\alpha_{P1}\alpha_{P2}}\sqrt{\alpha_{C1}^2\sigma_1^2 + \alpha_{C2}^2\sigma_2^2 + 2\rho_T\sigma_1\sigma_2\alpha_{C1}\alpha_{C2}}} \tag{3.5}$$

Here FCM is the value of the fitness correlation metric in a population, σ_i is a variation of average trait X_i across collectives in the population, and $\rho_T = \text{Cov}(X_1, X_2)/\sigma_1\sigma_2$ is the correlation coefficient of average traits X_1 and X_2.

This result has an intuitive geometric interpretation if two conditions are fulfilled. The first condition is a non-correlated traits distribution $\rho_T = 0$. The second condition is an equality of the traits variation $\sigma_1 = \sigma_2$. Under both conditions, Eq. 3.5 becomes:

$$\text{FCM} = \frac{\alpha_{P1}\alpha_{C1} + \alpha_{P2}\alpha_{C2}}{\sqrt{\alpha_{P1}^2 + \alpha_{P2}^2}\sqrt{\alpha_{C1}^2 + \alpha_{C2}^2}} \tag{3.6}$$

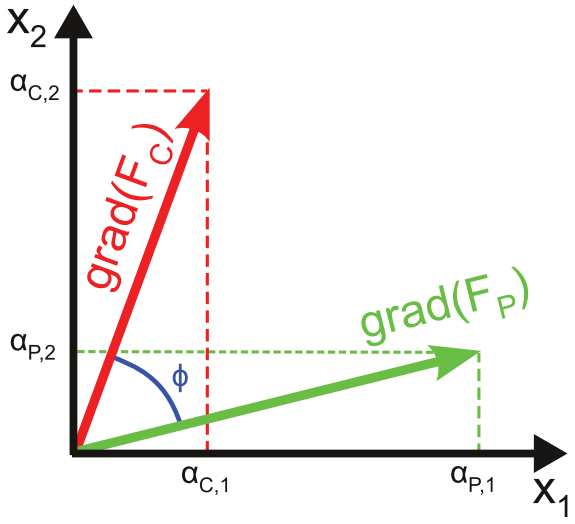

Figure 3.5: **Geometric interpretation of traits-to-fitnesses functions, which promote fitness decoupling.** The selection pressure applied to the population with two traits can be characterized by the vector of the fitness gradient $(\text{grad}(F))$ in the space of traits (X_1, X_2), which indicates the direction of selection. Multilevel selection can be characterized by two vectors: particle fitness gradient $(\text{grad}(F_P) = (\alpha_{P1}, \alpha_{P2}))$ and collective fitness gradient $(\text{grad}(F_C) = (\alpha_{C1}, \alpha_{C2}))$, which indicate the direction of fastest increase of particle and collective fitnesses, respectively. In the absence of traits correlation, FCM is equal to the cosine between fitness gradients $\text{FCM} = cos(\phi)$.

The right hand side of Eq. 3.6 is equal to the cosine between vectors of the particle fitness gradient $(\text{grad}(F_P) = (\alpha_{P1}, \alpha_{P2}))$ and collective fitness gradient $(\text{grad}(F_C) = (\alpha_{C1}, \alpha_{C2}))$ as illustrated in Fig. 3.5. Fitness gradients indicate the directions in the space of traits (X_1, X_2), which corresponds to the maximal increase in particle and collective fitness values. In other words, the gradient of the fitness at a particular level states the direction of evolution in the absence of selection at another level. This interpretation also works for a population with unequal traits variations after substitution $(x_1 \to \frac{x_1}{\sigma_1},\ x_2 \to \frac{x_2}{\sigma_2})$, as shown in appendix 3.5.3.

The geometrical interpretation shows the properties of fitness gradients necessary for the fitness (de-)coupling. The situation of fitness coupling corresponds to FCM close to 1, which can only be produced by the co-directional fitness gradients vectors. By contrast, the situation of fitness decoupling corresponds to FCM close to 0, which can be produced by fitness gradients vectors orthogonal to each other. Interestingly, the independent influence of each trait on fitnesses is irrelevant to the fitness decoupling: the only important factor is the relative

difference between fitness gradients directions.

The geometric interpretation also helps to outline the selective conditions that may promote fitness decoupling at the earliest stages of multicellular evolution. In early collectives, reproduction of collectives was causally linked to the reproduction of particles in them. Thus, cell growth rate was likely to be a universally beneficial trait: its increase enhanced fitnesses at the particle and collective levels. The question arises "what type of selective conditions, i.e. what character of the second trait, provide the most pronounced fitness decoupling (FCM $= 0$) in such populations?" Since fitness decoupling is a hallmark of the transition in individuality at the collective level, the intuitive answer is – the trait which affects collective fitness while leaving particle fitness indifferent to it. However, analysis of the traits space (see Fig. 3.6) shows that the best option of the second trait is the "lawless" one, which increases particle fitness at the expense of collective fitness[7] or its complete opposite – a "lawful" trait that promotes collective fitness at the expense of the particle fitness. The combination of universally beneficial and "lawless" (or "lawful") traits provides more pronounced fitness decoupling (FCM ≈ 0) than the combination of universally beneficial and collective-only traits (FCM ≈ 0.7).

Results show that in a population under weak multilevel selection the FCM is determined by the gradients of selection and the parameters of the traits distribution. In the case of non-correlated traits with equal or known variations, the FCM is equal to the cosine of the angle between gradients of particle and collective fitnesses in the space of traits. Fitness decoupling is achieved in a population with orthogonal fitness gradients, which requires selection to act on at least two traits with different effects on particle and collective fitnesses.

3.3.3 Dynamics of the FCM in the course of evolution

Under weak selection, the FCM is determined by the variations and covariation of traits $(\sigma_1, \sigma_2, \rho_T)$ and fitnesses gradients (α_P, α_C), according to Eq. 3.5. Variations and covariation

[7] Please note the difference from the selfish trait, which increases owner's particle fitness at the expense of particle fitness of others, instead of collective fitness. The "lawless" trait may be also selfish but in general case they are not identical.

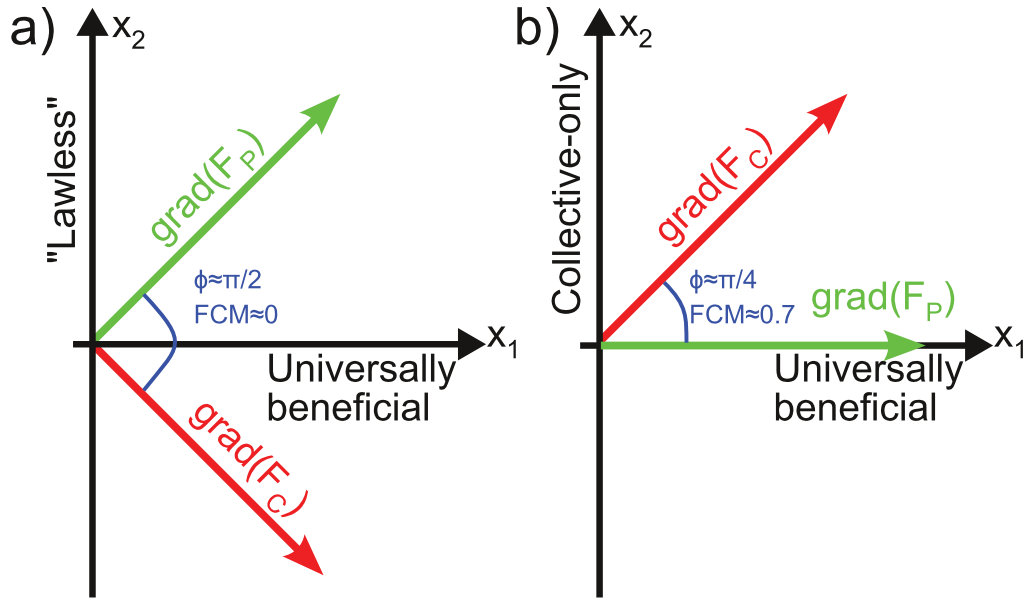

Figure 3.6: **In a population with a universally beneficial trait, a "lawless" trait provides a FCM closer to zero than a collective-only trait.** a) population in which one trait (X_1) is universally beneficial on both levels and another trait (X_2) is "lawless", i.e. increases particle fitness, at the expense of collective fitness. In this case directions of selection on both levels are significantly different from each other $(\phi \approx \pi/2)$, so the fitnesses are decorrelated (FCM ≈ 0). b) population with one universally beneficial trait (X_1) and one trait that improves collective-level fitness only (X_2), without any effect on the particle fitness. In this case directions of selection are more correlated $(\phi \approx \pi/4)$ than in previous one, so the fitness decoupling is much less pronounced (FCM ≈ 0.7).

of traits may change in the course of evolution, so the FCM will change accordingly. In this section, I investigated the change of the FCM in the course of evolution in populations with different initial covariations of traits. Two different selective conditions were considered: one that promotes fitness decoupling and another that keeps fitnesses coupled. As a result of simulations, I found that the average value of the FCM eventually becomes independent of the initial covariation of traits (ρ_T). Therefore, the average FCM is determined only by applied selection pressure (α_P, α_C) according to Eqs. 3.6 (or 3.14 for unequal variations traits (σ_1, σ_2)).

3.3.3.1 Model of evolution of a population under weak multilevel selection

To investigate the dynamics of the FCM in the course of evolution, I developed a model of evolution of a population under weak multilevel selection.

The modelled population consists of $N = 10000$ collectives, each containing $M = 100$ particles. Each particle has two numerical traits x_1 and x_2. The fitness of particles and collectives are determined as

$$\begin{aligned} F_P &= e^{w(\alpha_{P1}x_1+\alpha_{P2}x_2)} \\ F_C &= \sum_{i\in\text{particles}} e^{w(\alpha_{C1}x_{1,i}+\alpha_{C2}x_{2,i})} \end{aligned} \tag{3.7}$$

Here F_P and F_C are particle and collective fitnesses, w is intensity of selection, $x_{.,i}$ is the trait value of i-th particle in a collective and α_{P1} and α_{P2} are effects of traits on the particle fitness, α_{C1} and α_{C2} are effects of traits on the collective fitness. The exponential trait to fitness functions are chosen to prevent negative values of fitnesses that may arise in the course of evolution if the original linear functions (Eq. 3.4) had been used. The intensity of selection parameter was chosen to be small $(w = 0.2)$, so the population evolves under weak selection.

The initial values of the traits were sampled from two-dimensional normal distribution. The variations of the traits were equal to one in all simulations. he covariations of the traits were independently chosen for each simulation run from the range $(-1, 1)$.

The population was subjected to a series of Death-birth process at the particle and collective levels. At the each step, one instance of Death-birth process at the particle level occurred first, followed by one instance of Death-birth process at the collective level.

Death-birth process at the particle level updates the composition of each collective independently of other collectives. In this process, some particles in a collective are marked for extinction, while other particles reproduce. The probability of particle survival is proportional to its particle fitness F_P, such that the probability of survival of the particle with maximal fitness within the collective is equal to 1. The probability that a surviving particle reproduces is equal for each particle. The number of reproducing particles is chosen to keep the total size of collectives equal to M particles. When a particle reproduces, it creates a new particle whose traits are random values normally distributed around the traits of progenitor particle with variation 0.1.

In Death-birth process at the collective level, some collectives in a population are chosen to go extinct, while other collectives reproduce. The probability of collective survival is proportional to its collective fitness F_C, such as the probability of survival of the collective with maximal fitness is equal to 1. The probability that surviving collectives reproduce is equal for each collective. The number of reproducing collectives is chosen to keep the total size of the population equal to N collectives. When a collective reproduces, each particle in a progenitor collective reproduces and the newborn particles form the new collective.

3.3.3.2 Results of simulations

The evolution of populations with various initial traits covariations were investigated. I measured the dynamics of the FCM under two different selective conditions. In the first series of simulations, fitness gradients were almost co-directional $(\alpha_{C1}, \alpha_{C2}) = (0.7, 0.8)$ and $(\alpha_{P1}, \alpha_{P2}) = (0.8, 0.7)$, so according to Eq. 3.6 fitnesses would be coupled if traits were non-correlated. In the second series of simulations, fitness gradients were orthogonal $(\alpha_{C1}, \alpha_{C2}) = (\sqrt{3}/2, 0.5)$ and $(\alpha_{P1}, \alpha_{P2}) = (-0.5, \sqrt{3}/2)$, so according to Eq. 3.6 fitnesses would be decoupled if traits were non-correlated. Results of simulation are presented in

Fig 3.7.

Simulation results show that the value of the FCM after a sufficiently long time period does not depend on the initial state of the population. Under selective conditions preventing fitness decoupling, the FCM approaches 1 (see Fig. 3.7 a) and b)). Under selective conditions promoting fitness decoupling, the FCM fluctuates around 0 Fig. 3.7 c) and d)), independent of the initial state of the population.

In the section 3.3.2 I showed that in the simple model of population under multilevel selection the FCM is determined by both traits distribution and selection pressure applied to the population, as represented by Eq. 3.5. However, results of the simulations indicate that the average value of the FCM eventually becomes independent of the initial distribution of traits, and therefore, is determined by selection only. Thus, the simplified Eqs. 3.6 and 3.14 and the geometric interpretation of selective conditions promoting fitness decoupling proposed in the section 3.3.2 can be applied to any population subjected to constant weak multilevel selection.

3.4 Discussion

In this work I have proposed a method for detecting fitness decoupling, based on the simultaneous measurement of the fitness of collectives and the particles of which they are comprised. The distribution of fitnesses is expected to be significantly correlated during early stages of the evolution of multicellular life, before collectives developed Darwinian properties. However, once selection begins to transition to the level of collectives a tractable decorrelation between particle and collective fitnesses is thought to occur.

3.4.1 Measurement of the collective fitness of early collectives

My approach requires the measurement of collective fitness. However, the meaning of this term varies among populations at the different stages of multicellularity development. Damuth and Heisler in their paper (1987) defined two classes of multilevel selection (MLS) model.

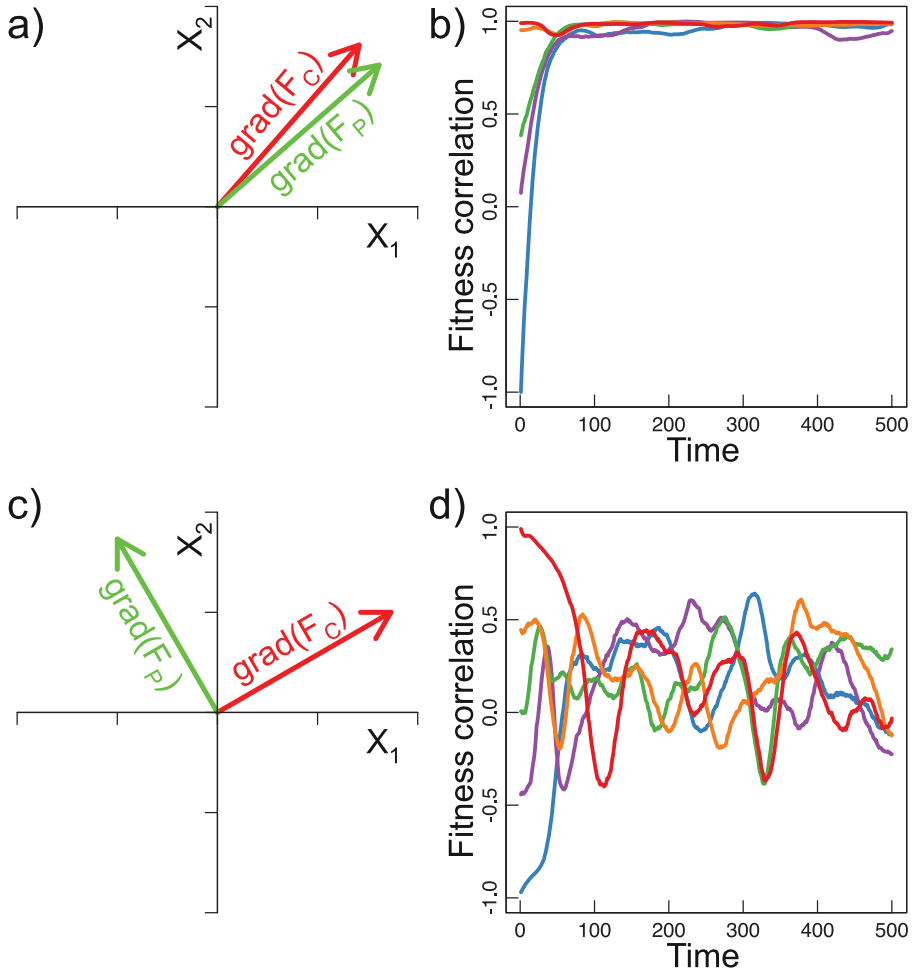

Figure 3.7: **Dynamics of the FCM in the course of evolution of the model population under different selective conditions.** a) Fitness gradients that prevent fitness decoupling. Fitness gradients have similar directions: $(\alpha_{C,1}, \alpha_{C,2}) = (0.7, 0.8)$ and $(\alpha_{P,1}, \alpha_{P,2}) = (0.8, 0.7)$. b) Evolution of FCM under selective conditions specified in panel (a). Each line represent one population. Independently of the initial traits distribution, the FCM approaches 1 in the course of evolution. c) Fitness gradients that promote fitness decoupling. Fitness gradients are orthogonal: $(\alpha_{C,1}, \alpha_{C,2}) = (\sqrt{3}/2, 0.5)$ and $(\alpha_{P,1}, \alpha_{P,2}) = (-0.5, \sqrt{3}/2)$. d) Evolution of FCM with time under selective conditions specified in panel (c). Each line represent one population. Independently of the initial traits distribution, the FCM approaches and fluctuates around 0. All simulations performed under weak selection.

In MLS1 models the fitness of collectives is defined as the average number of particles descending from a given collective. This number is characterized by the average particle fitness within the collective. MLS2 models define collective fitness as the number of offspring collectives. Both classes of models have their areas of application but what makes the distinction important is the fact that the very first and very last stages of an evolutionary transition to multicellularity are covered by different theoretical approaches. The earliest collectives were, most likely, the simplest ones, therefore, their evolutionary success was likely determined by the fitness of particles, which makes MLS1 models most applicable to these systems. In contrast, during the final stages of the evolution of multicellularity when collectives approach the point of becoming Darwinian individuals in their own right, evolutionary success of such collectives is determined by number of offspring collectives used in the MLS2 class of model.

In order to understand transitions in individuality, it is necessary to be able to compare models or populations prior to the transition in individuality with models of populations after the transition. Some shared "currency" is needed in order to be able to track the transition. I claim that the number of offspring collectives can be used as such "currency". This means that the MLS2 collective fitness can be measured for populations in which collectives do not reproduce as a units, for example, in the case of populations of deer herds as described by Williams (1966). This can be done formally. Collectives in a population prior to a transition in individuality do not reproduce as units but the particles inside them do. Any present particle can be traced via following offspring-parent relationships to some particle in the past. At the collective level, all particles in the present collective can be traced to particles in some collectives in the past. This forms links between past and present collectives. Thus, the fitness of a collective can be defined as the number of collectives connected by these links to an earlier collective, as in Figure 3.8.

The existence of such a value as the "number of collective offspring" does not mean the collectives can reproduce, it is merely an interpretation of observed events. A rockfall may split a narrow lake into two smaller ones and a single population of fish may become two or a researcher may take a sample from a Petri dish and plate this on a new one, so it is possible to

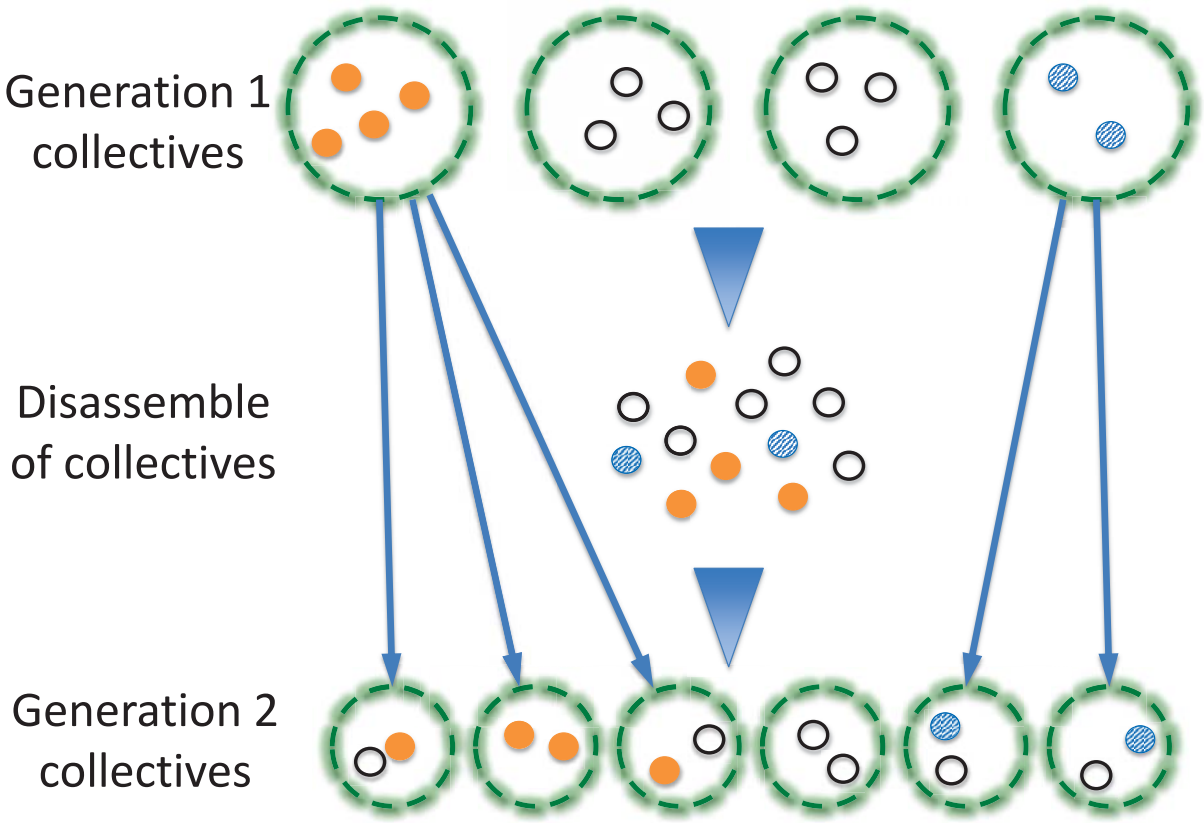

Figure 3.8: **Measurement of MLS2 fitness in a population in which collectives do not posses Darwinian individuality.** The population undergoes a cycle involving assembly and disassembly of collectives. Evolutionary success of a collective is determined by the number of particles produced. The parent-offspring relationships at the level of particles establish genealogical connections at the level of collectives. These connections are shown by lines for the rightmost and the leftmost collectives at generation 1. The collective-level offspring is any collective containing particles descended from a given collective. For this population, the MLS2 fitness (number of offspring collectives) is similar to the MLS1 fitness (number of offspring particles): the rightmost collective containing the largest number of particles has more collective offspring than the leftmost collective with the lowest umber of particles. For populations that have made the transition in individuality the numbers of offspring particles and offspring collectives may be significantly different.

formally consider the newly inoculated plate as "collective level offspring" of another plate. This definition does not imply any biological process such as reproduction.

The MLS2 collective fitness formally defined for populations prior to a transition in individuality is still a byproduct of particle-level fitness. For such a population, knowledge of MLS2 collective fitness in addition to known particle fitness does not provide much information about the evolution of the population. In contrast, for a population that has passed through a transition in individuality, MLS2 fitness of collectives provides information about collective reproduction that cannot be inferred from particle fitness. The measurement of MLS2 collective fitness conveys no information about collective reproduction prior to the transition in individuality, but is informative after the transition. The transition manifests itself by making MLS2 collective fitness an informative characteristic of evolution, independent of particle fitness. The proposed FCM makes it possible to detect this process.

3.4.2 Fitness decoupling in non-intuitive scenarios

This work has been motivated by the shortcomings in the methods currently used in the identification of Darwinian individuality, such as covariance and the contextual approaches. These methods provide counter-intuitive conclusions when applied to some populations under multilevel selection (Sober 1993, Okasha 2006). Here I review how the method proposed in this work handles these examples.

The covariance approach may detect the presence of selection at the collective level, while, in fact, selection is absent. Wallace (1968) suggested a "soft selection" scenario where each collective contributes an equal number of cells to the next generation, however, cells within a collective differ in the reproductive output. In this scenario, selection acts at the level of cells but does not act at the level of collectives. However, application of the covariance approach to this model results in a non-zero collective-level selection term (Wade 1985). Thus, the covariance approach provides incorrect results in this case.

Application of my method to the "soft selection" scenario results in the zero divided by zero expression in Eq. 3.1. The FCM is a ratio of covariance of particle and collective

fitnesses to the variances of particle and collective fitnesses. Under "soft selection", each collective has the same number of collective-level offspring, so the variance of collective level fitness is zero. The covariance of particle and collective fitnesses is equal to zero for the same reason. Thus, the FCM cannot be determined for the "soft selection" scenario. While my method does not give an answer on the presence of fitness decoupling in this case, it provides a warning that there is no answer, unlike to the covariance approach which draws an incorrect conclusion.

Another example is a population where the collectives are composed of a mixture of cooperating and defecting particles. Defectors are favoured by particle-level selection but collectives with high frequencies of cooperating types perform better than collectives dominated by defecting types. Since the fitness of a particle depends on the composition of the collective to which the particle belongs, both the covariance and the contextual approach are in agreement - both indicate that selection takes place at the level of collectives. However, collectives in this system may be Darwinian individuals only in a very marginal sense. For instance, if collectives at the next generation are formed by the random assortment of cells released by collectives at the previous generation, like in the trait group models (Wilson 1975), then heredity at the collective level will be small. Thus, the detection of selection at the collective level by the contextual and covariance approaches does not detect the presence of Darwinian individuality at the collective level.

The application of my method to the trait groups model results in high correlation between particle and collective fitnesses. Under random assortment of particles, the only factor determining the number of collective-level offspring is the number of particles produced. As such, the number of offspring collectives is not an independent characteristic of the population, so my method correctly indicates that in this example collectives cannot participate in natural selection in their own right.

My method also helps to better understand results of evolutionary experiments. Hammerschmidt et al (2014) investigated the evolution of fitness decoupling under two different selection regimes (see section 1.2.3.2 for details of experiment). They observed fitness de-

coupling in a two-phase "cheat-embracing" life cycle where each phase favoured cells of a specific phenotype. At the same time, populations propagated under a "cheat-purging" life cycle, which sustained a single phenotype, meant that particle and collective fitness remained coupled. These results pose the question: what was so important in the cheat embracing life cycle that made fitness decoupling possible? Analysis of this system with my method provides an explanation – fitness decoupling occurred when the selection regime favoured different traits at the different levels. The cheat embracing life cycle established the collective level selection that favoured an increase in transition rate between two phenotypes. At the same time, selection at the particle level promoted the growth rate of cells. Thus, transition and growth rates were independent traits with uncorrelated effects on particle and collective fitness, which lead to the fitness decoupling according to geometrical interpretation of Eq. 3.6. In contrast, under the cheat purging life cycle, selection at the collective level promoted only the stability of the bacterial mat. The mat stability can be improved by increasing the number of glue-producing cells, i.e., by improvement of growth rate. As such, in the cheat purging life cycle, there was only one trait affecting both the particle and collective-level fitness and fitness decoupling is impossible if there is a selection for only one trait. My method provides a possible explanation for presence or absence of fitness decoupling in cheat embracing and cheat purging life cycles respectively.

Insights from the experiment of Hammerschmidt et al (2014) combined with an analysis by my method allows me to outline a set of conditions in which fitness decoupling will emerge. My method shows that at least two traits with non-correlated effects on particle and collective-level fitness are necessary to achieve fitness decoupling. Hammerschmidt et al (2014) have shown that the second collective fitness-specific trait naturally emerges when there are two phases to a life cycle. A combination of these two results predicts that fitness decoupling will likely emerge under a life cycle involving two distinct phenotypes where survival and reproduction of collectives is unrelated to the growth rate of the particles comprising them[8].

[8]This does not mean that any possible two-phase life cycle will exhibit fitness decoupling. If the particle fitness is determined by something else than growth rate trait, then fitnesses can be coupled. I cover several such

3.4.3 Fitness decoupling as a manifestation of Darwinian individuality

In this study I have adopted a Darwinian definition of multicellularity: a collective of cells is a multicellular organism if it participates to some extent as a unit of selection. This definition concerns the observed outcomes of the process but does not capture the mechanistic underpinning of such outcomes. Similarly, Lewontin's conditions for natural selection (variation, reproduction and heredity) do not say anything about the mechanisms underlying the expression of these properties. As such, my method for the detection of Darwinian individuality by assaying for fitness decoupling can indicate when recurrences of collectives depends on something else other than just reproduction of particles. It says nothing about the underlying mechanistic details, for example those that bring about collective level reproduction.

The mechanistic details of collective recurrence will play role if the transition in individuality occurs without fitness decoupling. The fitness coupling detected by FCM indicates that fitness at one level is a byproduct of fitness at another level. However, it is impossible to determine which level is a byproduct, without knowing the causal relationship between particle and collective fitnesses. The example of collective fitness being a byproduct of particle fitness is a "deer herd" system (Williams 1966). The fitness of the herd as a whole is determined by the fitnesses of each individual deer in it. An adaptation improving the running speed of individual deer increases the fitness of each particular deer, and as a consequence increases the fitness of the deer herd as a whole. The example of particle fitness being a byproduct of collective fitness is *G. pectorale*, which contains 16 cells in a collective phase (Stein 1958) each capable to give rise to a new colony. The colony behaves as a unit and an adaptation improving the performance of the colony leads to higher uptake of resources, and as a consequence, increases the fitness of each cell in it. In both examples, FCM detects coupled fitnesses[9] that means that selection operates only at one level. FCM and all other phenomenologic methods including MVSHN index, Price's and contextual decompositions

cases in chapter 4.

[9]This is correct for adaptations improving only the growth rate in *G. pectorale*. However, if some adaptation affected the mode of reproduction cycle of *G. pectorale*, then the Darwinian properties of *G. pectorale* colonies would have an influence on the evolution of a population and at the same moment this population would exhibit fitness decoupling.

are unable to identify at which level selection operates.

While fitness decoupling (and subsequently FCM) ignores the mechanistic interactions between levels of organization, it still has a use for the characterization of the evolutionary response of a population to applied selection. The change in composition of population with time is determined by fitnesses of particles and collectives. Under fitness coupling scenario, knowledge of the fitness at one level provides information about fitness at another level. Therefore, populations expressing fitness coupling are in a special position: the response to selection is independent from the level at which selection operates in these populations. Adaptations that have similar effect on the fitness will result in a similar evolutionary changes in both deer herd and *G. pectorale* populations. Thus, the Darwinian properties of collectives in populations with coupled fitnesses do not alter the response to selection, if compared with populations prior to the transition in individuality.

Another aspect of multilevel selection and transition in individuality has been proposed by Bourrat (2015). He noted that the measure of the particle fitnesses over sufficiently long time scale is equivalent to the measurement of collective fitness. As such, instead of two fitnesses persisting at two different levels, the multilevel selection may be described by a single fitness measured at different time scales. Based on these findings Bourrat claims (2015) that the whole concept of the collective fitness is unnecessary for the understanding of the transition in individuality, and therefore, the application of derivative concepts such as fitness decoupling may be misleading. However, even from his perspective, the emergence of Darwinian individuality is accompanied by the emergence and development of the novel selective processes, in this case – acting at the longer time scales. As such, the direct link can be drawn between concepts used in each approach: concepts generally addressed to the particle-level correspond to the short-term processes and concepts addressed to the collective level correspond to the long-term processes. Therefore, the switch to Bourrat's point of view does not change the nature of the questions discussed in this chapter.

3.4.4 Interpretation of the FCM value

FCM was developed as a metric of fitness decoupling. Fitness decoupling is considered to be a binary entity; a population can either exhibit it or not. FCM, instead, takes a value from a continuous range $(-1, 1)$. The boundary values have clear interpretations. Populations with coupled fitnesses express a FCM close to 1. Populations in which fitnesses are decoupled and independent of each other have the FCM close to 0. Populations in which fitnesses are decoupled and conflicted have the FCM close to -1. Intermediate values of the FCM correspond to the intermediary states between these boundary cases. The question is: what do these intermediary states mean?

As indicated in section 3.4.3, the FCM deals with the expected response of a population to an applied selection pressure. When fitnesses are coupled $(\text{FCM} = 1)$, the response of a population to selection at the particle and collective level is the same. As fitnesses begin to decouple, collective-level fitness is no longer identical to particle fitness $(\text{FCM} < 1)$. However at the earliest stages, evolutionary success of the collective may still rely on particle fitness to some extent, thus the FCM remains positive $(0 < \text{FCM} < 1)$. Generally, the intermediary states between coupled and decoupled fitnesses are not discussed but they may potentially exist in the course of evolution of multicellularity.

An example of a population with an intermediate value of the FCM is a population in which fertility of collectives is independent of particle reproduction but viability is determined by collective size. Consider a population where collectives were formed to provide a defence against predators. Imagine then that these collectives developed a means of reproduction, which does not depend on the size of the collective. In this case, the fertility of the collective is independent of the particle fitness. However, the larger size of the collective is determined by the particle fitness[10] and provides a better defence against predators, thus particle fitness contributes to collective viability. In this example, the fertility of the collective is independent of particle fitness and viability of collectives is determined by particle

[10]Here I consider collectives at the early stages of development, so the number of cells in a collective is a result of actions at the particle level. The paradigm multicellular organisms do not fit this example because their body size is determined by the development program which is a collective-level trait.

fitness, so the total collective fitness is neither identical to the particle fitness, nor completely independent of it $(0 < \text{FCM} < 1)$.

The FCM indicates the extent to which the fitness of collectives relies on the fitness of particles comprising them. Prior to the transition in individuality, collective fitness is a byproduct of particle fitness, so fitnesses at both levels are identical to each other. However, adaptations that make them different do not necessarily establish complete independence of evolutionary responses at two levels of life's hierarchy. The FCM can detect the partial decoupling as the spectrum of intermediate values of the metric.

3.4.5 Possible applications of the FCM

The FCM is a useful tool for investigation of populations subjected to selection at more than a single level.

Measurement of the FCM allows a direct comparison of populations with different properties. The FCM can be evaluated for any population featuring distinct groups and tractable genealogy. These conditions are met in various natural and experimental populations: volvocales, populations of *Saccharomyces cerevisiae* and *Chlamydomonas reinhardtii* evolved in settling experimental studies (Ratcliff et al. 2012, 2013a), populations of *Pseudomonas fluorescens* evolved in life cycle experimental studies (Hammerschmidt et al. 2014) and to some extent in slime molds. Each of these populations exhibit features of multicellularity in a unique way and yet they can be compared on the basis of the FCM.

Godfrey-Smith in his book (2009) developed a framework with similar capabilities. However, in his approach, Darwinian individuality at the collective level is characterized by three parameters: reproductive bottleneck, reproductive specialization and integration. Each of these parameters is a qualitative characteristic of a population. Godfrey-Smith did not specify how to measure any of these parameters, instead he assigned the values according to his interpretation of events occurring during life cycles of considered populations. My method, while being not so detailed as Godfrey-Smith's framework, allows a numerical characterization of a population by a single parameter (FCM) that can be obtained by direct measurement.

3.4.6 Measurement of fitness decoupling in natural and experimental populations

My method has been designed to be more than just a theoretical toy. Throughout I have kept in mind possibilities for application of my method to experimental and natural populations. As such, a few notes should be made about applications of the FCM as a measure of interdependence of evolution at the particle and collective levels. Obtaining the FCM requires measurement of fitnesses themselves and this is possible only with limited accuracy. Noise in the determination of fitness affects the value of the FCM. Even the unbiased uncorrelated noise in the measurement of fitness values leads to a bias in the estimated value of the correlation coefficient. For example, in the case of complete correlation between particle and collective fitness ($F_C = kF_P$, so $\text{FCM}_{real} = 1$), any uncertainty in measurement of fitnesses means that the observed values of fitnesses will be only approximately proportional to each other, so the observed correlation coefficient will be less than 1 ($\text{FCM}_{observed} < 1$). This effect is important for any real world application of my method and anyone who is going to use it is advised to pay attention to the accuracy of fitness measurements.

The application of my method requires measurement of the particle and collective-level fitness. Calculation of the number of offspring performed over different time scales may provide different results. For example, consider a group-structured population subjected to infrequent but regular mass-extinction events. At such events, most particles in each collective die and some collectives die completely. During the following growth period, collectives rebuild themselves and new collectives emerge to replace extinct collectives. In this system, particle fitness can be measured over multiple time scales with different results. If the time scale is much shorter than the period between extinction events, then the fitness of the particle will be determined by its rate of reproduction. If the time scale is about the period between extinctions, then the fitness of the particle will be also influenced by the chances of its survival compared to the chances of other particles in the same collective. However, if the time scale is much longer than the period between extinctions, then the fitness of particles will be additionally affected by the chances that the host collective survives extinctions and produces

new collectives between extinctions. Implementation of different time scales in my method leads to different values of the FCM, so the choice of the time scale is an important part of the investigation (Bourrat 2015).

There is no universal rule how to choose the time scale for fitness measurement. Generally, a fitness of some entities is calculated over a single generation time of these entities. However, this choice is not always optimal. For instance, the 1:1 sex ratio observed in natural populations can be explained only if the fitness is measured over a period of two generations instead of one (Fisher 1958). Thus, prior to application of my method, the time scale should be chosen based on the dynamics of the studied population.

The method proposed in this paper allows the numerical characterization of a fitness decoupling value. A model or a real multilevel population can be tested using my approach if the average particle and collective level fitnesses can be measured for the same collectives of the given population. The collective level fitness used in my method is MLS2 fitness but it can be measured even in MLS1 populations using genealogical links of particles as progenitor-offspring connectors between collectives. The simple model of a multilevel population shows that decoupling of fitnesses requires selection with at least two degrees of freedom (traits) with the value of the FCM depending on the directions of selection pressures at the particle and collective levels, in the space of traits. The last result reveals the properties of models, necessary for investigation of fitness decoupling.

3.5 Appendix

3.5.1 Models used in illustrations of fitness correlation

These models serve as an illustration of the principle and do not accurately represent any real life cycle. Therefore, these models are extremely simplified.

Models presented here calculate the co-distribution of particle and collective fitnesses in simple populations undergoing different life cycles. Calculation of the co-distribution of particle and collective fitnesses consists of two stages: simulation of evolution and measurement

of fitness in evolved populations. At the first stage, a population of particles nested within collectives is subject to natural selection. At the second stage, parameters of evolved population are used to calculate the expected average particle fitness and the collective fitness for each collective in the population. The resulted co-distribution of particle and collective fitness are presented in Figure 3.2.

Model of population with correlated fitnesses

This model simulates the evolution of a group-structured population where each collective splits in two when it reaches a critical number of particles. Each particle in the population has a growth rate dependant only of its own characteristics. Thus, in this model, the collective level fitness (rate of collective splitting) is a byproduct of the particle level fitness (particle growth rate).

The population consists of $M = 100$ collectives. Each collective initially consists of $N = 5$ particles. Each particle has a single numerical trait, its doubling time is equal to the value of this trait. Initial values of the trait are set as uniformly distributed random numbers in an interval $(1; 3)$. When a particle divides, a new particle arises in the same collective with the doubling time equal to a random number uniformly distributed in the interval $(0.9; 1.1)$ of the progenitor's doubling time. When any collective reaches the size of $2N = 10$ particles, it splits in two collectives of N particles each. Particles comprised the progenitor collective are randomly distributed between newborn collectives. When any collective splits, a single other collective in the population dies, so the total number of collectives is always equal to M. The simulation of evolution was calculated for $100 * M * N = 50000$ particle divisions. The state of the population (traits of the particles and their distribution among collectives) was recorded at the end of the simulation and then used in the fitness measurement.

Collective fitness and the average particle fitnesses were calculated for each collective. The average particle fitness was calculated as the average doubling time of all particles in the collective. The collective fitness of a given collective was calculated as the time required to split for the collective constructed from N particles randomly chosen from a given collective.

Model of population with decorrelated fitnesses

This model simulates the evolution of a group-structured population where each collective splits in two when its internal countdown reaches zero. The growth rate of each cell in this population depends only on its own characteristics. Thus, in this model, the collective fitness is independent of the particle fitness.

The population consists of $M = 100$ collectives. Each collective initially consists of $N = 5$ particles. Each particle has two numerical traits: a particle's doubling time and the influence of this particle on the collective doubling time. Initial values of both traits are set as uniformly distributed random numbers in an interval $(1; 3)$. When the particle divides, a new particle arises in the same collective with values of traits equal to random numbers that are uniformly distributed at an interval $(0.9; 1.1)$ of the progenitor's traits values (both traits can change independently of each other). The collective doubling time is determined at the moment of collective birth and is equal to the mean value of the second trait among particles present in the collective at the moment of birth. When the collective divides, it splits in two. Particles comprising the progenitor collective are randomly distributed between newborn collectives. If the split collective had an even number of particles, then both newborn collectives have equal size. If the split collective had an odd number of particles, then one newborn collective has one more particle than other newborn collective. If the split collective contained a single particle, then the splitting does not happen and countdown time is reset. When any collective splits, a single other collective in the population dies, so the total number of collectives is always equal to M. The simulation of evolution was calculated for $100 * M * N = 50000$ particle divisions. The state of population (traits of the particles and their distribution among collectives) was recorded at the end of the simulation and then used in the fitness measurement.

Collective fitness and the average particle fitness were calculated for each collective. Average particle fitness was calculated as the average doubling time of all particles in the collective. Collective fitness was calculated as the doubling period of the collective, i.e. the average value of the second trait of all particles in the collective.

Model of population with fitnesses tradeoff

This model simulates the evolution of a group-structured population where each collective splits in two when it collects a critical amount of a resource in the collective storage. At each time step, the collective evenly shares the same amount of resource among all particles in it. Each particle distributes the gained resource between investment in its own reproduction and donation to the collective storage. Thus, in this model, the collective fitness tradesoff against particle fitness.

The population consists of $M = 100$ collectives. Each collective initially consists of $N = 5$ particles. Each particle is described by the single numerical trait, which value is the fraction of resource that cell keeps to itself. Initial values of the trait are set as uniformly distributed random numbers in an interval $(0; 1)$. At each time step, each collective evenly distributes 1 unit of resource among all particles within it. When a particle collects $z = 1$ unit of resource for its own needs, it divides. When the particle divides, a new particle arises in the same collective with the trait value equal to the random number uniformly distributed in interval $(0.9; 1.1)$ of the progenitor's trait value (values higher than 1 are forbidden). The amount of resource collected by divided particle is lost after division. When a collective allocates $Nz = 5$ units of resource in a collective storage (donated by particles), it splits in two. Particles are randomly distributed between newborn collectives. If the dividing collective had an even number of particles, then both newborn collectives have equal size. If the dividing collective had an odd number of particles, then one newborn collective has one more particle than another one. If the dividing collective contained a single particle, then collective division does not happen and the accumulated resource is lost. When collective division occurs, a single other collective in the population dies, so the total number of collectives is always equal to M. The simulation of evolution was calculated for $100 * M * N = 50000$ particle divisions. The state of population (traits of the particles and their distribution among collectives) was recorded at the end of the simulation and then used to determine the fitness.

Collective fitness and the average particle fitness were calculated for each collective. The average particle fitness was calculated as average doubling time of all particles in collective. Collective fitness was calculated as the doubling period of the collective, given the initial

amount of resource in the collective storage is zero.

3.5.2 Fitness covariation in the case of more than two traits

If there are n traits in the population, the fitnesses are equal to:

$$\begin{aligned} F_P(x_1, .., x_n) &= \sum_{i=1}^{n} \alpha_{P,i} X_i \\ F_C(x_1, .., x_n) &= \sum_{i=1}^{n} \alpha_{C,i} X_i \end{aligned} \tag{3.8}$$

The combination of 3.1 and 3.8 leads to:

$$\text{FCM} = \frac{\sum_{i=1}^{n}\sum_{j=1}^{n} \alpha_{P,i}\alpha_{C,j} \left(\mathbb{E}\left(X_i X_j\right) - \mathbb{E}\left(X_i\right)\mathbb{E}\left(X_j\right)\right)}{\sqrt{\sum_{i=1}^{n}\sum_{j=1}^{n} \alpha_{P,i}\alpha_{P,j} \left(\mathbb{E}X_i X_j - \mathbb{E}X_i \mathbb{E}X_j\right)} \sqrt{\sum_{i=1}^{n}\sum_{j=1}^{n} \alpha_{C,i}\alpha_{C,j} \left(\mathbb{E}X_i X_j - \mathbb{E}X_i \mathbb{E}X_j\right)}} \tag{3.9}$$

Taking into account that variation of trait X_i is equal to $\sigma_i^2 = \mathbb{E}X_i X_i - \mathbb{E}X_i \mathbb{E}X_i$ and covariation of traits X_i and X_j is equal to $\rho_{ij} = \mathbb{E}X_i X_j - \mathbb{E}X_i \mathbb{E}X_j$ we get:

$$\text{FCM} = \frac{\sum_{i=1}^{n} \alpha_{P,i}\alpha_{C,i}\sigma_i^2 + \sum_{i,j=1, i\neq j}^{n} \alpha_{P,i}\alpha_{C,j}\rho_{i,j}}{\sqrt{\sum_{i=1}^{n} \alpha_{P,i}^2\sigma_i^2 + \sum_{i,j=1, i\neq j}^{n} \alpha_{P,i}\alpha_{P,j}\rho_{i,j}} \sqrt{\sum_{i=1}^{n} \alpha_{C,i}^2\sigma_i^2 + \sum_{i,j=1, i\neq j}^{n} \alpha_{C,i}\alpha_{C,j}\rho_{i,j}}} \tag{3.10}$$

The equation 3.10 is an analogue of the equation 3.5. With the absence of traits correlations and equal variations this equation transforms into:

$$\text{FCM} = \frac{\sum_{i=1}^{n} \alpha_{P,i}\alpha_{C,i}}{\sqrt{\sum_{i=1}^{n} \alpha_{P,i}^2} \sqrt{\sum_{i=1}^{n} \alpha_{C,i}^2}} \tag{3.11}$$

This result is an equation 3.6 in the case of many traits. The geometrical interpretation holds true with this result but the gradients are calculated in n-dimensional space of traits.

3.5.3 Fitness decoupling in the population with uncorrelated traits but unequal traits variations

If the traits variations are not equal $\sigma_1 \neq \sigma_2$, then the analogue of the equation 3.6 still can be obtained. In order to achieve this result, the trait values should be normalized:

$$\begin{aligned} x'_1 &= \frac{x_1}{\sigma_1} \\ x'_2 &= \frac{x_2}{\sigma_2} \end{aligned} \tag{3.12}$$

With this normalized trait values the fitnesses values are equal to:

$$\begin{aligned} F_P(x'_1, x'_2) &= \alpha_{P1}\sigma_1 x'_1 + \alpha_{P2}\sigma_2 x'_2 = \alpha'_{P1}x'_1 + \alpha'_{P2}x'_2 \\ F_C(x'_1, x'_2) &= \alpha_{C1}\sigma_1 x'_1 + \alpha_{C2}\sigma_2 x'_2 = \alpha'_{C1}x'_1 + \alpha'_{C2}x'_2 \end{aligned} \tag{3.13}$$

Here I made the substitution $\alpha'_{P/C,i} = \alpha_{P/C,i}\sigma_i$. Under the assumption of the non correlated traits distributions we get:

$$\text{FCM} = \frac{\alpha'_{P1}\alpha'_{C1} + \alpha'_{P2}\alpha'_{C2}}{\sqrt{\alpha'^2_{P1} + \alpha'^2_{P2}}\sqrt{\alpha'^2_{C1} + \alpha'^2_{C2}}} \tag{3.14}$$

The equation 3.14 has the same geometric interpretation as the equation 3.6 but does not require the equality of the traits variations. However, in order to use this result the variations of traits (σ_i) should be known.

Chapter 4

Using the FCM to make predictions concerning fitness decoupling

4.1 Introduction

The transition in Darwinian individuality to the level of collectives is a major step in the evolution of multicellularity (Godfrey-Smith 2009). While collectives gain an ability to participate in natural selection in their own right, the fitness of collectives may become independent of the fitness of the particles comprising them. This is known as *fitness decoupling* and it is a likely the hallmark of the transition in individuality (Michod and Roze 1999). In Chapter three, I suggested the fitness correlation metric (FCM) as a measure of fitness decoupling. The FCM can be obtained for any group-structured population and makes it possible to detect the transition in individuality in populations on the brink of multicellular life.

In Chapter three, FCM has been defined as a correlation coefficient between particle and collective fitnesses (see Eq. 3.1). This approach requires prior measurement of particle and collective fitnesses, though the measurement of fitnesses in natural and experimental populations may be a complex task.

However, the FCM can be inferred from fitness gradients (Eq. 3.6) if fitnesses are linear functions of traits (Eq. 3.4). This approach provides an alternative way to calculate the FCM

that does not require prior measurement of fitnesses. Moreover, the FCM can be obtained before evolution takes place.

In this chapter, FCM values inferred according to the FCM definition (Eq. 3.1) are referred to as *measured* FCM values and FCM values inferred from fitness gradients (Eq. 3.6) are referred to as *predicted* values.

The ability to predict FCM from fitness gradients can be of particular importance to the design and analysis of experimental evolution studies of fitness decoupling by making it possible to estimate fitness decoupling prior to conducting an experiment. In using predicted FCM values, however, it is necessary to assume that both particle and collective fitnesses are linear functions of traits (Eq. 3.4). If this assumption is not fulfilled, the predicted FCM value will deviate from the measured value. In this chapter, I investigate the accuracy of the FCM prediction in a bacterial population from an experimental evolution study performed by Hammerschmidt et al. (2014, data)

In the experimental evolution study of Hammerschmidt et al. (2014, data), collectives of *Pseudomonas fluorescens* were subjected to multilevel selection imposed by an artificially designed life cycle. Below I present a brief description of the experimental setup, see section 1.2.3.2 for a more detailed description.

P. fluorescens features two distinct morphotypes: a freely swimming smooth morphotype (S) that populates the broth of the liquid media, and the glue-producing wrinkly spreader morphotype (W) that forms mats on the surface of liquid media. Each life cycle consists of two growth phases: S→W and W→S, separated by bottlenecks (Fig. 4.1). The life cycle required a switch between S and W morphotypes. W→S phases were inoculated by W-morphotype cells and S-morphotype cells were sampled after W→S phase. S→W phases were inoculated by S-morphotype cells and W-morphotype cells were sampled after S→W phase.

Two variants of the life cycle were implemented in the experimental evolution study: *non-mixed* and *mixed* selection regimes. In the non-mixed regime, samples taken after W→S and S→W phases were independently used to inoculate collectives at the next phase. Therefore,

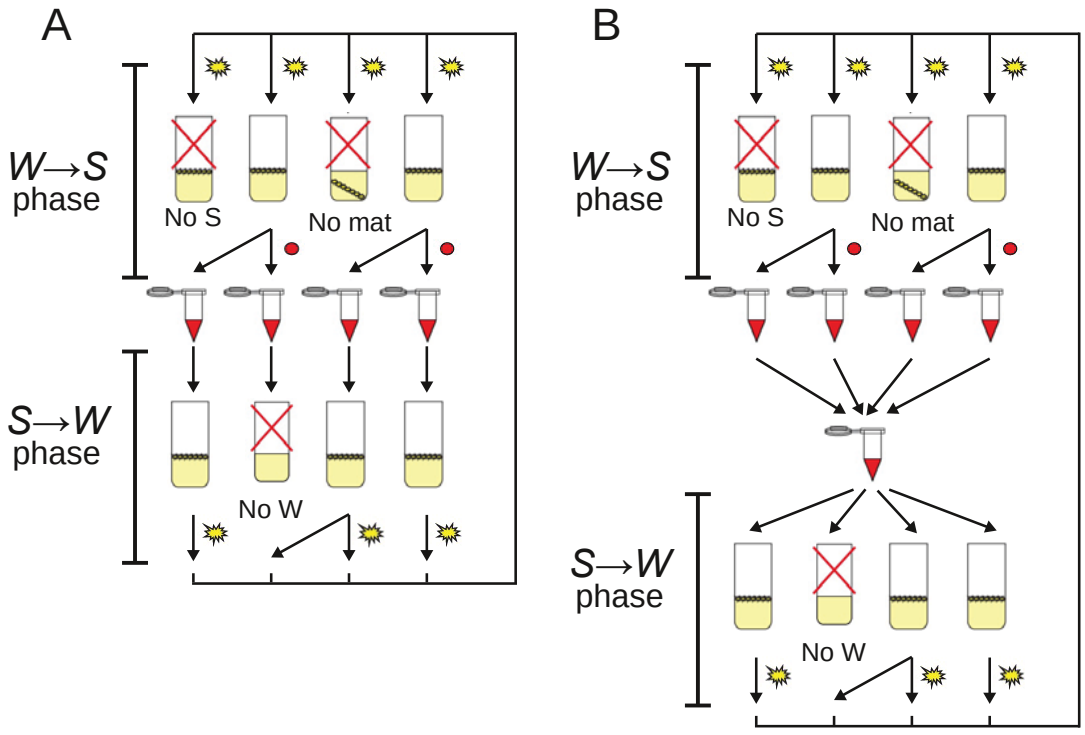

Figure 4.1: **Schemes of life cycles used in the experimental evolution study.** Panel A shows the scheme of life cycle used in the non-mixed selection regime. Panel B shown the scheme of life cycle used in the mixed selection regime. In both selection regimes, the life cycle consisted of two phases with bottlenecks between them. At the W→S phase, collectives were inoculated with W-morphotype cells. Only S-morphotype cells were sampled after W→S phase. Collectives with collapsed mats or without S-morphotype cells were considered extinct. The extinct collectives were replaced with samples from successful ones. At the S→W phase, collectives were inoculated with S-morphotype cells. Only W-morphotype cells were sampled after S→W phase. Collectives, which did not produce W-morphotype cells were considered extinct and were replaced with the samples from successful collectives. In the mixed regime, all samples taken after W→S phase were mixed together before inoculation of the following S→W phase. Adapted from Hammerschmidt et al. (2014)

at any phase each collective can be considered a descendant of a single collective that existed at the previous phase. By contrast, in the mixed regime, all samples taken after W→S phase were mixed together into a common pool. Collectives at the next S→W phase were inoculated by the mixed sample. Therefore, collectives at S→W phase in the mixed regime can be considered a descendant of all collectives that existed at the previous W→S phase. Evolution under the non-mixed selection regime resulted in decoupling between particle and collective fitnesses, so in at least one selection regime, selection at the collective level acted independently of selection at the level of cells.

In this chapter I tested the accuracy of the FCM prediction approach applied to the experimental evolution study performed by Hammerschmidt et al. (2014, data). This test showed that the accuracy of the predictive model is by an order of magnitude better than the difference between FCM values in mixed and non-mixed regimes. My findings show that the FCM can be reliably predicted in a complex experimental system under a wide range of selection regimes.

4.2 Methods

Section 4.2.1 describes the model that performs the evolution of the modelled population based on the selection regime used in the experimental evolution study of Hammerschmidt et al. (2014, data); this model is later referred to as the *simulative model*. Section 4.2.2 describes the model that calculates fitness gradients and from these computes the FCM; this model is later referred to as *predictive model*. Section 4.2.3 describes additional selective regimes, which provide a wide range of selective conditions beyond two experimentally studied regimes for assessment of the accuracy of FCM prediction.

4.2.1 The simulative model

The simulative model calculates the evolution of the model population under a given selection regime. The design of the simulative model is based on the setup of the experiment

performed by Hammerschmidt et al. (2014, data). This section contains a brief description of the simulative model; see Appendix 4.5.1 for further details.

The model population consists of $M = 10$ collectives. Each collective may contain multiple different *cell lines* that represent sets of identical cells, i.e. having the same growth rate (k), transition rate (p), and morphotype (W or S). Following the experimental setup, the cell lines within each collective are distributed between two niches: "mat" representing bacteria inhabiting the bacterial mat on the surface of liquid media, and "broth" representing the population inside the liquid media. In the model, cell lines in different niches grow independently of each other according to the logistic equation with carrying capacity shared among all cell lines in an ecological niche:

$$\frac{dN_i}{dt} = k_i N_i \left(1 - \frac{\sum_{i \in \text{niche}} N_i}{N_{\text{MAX}}}\right) \tag{4.1}$$

Here, N_i is the number of cells of i-th cell line; k_i is the growth rate of i-th cell line $\sum_{i \in \text{niche}} N_i$ is total size of the population within the same ecological niche; N_{MAX} is maximum population size in that ecological niche. Eq. 4.1 was numerically solved for both niches in each collective of the modelled population.

New cell lines emerge in the course of cell lines growth as a result of mutations with probability equal to:

$$P_i^{\text{mut}}(t, t + dt) = p_i \cdot (N_i(t + dt) - N_i(t)) \tag{4.2}$$

Here, $P_i^{\text{mut}}(t, t + dt)$ is the probability that i-th cell line will produce a new cell line in a time interval between t and $t + dt$; p_i is the transition rate of i-th cell line; $N_i(t)$ is the number of cells in i-th cell line at the time t.

The new cell line has W-morphotype with probability equal to 0.77, otherwise it has S-morphotype. The growth and transition rates of a new cell line are equal to the rates of the progenitor cell line with small random perturbation added.

The population is subjected to a selection regime which consists of two *phases*: W→S

phase and S→W phase (Figs. 4.2 and 4.3, steps 1 and 3). At the beginning of each phase, each collective in a population is inoculated with cell lines of a particular morphotype: W morphotype at the beginning of W→S phase and S-morphotype at the beginning of S→W phase. The cell lines of another morphotype are sampled after each phase to inoculate the next phase. So, cell lines of S-morphotype are sampled after W→S phase (Figs. 4.2 and 4.3, step 2) and cell lines of W-morphotype are sampled after S→W phase (Figs. 4.2 and 4.3, step 4). After two phases, the population returns to the initial morphotype and completes a single generation of the life cycle.

Collectives, which did not produce any cell line of the morphotype by the end of S→W or W→S phases were considered extinct. At the next phase, these collectives were inoculated by a randomly chosen sample. Thus, the total number of collectives remained constant.

The simulation run lasted for 30 life cycle generations. For each collective in each generation, traits (growth rate k and transition rate p) of the samples taken after S→W phase were recorded, so each collective is represented by a single cell line. The collective fitness and the average particle fitness were calculated from recorded growth and transition rates for each collective (see Appendix 4.5.2 for details of fitnesses calculation). For each simulation run, the FCM was calculated from collective and average particle fitnesses according to Eq. 4.3.

$$\text{FCM} = \frac{\langle (F_P - \langle F_P \rangle)(F_C - \langle F_C \rangle) \rangle}{\sqrt{\langle (F_P - \langle F_P \rangle)^2 \rangle} \sqrt{\langle (F_C - \langle F_C \rangle)^2 \rangle}} \tag{4.3}$$

Here, F_P is the particle fitness averaged within collectives; F_C is the collective fitness, $\langle x \rangle$ is the mean value of x where averaging is performed across all collectives in a population.

There were 500 independent simulation runs for each selection regime: mixed and non-mixed. The resultant FCM was calculated by averaging the FCM values across all independent simulation runs.

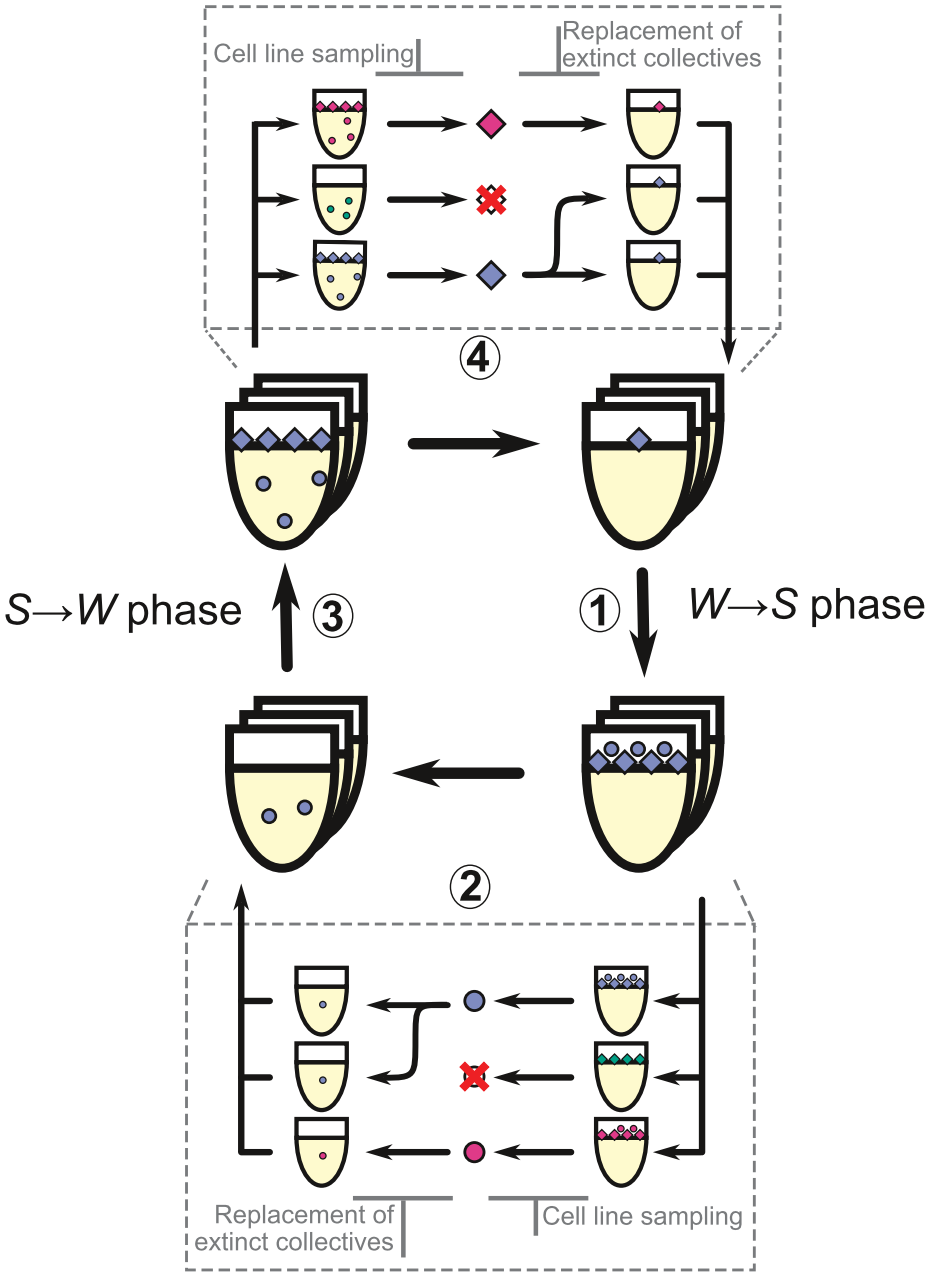

Figure 4.2: **Scheme of non-mixed life cycle in the simulative model**. Life cycle consists of two phases with two sampling procedures between them. (1) W→S phase starts with one W-cell in each collective, while S-cells emerge in the course of growth. (2) S-cells are sampled from each collective. Collectives, which did not produce S-cells are replaced. (3) S→W phase starts with S-cells in all collectives, W-cells emerge in the course of growth. (4) One W-cell is sampled from each collective, while collectives without W-cells are replaced. Circles represent S-morphotype cells, rhombuses represent W-morphotype cells. White and yellow areas in collectives represent "mat" and "broth" ecological niches, respectively.

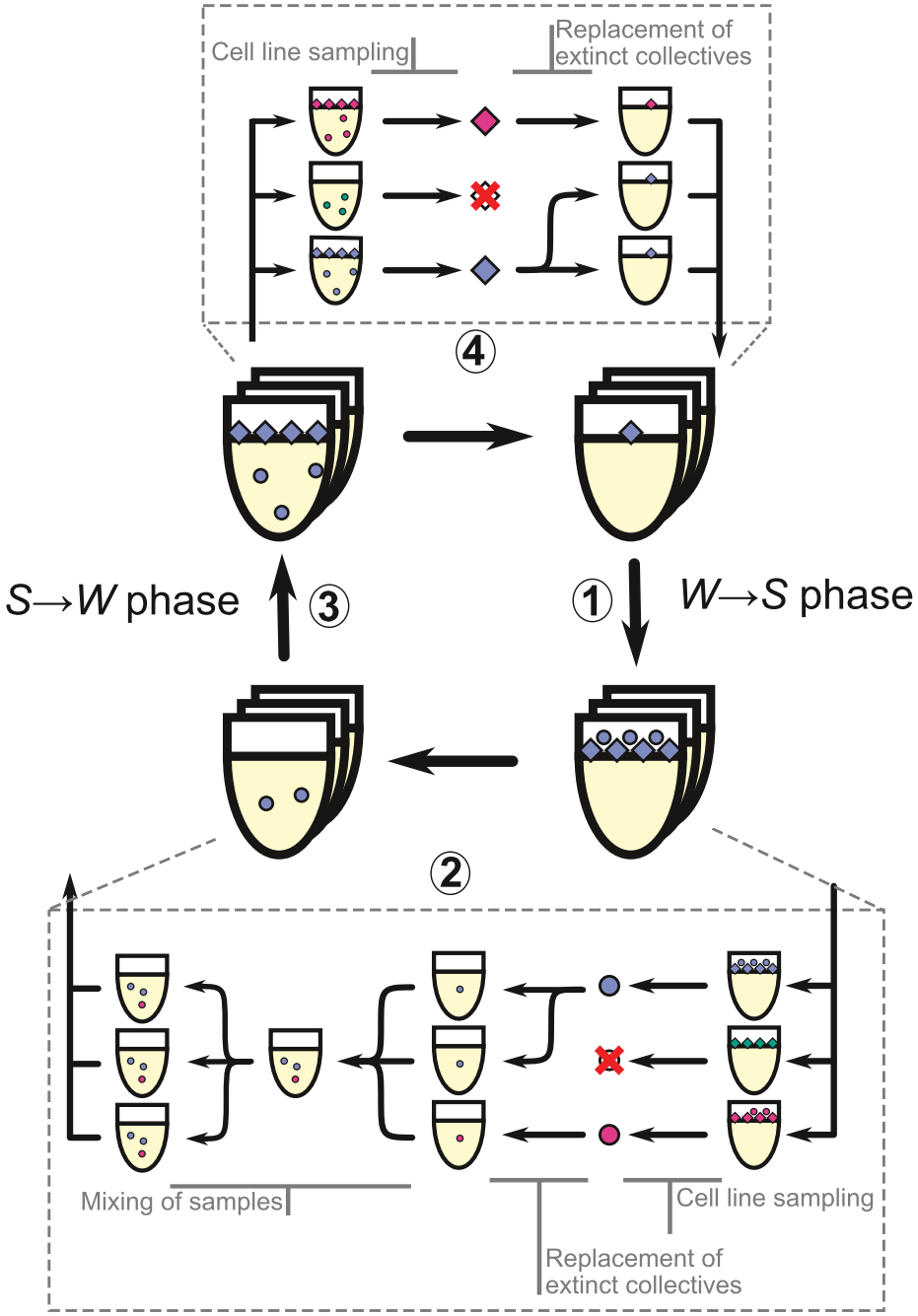

Figure 4.3: **Scheme of mixed life cycle in the simulative model**. Life cycle consists of two phases with two sampling procedures between them. (1) W→S phase starts with one W-cell in each collective, while S-cells emerge in the course of growth. (2) S-cells are sampled from each collective. Collectives, which did not produce S-cells are replaced. All samples are pooled together before inoculation of the next phase. (3) S→W phase starts with S-cells in all collectives, W-cells emerge in the course of growth. (4) One W-cell is sampled from each collective, while collectives without W-cells are replaced. Circles represent S-morphotype cells, rhombuses represent W-morphotype cells. White and yellow areas in collectives represent "mat" and "broth" ecological niches, respectively.

Table 4.1: **Parameters used in the simulative model.**

Parameter	Value
Number of runs for each selection regime	500
Number of life cycle generations in each run	30
Number of collectives in population	10
Maximal number of cells in ecological niche, N_{MAX}	10^7
Length of S→W (W→S) phase (days)	3 (6)
Probability for a mutant line to have W (S) morphotype	0.77 (0.23)
Initial growth rate, k_0 (days^{-1})	10.3
Variation of growth rate at mutation, v_k (days^{-1})	1
Initial transition rate, p_0	$3 \cdot 10^{-7}$
Variation of transition rate at mutation, v_p	$3 \cdot 10^{-8}$

4.2.2 The predictive model

The predictive model determines the FCM from the fitness gradients at the particle and collective levels without the simulation of evolution. This section contains a brief description of the predictive model, see Appendix 4.5.3 for further details.

In chapter three, I showed that FCM in a population with linear traits-to-fitness function can be calculated as

$$\text{FCM} = \frac{\alpha_{Pk}\alpha_{Ck} + \alpha_{Pp}\alpha_{Cp}}{\sqrt{\alpha_{Pk}^2 + \alpha_{Pp}^2}\sqrt{\alpha_{Ck}^2 + \alpha_{Cp}^2}} = \cos(\theta_{\overline{\alpha}_P\overline{\alpha}_C}) \tag{4.4}$$

Here, α_{Pk} and α_{Pp} are the components of the particle fitness gradient vector in the space of traits; α_{Ck} and α_{Cp} are the components of the collective fitness gradient; and $\theta_{\overline{\alpha}_P\overline{\alpha}_C}$ is the angle between the fitnesses' gradients.

Eq. 4.4 assumes that the trait values are uncorrelated ($\rho_T = 0$). Biological mechanisms responsible for expression of traits used in my model (growth and transition rates) are very different. The growth rate depends on rates of resource uptake and processing, while the transition rate depends on the performance of the replication machinery. Thus, it is unlikely that the growth and transition rates are causally connected in the experimental population, therefore, the predictive model assumes that these traits are non-correlated ($\rho_T = 0$).

Components of the fitness gradients in Eq. 4.4 are calculated in the space of scaled traits k' and p' in which variations in growth and transition rates in a given population are equal to each other.

The predictive model calculates the FCM according to Eq. 4.4. In order to apply Eq. 4.4, the predictive model infers the fitness gradients $\overline{\alpha}_P$ and $\overline{\alpha}_C$ from selection rules as a direction of the maximal increase in particle and collective fitness for the initial values of traits (k_0, p_0). The scheme of the extraction of fitness gradients and calculation of the FCM is presented in Fig. 4.4.

4.2.3 Additional selection regimes

A series of additional selection regimes has been developed to extend the set of investigated selection conditions beyond the two experimentally studied regimes. This section contains a brief description of the additional selective regimes, see Appendix 4.5.6 for further details.

In additional selective regimes (Fig. 4.5), the rules of selection, i.e. rules that determines which cell lines and collectives will survive at the end of each phase, was different from rules used in the experimentally investigated selection regimes. To incorporate the new rules of selection to the model, *guiding selective events* were imposed at the particle and collective levels. Each additional selection regime features a unique combination of guiding events at the particle and collective levels. The choice of the scoring function influences directions of the fitness gradients, so each additional selective regime features a unique set of rules of selection. So the whole set of regimes covered a wide range of selective conditions.

At the particle level, the guiding selective event replaced the procedure of cell line sampling used in the experimentally investigated selection regimes (Fig. 4.5, steps 2 and 4). The probability of the cell line of being sampled is proportional to the value of the particle scoring function $S_P(k, p)$, which is independently chosen for each additional regime from a list of eight functions: $S_P(k, p) \in \{k, kp, p, \frac{p}{k}, \frac{1}{k}, \frac{1}{kp}, \frac{1}{p}, \frac{k}{p}\}$. Thus, the set of particle scoring functions covers eight major directions of the particle-level selection in the space of traits (see Fig. 4.6 and Table 4.2).

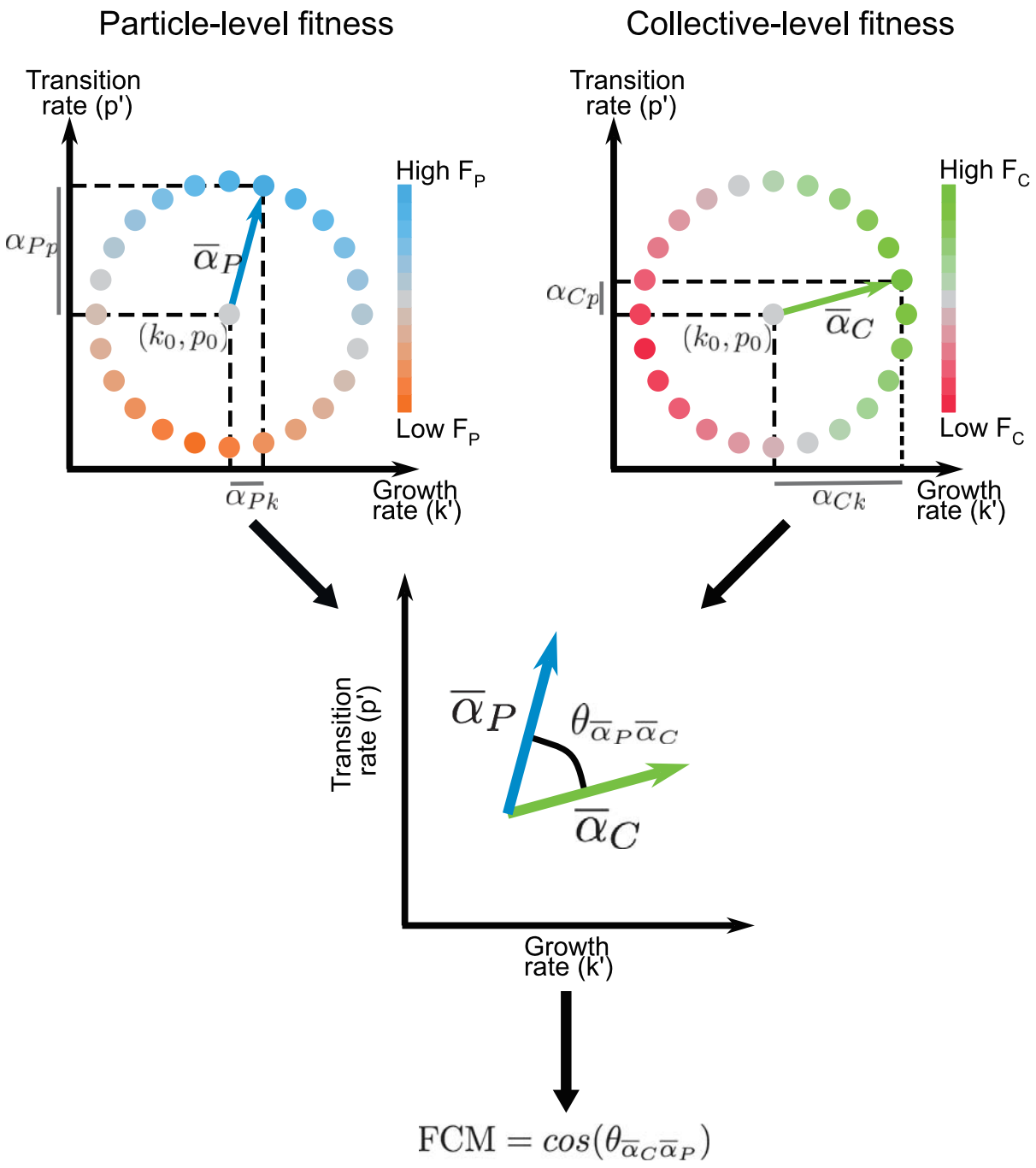

Figure 4.4: **Scheme demonstrating how the predictive model calculates the FCM**. The particle and collective-level fitness is calculated for a constructed set of cell lines that are evenly placed on the circle in the space of traits. The centre of the circle reflects the initial values of traits (k_0, p_0). The location of the cell line with the highest particle (F_P) or collective (F_C) fitnesses is used to calculate directions of the fitness gradients $\overline{\alpha}_P$ and $\overline{\alpha}_C$, respectively. The FCM is calculated as the cosine of the angle between the particle and collective fitness gradients $\mathrm{FCM} = \cos(\theta_{\overline{\alpha}_P\overline{\alpha}_C})$.

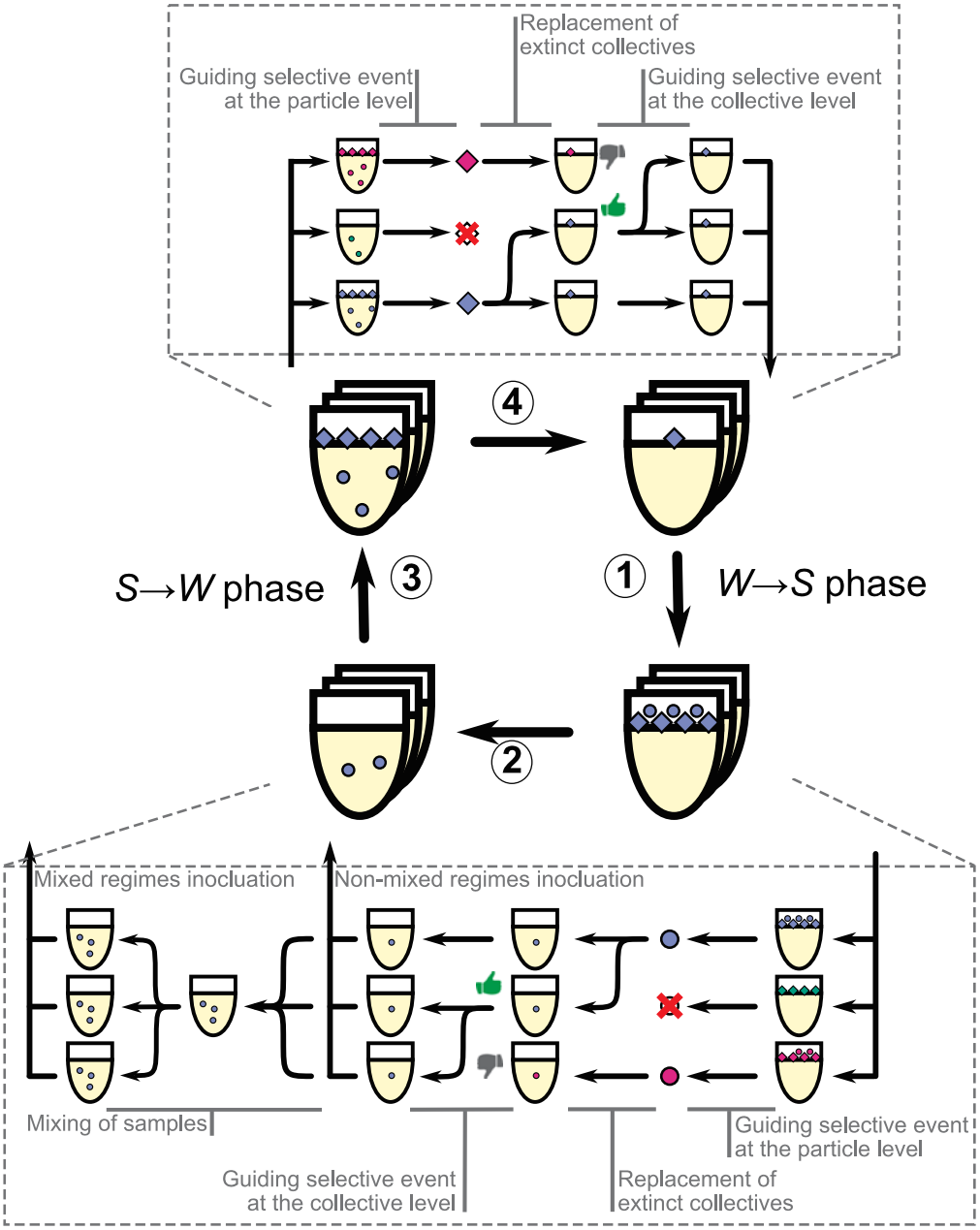

Figure 4.5: **Scheme of life cycle in additional selection regimes.** (1) W→S phase starts with one W-cell in each collective, while S-cells emerge in the course of growth. (2) S-cell lines are sampled from each collective by the guiding selective event. Collectives, which did not produce S-cell lines are replaced. Then in the guiding selective event, one collective is chosen to extinct while one other collective replaces it. In the mixed regime, all samples are pooled together before inoculation of the next phase. (3) S→W phase starts with S-cells in all collectives, W-cells emerge in the course of growth. (4) One W-cell is sampled from each collective, while collectives without W-cells are replaced. After that, the collective-level guiding selective event replaces one collective with one other. Circles represent S-morphotype cells, rhombuses represent W-morphotype cells.

Table 4.2: **Scoring functions in the additional selection regimes**. Each scoring function corresponds to the inclination angle of the fitness gradient with respect to the k-axis; see the scheme on Fig. 4.6.

Scoring function S	$grad(S)$ components: (α_k, α_p)	Inclination angle (degree)
k	$(1, 0)$	0
$k \cdot p$	$(\frac{1}{\sqrt{2}}, \frac{1}{\sqrt{2}})$	45
p	$(0, 1)$	90
p/k	$(-\frac{1}{\sqrt{2}}, \frac{1}{\sqrt{2}})$	135
$1/k$	$(-1, 0)$	180
$1/(k \cdot p)$	$(-\frac{1}{\sqrt{2}}, -\frac{1}{\sqrt{2}})$	225
$1/p$	$(0, -1)$	270
k/p	$(\frac{1}{\sqrt{2}}, -\frac{1}{\sqrt{2}})$	315

At the collective level, the guiding selective event is introduced after the replacement of the extinct collectives (Fig. 4.5, steps 2 and 4). A single collective is chosen to become extinct and another collective is chosen to replace the extinct collective. The probability to replace is proportional to the collective scoring function $S_C(k, p)$. The probability of going extinct is inversely proportional to the same scoring function. Therefore, collectives expressing larder values of the scoring function S_C gain a boost in the collective fitness, while collectives expressing low values of S_C are constantly removed from the population. Thus, the rules of selection at the collective level in additional selective regimes with different scoring functions are different. The collective scoring function used in the guiding event is independently chosen for each regime from the same list of functions as used at the particle level: $S_C(k, p) \in \{k, kp, p, \frac{p}{k}, \frac{1}{k}, \frac{1}{kp}, \frac{1}{p}, \frac{k}{p}\}$.

Each selection regime is determined by three components: selection pressure imposed by the guiding event at the particle level (eight variants of S_P), selection pressure imposed by the guiding event at the collective level (eight variants of S_C), and the organisation of the life cycle (two variants: mixed and non-mixed). In total, $8 \cdot 8 \cdot 2 = 128$ different additional selection regimes have been investigated, in addition to two selection regimes for which experimental data have been available.

In the simulative model, 500 independent runs have been computed for each additional

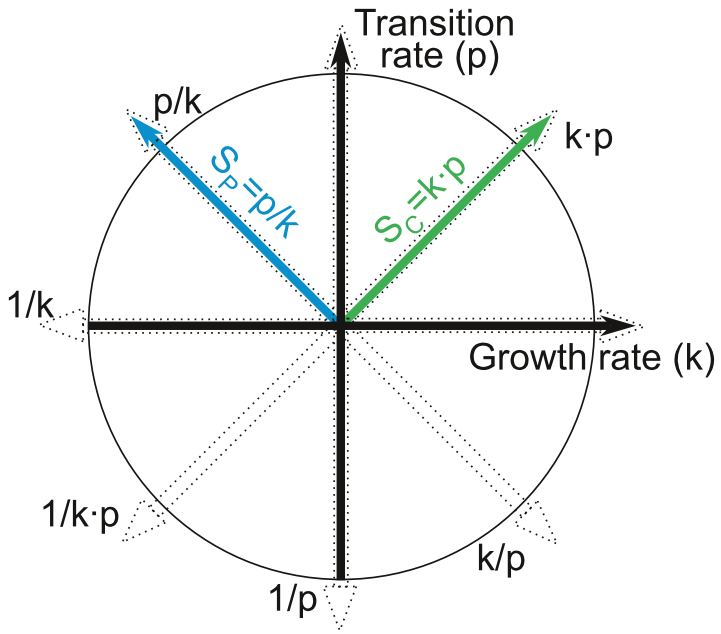

Figure 4.6: **Directions of scoring function gradients in the space of traits (k, p) for different variants of S_P and S_C.** Each additional selective regime uses one scoring function for the particle-level selection and one scoring function for the collective-level selection. The choice of the scoring functions influences the directions of particle and collective fitness gradients. The set of eight scoring functions ($S(k, p) \in \{k, kp, p, \frac{p}{k}, \frac{1}{k}, \frac{1}{kp}, \frac{1}{p}, \frac{k}{p}\}$) used in this study cover major directions in the space of traits. Directions of scoring function gradients imposed by guiding events in the selection regime with $S_P = \frac{p}{k}$ and $S_C = kp$ are highlighted.

regime. Each run lasted for 30 generations. FCM values have been calculated for the populations in the final generation. The resulting FCM provided by a selection regime was calculated by averaging the FCM values across all independent simulation runs.

4.3 Results

4.3.1 The predictive model calculates highly accurate FCM in both mixed and non-mixed selection regimes

I investigated how accurately FCM calculated from experimental data (Section 4.5.4) are reproduced by the predictive model (see appendix 4.2.2). FCM for experimental populations was obtained for two selection regimes: mixed and non-mixed (Fig. 4.7, panel C and panel D). For the non-mixed regime, the predicted FCM lies within the 95% confidence interval of the experimentally measured FCM (Table 4.3). For the mixed regime, in contrast, the predicted FCM lies outside of the 95% confidence interval of the experimentally measured FCM. Thus, the predictive model reproduces the FCM for the non-mixed regime but does not for the mixed regime. However, the difference between the predicted and experimentally measured FCM within each regime is smaller than the difference between the FCM obtained for different regimes. Therefore, the predictive model can reliably distinguish between the mixed and non-mixed selection regimes.

The accuracy of the predictive model can be estimated by observing the difference between predicted and measured FCM values. However, this difference is affected by the precision of the FCM measurement (see appendix 4.5.5). For example, in the non-mixed regime, the 95% confidence interval of the experimentally measured FCM $(-0.7, 0.27)$ is larger than the difference between predicted and measured FCM values, which is equal to 0.33 (Table 4.3). This difference may be explained by the statistical error of FCM measurement. Therefore, the accuracy of the predictive model in the non-mixed regime can be estimated as being at least 0.33.

Table 4.3: **FCM calculated from experimental data, predictive model and simulative model in the mixed and non-mixed regimes**. Upper and lower bounds outline 95% confidence intervals of the FCM obtained from experimental data and the simulative model, and estimated uncertainty of the predictive model. SEM is a standard error of mean for 500 independent populations calculated in the simulative model.

	Experimental data	Predictive model	Simulative model
Non-mixed regime	$-0.33^{+0.60}_{-0.37}$	$0^{+0.06}_{-0.06}$	$0.05^{+0.84}_{-0.97}$, SEM$= 0.02$
Mixed regime	$0.91^{+0.04}_{-0.48}$	$0.99^{+0.01}_{-0.01}$	$0.95^{+0.05}_{-0.19}$, SEM$= 0.01$

The simulative model (Section 4.2.1) has been developed to estimate the accuracy of the predictive model. The simulative model calculates evolution of the model population according to the rules used in the experimental setup and obtains the FCM from the distribution of fitnesses in the evolved population (Fig. 4.7, panel E and panel F). The FCM measured for the experimental and simulated populations lie within each other's 95% confidence intervals (Table 4.3), so the simulative model can be used as a proxy of the experiment. The simulative model also measured the mean FCM with higher accuracy than experimental data (SEM ≤ 0.02) due to the large number of independent simulations. Thus, the comparison of results obtained by the predictive and simulative models allowed an estimation of the accuracy of the predictive model.

In the non-mixed regime, the difference between simulated and predicted FCM values is $0.05 - 0 = 0.05$. This is smaller than the accuracy of the predictive model, which is equal to 0.06 (see Table 4.3). Thus, in the non-mixed regime, the accuracy of the predictive model is smaller than 0.05. In the mixed regime, the difference between predicted and simulated FCM values is $0.99 - 0.95 = 0.04$ which is higher than the accuracy of both models at 0.01 (see Table 4.3). So for the the mixed regime, the accuracy of the predictive model can be estimated as 0.04. Results show that the accuracy of the predictive model is an order of magnitude smaller than the difference between FCM values obtained in mixed and non-mixed selection regimes ($\text{FCM}_{\text{mixed}} - \text{FCM}_{\text{non-mixed}} \approx 1$).

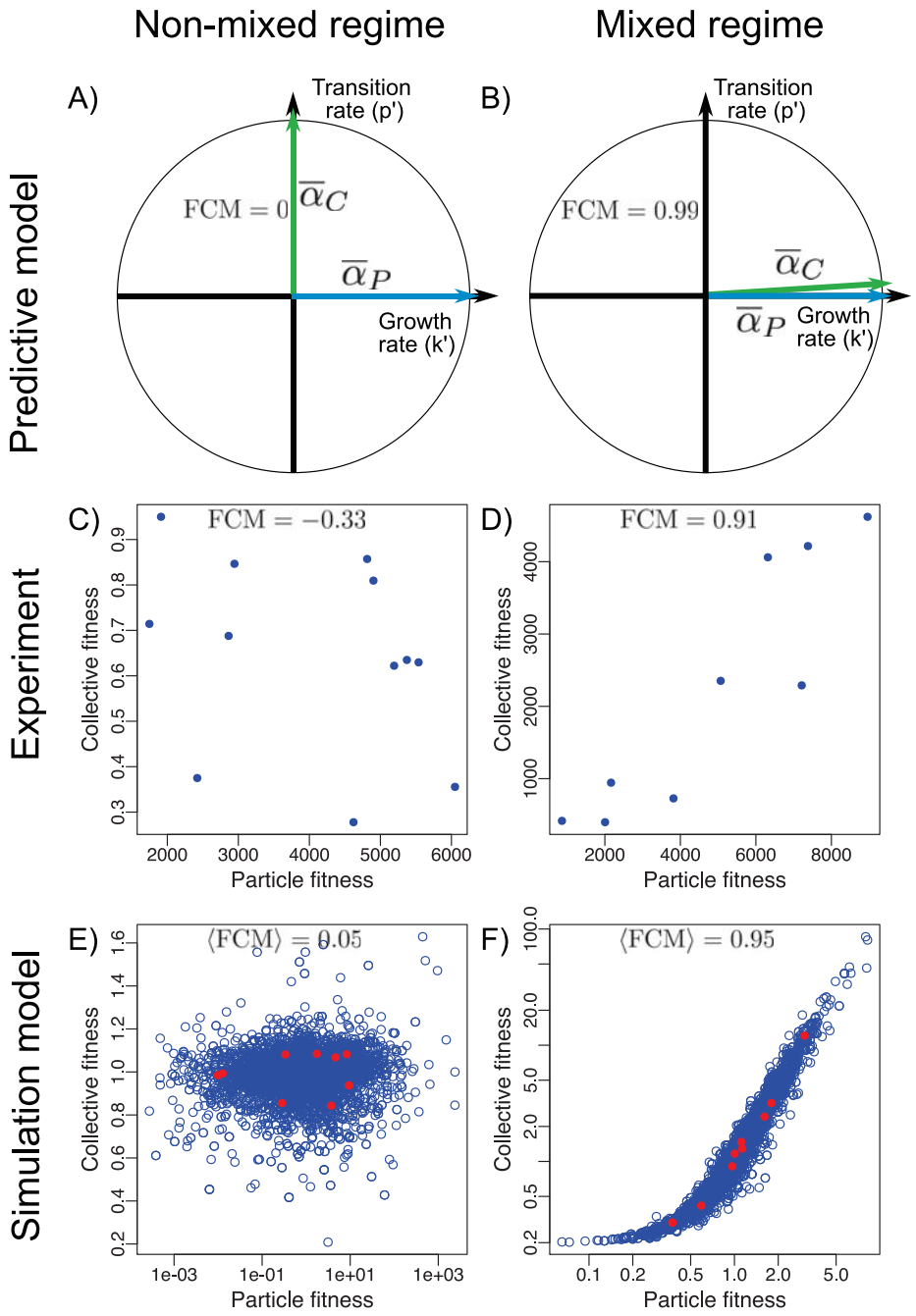

Figure 4.7: **FCM values in mixed and non-mixed selection regimes significantly differs between regimes.** Panels A and B show FCM from fitness gradients by the predictive model in non-mixed and mixed regimes, respectively. Vectors α_P (blue arrow) and α_C (green arrow) represent gradients of particle and collective fitnesses in the space of traits, respectively. Panels C and D show the FCM measured from experimental data in non-mixed and mixed regimes, respectively. Each dot represents a single independent population. Panels E and F show the FCM calculated by the simulative model in non-mixed and mixed regimes, respectively. Each circle represents a single collective. Sets of red dots represent collectives from a single independent run of simulation.

4.3.2 In additional selection regimes, predicted and simulated FCM are highly correlated

To test the accuracy of predictions arising from the FCM under a range of selective conditions, which have not been studied experimentally, a set of 128 additional selection regimes have been analysed (see Section 4.2.3). The additional selection regimes are based on the experimental life cycles: 64 regimes used the non-mixed life cycle and 64 used the mixed life cycle. Each regime is characterised by a unique combination of fitness gradients at the particle and collective level. So, the whole set of additional regimes covers a wide range of selective conditions.

The FCM obtained by predictive and simulative models are highly correlated (see Fig. 4.8). Pearson's correlation coefficient between predicted and simulated FCM for non-mixed regimes is equal to $r = 0.88$ and for mixed regimes is equal to $r = 0.93$. Such high correlation confirms that the predictive model can assess the FCM value with high accuracy. Collectively, my results support that the directions of the fitness gradients at the particle and collective levels are the key factor in determining FCM and, as a result, these directions primarily determine the fitness (de-)coupling state in the course of evolution.

4.3.3 The mixing procedure determines collective-level selection in additional mixed regimes

The co-distributions of predicted and measured FCM values differs between mixed and non-mixed regimes: FCM obtained in mixed regimes are clustered into distinct groups, while no clustering is observed in non-mixed regimes (Fig. 4.8). However, the design of the additional selective regimes make each regime express a unique combination of selection rules at the particle and collective levels and no clustering of selection rules by any character is embedded into models. Below, I investigated what caused the emergence of clusters in mixed selection regimes.

Clusters of selection regimes (Fig. 4.8, panel B) exhibit similar predicted FCM, which

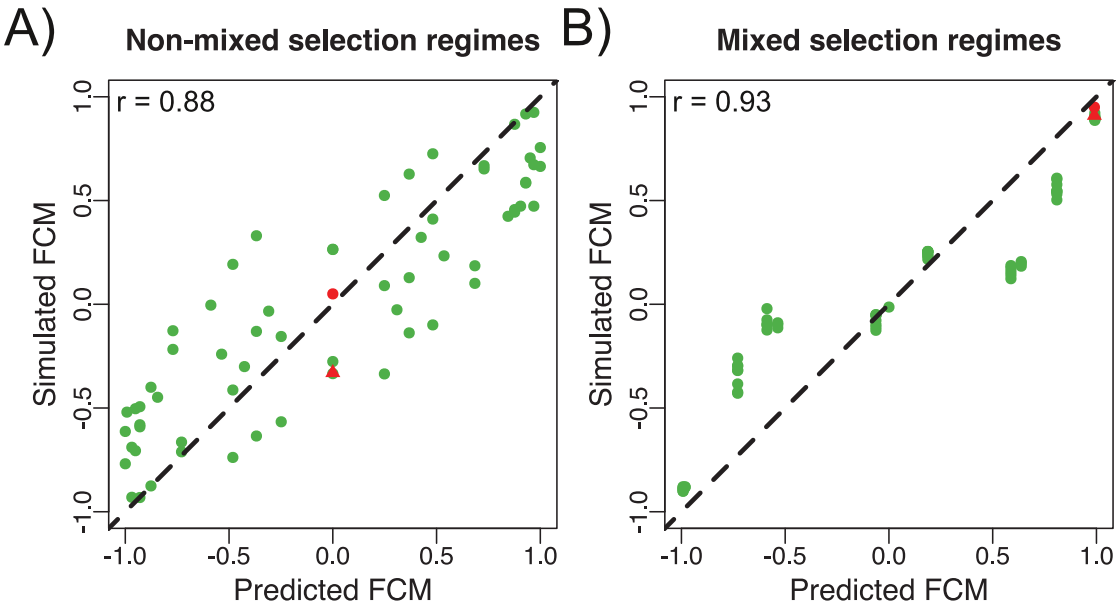

Figure 4.8: **Predicted and simulated FCM are highly correlated in additional selection regimes**. Panel A is non-mixed additional regimes. Panel B is mixed additional regimes. Every green circle represents a single selection regime. Pearson's correlation coefficient r shows a high level of correlation between predicted and simulated FCM in the additional selection regimes. The red circles represent the FCM calculated in the experimentally investigated non-mixed and mixed regimes by predictive and simulative models. The red triangles represent the FCM as determined by the experimental data and obtained by the predictive model in the experimentally investigated non-mixed and mixed regimes.

indicates that the directions of fitness gradients may be similar in these regimes. To confirm this I obtained the directions of fitness gradients operating at the particle and collective levels (Fig. 4.9) using the predictive model (Section 4.2.2), while directions of gradients of fitness component imposed by guiding selective events were obtained from scoring function gradients (Table 4.2).

Results presented in Fig. 4.9 indicate that guiding selective events are not the only factor affecting selection operating in population at the collective level. Other factors are the requirement to produce a novel morphotype by the end of each phase of the life cycle and the competition among cell lines within the mixed inoculation sample. Therefore, the directions of selection operating in a population is different from directions imposed by guiding selective events.

To find the contribution of guiding events I performed the fitting of fitness gradients ($\overline{\alpha}_P$ and $\overline{\alpha}_C$) found by the predictive model by linear combination of selection pressures imposed by the life cycle and guiding events (see appendix 4.5.7 for details):

$$\begin{aligned} &\measuredangle(\overline{\alpha}_P, \overline{\beta}_P) = \epsilon_P \to 0 \\ &\measuredangle(\overline{\alpha}_C, \overline{\beta}_C) = \epsilon_C \to 0 \\ &\overline{\beta}_P = grad(S_P) + Y_P \cdot grad(S_C) + \overline{Z}_P \\ &\overline{\beta}_C = X_C \cdot grad(S_P) + grad(S_C) + \overline{Z}_C \end{aligned} \tag{4.5}$$

Here, $\measuredangle(\overline{\alpha}, \overline{\beta})$ is an angle between vectors $\overline{\alpha}$ and $\overline{\beta}$; $\overline{\alpha}_P$ and $\overline{\alpha}_C$ are vectors of fitness gradients obtained using the predictive model; $\overline{\beta}_P$ and $\overline{\beta}_C$ are vectors of the fitted directions of selection at the particle and collective levels; $grad(S_P)$ and $grad(S_C)$ are the gradients of the scoring functions that represent the component of selection imposed by the guiding selective events at the particle and collective levels, respectively (see Table 4.2); X_C is the influence of the particle-level guiding event on selection operating at the collective level; Y_P is the influence of the collective-level guiding event on selection operating at the particle level; $\overline{Z}_P = (Z_{Pk}, Z_{Pp})$ and $\overline{Z}_C = (Z_{Ck}, Z_{Cp})$ are the impact of selection imposed by the life cycle (mixed or non-mixed); ϵ_P and ϵ_C are the residual errors, which were minimised in

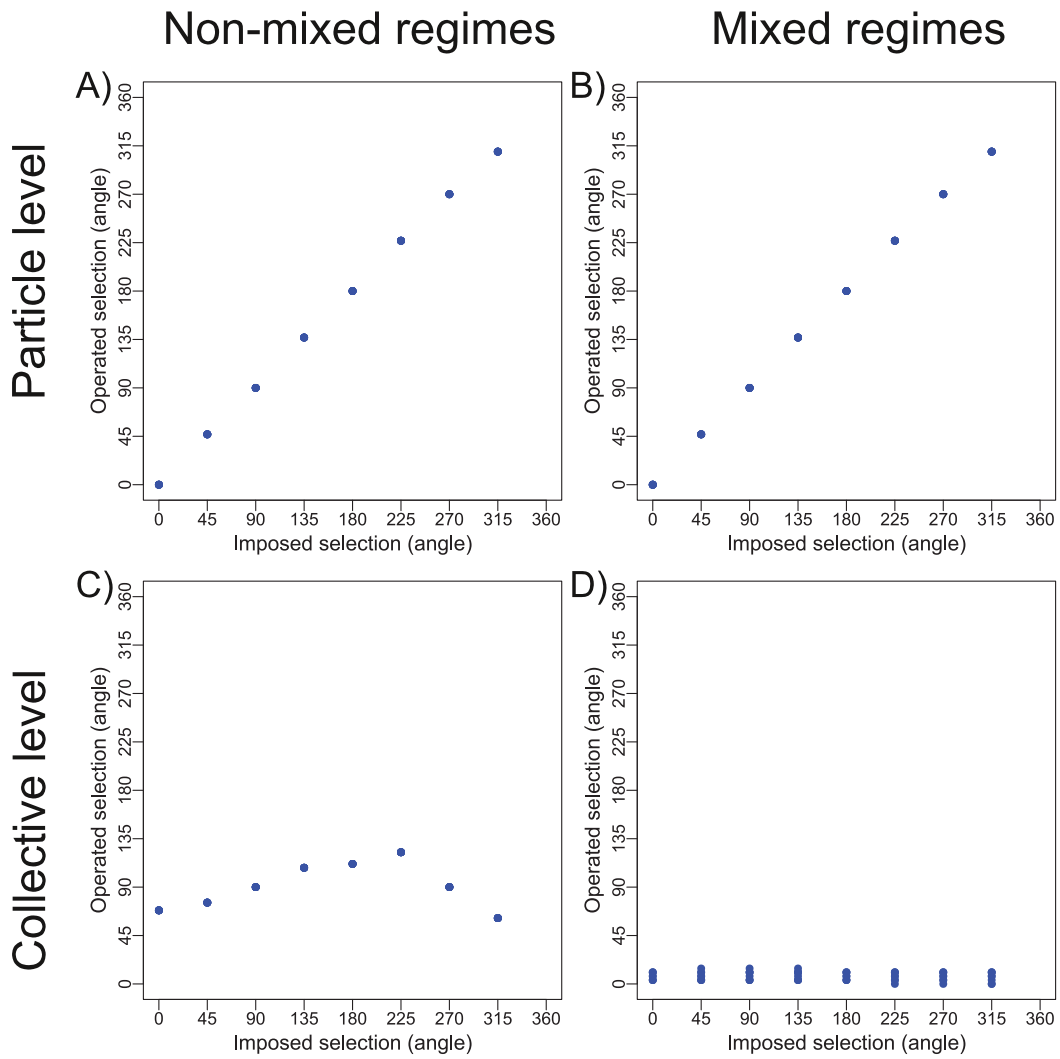

Figure 4.9: **At the particle level, guiding events determine the direction of fitness gradients, while at the collective level the guiding events are not the only factor of selection.** Directions have been characterised by the angle between the direction vector and the $k-$axis in the space of traits (k, p). Directions of fitness gradients at the particle level are similar to directions imposed by the guiding selective events – panel A in non-mixed and panel B in mixed regimes. Panel C shows that in non-mixed regimes, selection operating at the collective level is significantly different from selection imposed by guiding selective events. The direction of the fitness gradient is close to 90^0, which corresponds to selection for the transition rate p (Table 4.2). Panel D illustrates that in mixed regimes the direction of fitness gradient at the collective level is close to 0^0, which corresponds to selection for the growth rate k.

the fitting.

Data obtained for mixed and non-mixed selection regimes were fitted separately (Table 4.4).

Table 4.4: **Impact of the different components of selection on the fitness gradients at the particle and collective levels in additional selection regimes.** X is the relative strength of selection imposed by guiding events at the particle level; Y is the relative strength of selection imposed by guiding events at the collective level; Z_k is the relative strength of selection for the growth rate imposed by the life cycle; Z_p is the relative strength of selection for the transition rate imposed by the life cycle.

		X	Y	Z_k	Z_p
Non-mixed regimes	Particle level	1	$< 10^{-6}$	-0.02	-0.02
	Collective level	$< 10^{-6}$	1	-0.02	2.03
Mixed regimes	Particle level	1	$< 10^{-6}$	-0.02	-0.02
	Collective level	5.98	1	68.2	8.69

At the particle level, the guiding selective event applied at that level is the most influential factor of selection in both mixed and non-mixed additional selection regimes ($X = 1$ in Table 4.4). The effect of the selection regime itself is minimal ($|\overline{Z}| < 0.1$). The effect of the guiding selective event applied at the collective level is absent ($Y < 10^{-6}$). Thus, selection operating at the particle level is identical to selection imposed by the guiding selective event.

In non-mixed regimes, selection operating at the collective level is strongly influenced by the pressure imposed by the life cycle ($Z_p = 2.03$ in Table 4.4). This component represents the selection pressure encouraging collectives to produce cell lines of the novel morphotype to avoid the extinction of collectives at the end of each phase of the life cycle. Selection imposed by the guiding selective event at the collective level has an impact twice as weak as imposed by the life cycle ($Y = 1$ in Table 4.4). This explains why the direction of selection operating at the collective level generally promotes the transition rate p in non-mixed regimes (see Fig. 4.9, panel C).

In mixed regimes, selection acting at the collective level is influenced by all three of the considered factors (see Table 4.4). The strongest, most influential factor is selection for the highest growth rate k imposed by the life cycle ($Z_k = 68.2$). This is caused by competition of cell lines from different collectives in the mixed sample . The cell line with the highest growth rate k has the largest share of the "broth" niche during the following S→W phase (see Fig. 4.5). The fast growing cell line produces more W-morphotype cell lines than its competitors and this increases the chance that one of them will be sampled after S→W phase to inoculate the next W→S phase. Therefore, the collective containing cell lines with the highest growth rate is likely to produce more collective-level offspring. The same argument holds true for the transition rate p – a higher transition rate means more offspring W-morphotype cell lines in the S→W phase; however, the effect is weaker than high growth rate at $Z_p = 8.69$ (Table 4.4). Similarly, high particle fitness increases the chances of the offspring W-morphotype cell lines being sampled after the S→W phase, so selection imposed at the particle fitness has a strong impact on selection at the collective level $X = 5.98$ (Table 4.4). Thus, in mixed regimes, the selection pressure provided by the guiding selective event at the particle level is the weakest factor of selection at the collective level.

The results presented in Fig. 4.9 and Table 4.4 confirm the hypothesis that populations evolve under similar selection pressure in the regimes that clusters together (Fig. 4.8, panel B). In mixed regimes, selection at the collective level imposed by the guiding events has almost no effect in comparison to the selection pressure imposed by the mixing of samples ($Z_k \approx 70$). Therefore, the direction of selection at the collective level is similar in all mixed selection regimes. Any two selection regimes with the same scoring function at the particle level evolve under similar selective conditions which leads to similar predicted and simulated FCM values, i.e. clusters of FCM values in Fig. 4.8.

4.4 Discussion

Earlier in this chapter, I demonstrated that the predictive model calculates FCM with a high degree of accuracy in the studied selection regimes. The deviation between predicted and experimentally measured FCM was by an order of magnitude smaller than the difference of FCM between mixed and non-mixed regimes (Table 4.3). Furthermore, in additional regimes, the predicted FCM had a high correlation to values measured by the simulative model (Fig. 4.8). The predictive model calculates the FCM from the rules of selection (Section 4.2.2) and provides the FCM of a given population before evolution takes place. Thus, FCM can be reliably predicted from the rules of selection. This high accuracy of prediction confirms that the relationship between directions of fitness gradient at the particle and collective levels is the key factor of fitness decoupling.

The directions of fitness gradients inferred by the predictive model reveal the underlying mechanism of fitness decoupling. For instance, the predictive model confirms that fitness decoupling in the non-mixed selection regime was caused by the two-phase life cycle. According to Eq. 4.4, fitnesses are decoupled when fitness gradients in the space of traits are orthogonal to each other. Directions of fitness gradients identified by the predictive model in the non-mixed regime (Fig. 4.7, panel A) show that multilevel selection promotes different traits at particle and collective levels. At the particle level, selection promotes growth rate (see also Appendix 4.5.2.1). At the collective level, selection promotes transition rate (see also Appendix 4.5.2.2). Collective-level selection is the result of the two-phase life cycle that punished collectives unable to produce novel morphotypes. Thus, the two-phase life cycle results in fitness decoupling.

By contrast, my model shows that selection in the mixed regime favours the growth rate at both particle and collective levels. Collectives inoculated by mixed samples are likely to be the offspring of collectives that contained faster growing cell lines. Therefore, selection pressure imposed by mixing of inoculation samples promotes the growth rate. The predictive model showed that selection for growth rate is much stronger than selection for the transition rate imposed by the two-phase life cycle (see Fig. 4.7, panel B and components Z_k and Z_p for

mixed regimes in Table 4.4). So, for the mixed regime, selection operating at the collective level is determined mostly by the mixing event and, thus, is a by-product of selection at the particle level. Hence, the mixing of inoculation samples caused fitness coupling.

Additional selective regimes showed that the choice of selection rules in the guiding selective events has a major impact on the fitness (de-)coupling in the modelled population. The analysis of various combinations of guiding selective events applied at both the particle and collective levels revealed that FCM varies in the range $(-1, 1)$ in both mixed and non-mixed life cycles (Fig. 4.8). This implies that the life cycle (mixed, non-mixed) does not fully determine the fitness (de-)coupling state. For instance, fitnesses are coupled in non-mixed additional selective regime in which the guiding event at the particle level promotes transition rate (i.e. if $S_P = p$, see Fig. 4.6). Selection at both particle and collective levels has the same direction in the space of traits, so fitnesses are coupled. This shows that the choice of selection rules has a large impact on the fitness (de-)coupling, which is comparable to the influence of selection imposed by the life cycle.

Collectively my results provide a framework capable of predicting the fitness (de-)coupling state in an experimental population subjected to multilevel selection. In this study the predictive model was developed to the single experimental setup; however, such models can be constructed for any population subjected to multilevel selection. The predictive model is a new tool that can be used to design evolutionary experiments and to analyse experimental results. This approach is a step toward a unified model of the emergence of multicellularity.

4.5 Appendix

4.5.1 A detailed description of the simulative model

This section contains a detailed description of the simulative model. In section 4.5.1.1, the population state is described, i.e. population structure, cell lines and their parameters. In section 4.5.1.2, the evolution of the population in mixed and non-mixed regimes is explained.

Table 4.5: **Traits of cell lines in the simulative model.**

Trait	Role in the model
Growth rate, k	The rate of increase in the cell number.
Transition rate, p	The rate of production of new cell lines.
Morphotype, $\{$S, W$\}$	Affects the placement of cell line in ecological niche, and survival in bottlenecks.

4.5.1.1 Population structure, cell lines and traits

The population consists of $M = 10$ collectives. Each collective may contain several different *cell lines*. Every cell line represents a set of identical cells, i.e. all cells that share the same values of three traits: morphotype, growth rate (k) and transition rate (p) – see Table 4.5.

The *morphotype* trait can be either W-morphotype or S-morphotype; they represent glue-producing wrinkly spreader cells and freely swimming smooth cells, respectively. The morphotype affects the ecological niche where the cell line is located. Each cell line in a collective can exploit one of two ecological niches, later referred to as "broth" and "mat". These niches represent two environments in the experimental evolution study (Hammerschmidt et al. 2014). Each cell line is placed in the ecological niche at the moment of its appearance and remains there. W-morphotype cell lines are always located in the "mat" niche. The niche of the S-morphotype cell line is determined by a cell line's life history. If the S-morphotype cell line is used to inoculate the collective, then this cell line is put into the "broth" niche. If the S-morphotype cell line emerged from the another cell line as a result of mutation, then it remains in the same niche as the progenitor line.

The rule of assignment of morphotypes to ecological niches is a simplified representation of processes that occurred in the experimental evolution study of Hammerschmidt et al. (2014). There is no guarantee that cells cannot migrate between ecological niches, as assumed in the model. However, the selection regime forces the switch between W and S morphotypes, so S-migrants from "broth" to "mat" are unlikely to have any impact on the re-

sult of W-morphotype sampling. Therefore, the effect of possible migration between niches on the result of evolution is negligible, and as such, migration is ignored in the model.

The *growth rate* trait determines how fast a cell line grows. All cell lines located in the same ecological niche compete for the shared pool of resources. The growth of the i-th cell line in its ecological niche is determined by a logistic differential equation with the carrying capacity shared among multiple lines:

$$\frac{dN_i}{dt} = k_i N_i \left(1 - \frac{\sum_{i \in \text{niche}} N_i}{N_{\text{MAX}}}\right) \tag{4.6}$$

Here, N_i is the number of cells of i-th cell line; k_i is the growth rate of i-th cell line; $\sum_{i \in \text{niche}} N_i$ is total size of the population within the same ecological niche; N_{MAX} is maximum population size in that ecological niche. Eq. 4.6 was numerically solved for both niches in each collective of the modelled population.

The independence of cell growth in each ecological niche is a simplification of ecological interactions between niches. In the experiment, the growth of cells is limited by access to oxygen from the atmosphere; as such, cells in the mat, located in the air-liquid interface, have exclusive access to this resource. While the mat niche has low population, the broth has free access to the oxygen; however, the well-developed mat blocks the oxygen flow to the media, so cells in the broth are unable to grow. Several models of microcosm ecology have been investigated in preliminary simulations. The following models have been investigated: model in which S-cell lines in the mat have exclusive access to oxygen, the non-consumed part of the oxygen flow is delivered to the W-cell lines in the mat, the remainder of the oxygen flow goes to broth niche; model in which S- and W-cell lines in the mat have independent access to different oxygen flows, and remainder of the oxygen flow is diffused to the broth niche; model in which S- and W-cell lines in the mat share the same ecological niche with exclusive access to oxygen flow, and broth niche consumes the remainder of the flow. Preliminary simulations have shown that the result of selection is similar in all models of microcosm ecology, so the simplest ecological structure with two independent niches has been implemented in the simulative model.

The *transition rate* trait determines how frequently new cell lines emerge. The i-th cell line can produce a new cell line with the probability p_i per cell division. The newly emerged cell line has an initial population equal to 1. The traits of the new cell line are calculated based on the trait values of the parent line. The growth rate is a random number from the normal distribution with the mean equal to the parent line's growth rate and the standard deviation equal to $v_k = 1$. The transition rate of the new cell line is a random number from the normal distribution with the mean equal to the parent line's transition rate and the standard deviation equal to $v_p = 3 \cdot 10^{-8}$. The new line has W-morphotype with a probability of 0.77 or S-morphotype with a probability of 0.23 (Table 4.1). The new cell line is immediately put into the appropriate ecological niche. The influence of the newly emerged cell line on the growth of other cell lines is taken into account at the next step of the numerical solution of Eq. 4.6.

The values of the initial growth and transition rates (k_0, p_0), and the probabilities for a transition to the W/S morphotypes were chosen to mimic the extinction rates from the first generation of the life cycle in the experimental evolution study. The values of traits' variation at mutation v_k and v_p were chosen to be equal to 10% of initial traits' values k_0 and p_0. This way, the single mutation cannot lead to a significant change in traits' values but tens of mutations are able to significantly change the trait value (about 60 mutations are expected in each survived cell line by the end of the simulation run).

4.5.1.2 The life cycle

The life cycle is based on the experimental setup used by Hammerschmidt et al. (2014). The life cycle consisted of two *phases*, later referred to as W→S phase and S→W phase (Figs. 4.2 and 4.3, steps 1 and 3). At the beginning of each phase, the population is inoculated with cell lines of a particular morphotype: W morphotype at the beginning of W→S phase and S-morphotype at the beginning of S→W phase. In each phase, new cell lines with another morphotype may have emerged as a result of mutation (Section 4.5.1.1). The cell lines of another morphotype are sampled after each phase to inoculate the next phase. So, cell lines of S-morphotype are sampled after W→S phase (Fig. 4.2 and 4.3, step 2) and cell lines of

W-morphotype are sampled after S→W phase (Fig. 4.2 and 4.3, step 4). Samples are used to inoculate the population at the next phase of the life cycle. After two phases, the population returned to initial morphotype and completed a single generation of the life cycle.

Two selection regimes were studied in the experiment: *mixed* and *non-mixed*. These selection regimes were different in the manner in which inoculation samples were obtained after the W→S phase.

In the non-mixed selection regime, after the W→S phase a small sample of S-morphotypes cells were sampled from each collective (see Fig. 4.2, step 2). The sample from any given collective contains all S-morphotype cell lines present in this collective by the end of the W→S phase. However, different cell lines contribute a different number of cells, proportional to the number of cells in that cell line at the end of the W→S phase (N_i). Each sample was used to independently inoculate collectives at the start of the next S→W phase.

In the mixed selection regime, an additional mixing procedure occurred after the W→S phase, after taking inoculation samples. All samples taken were mixed together and this mixture used to inoculate all collectives at the next S→W phase (see Fig. 4.3, step 2). Thus, all inoculation samples became identical to each other and each sample contained the mixture of all S-morphotype cell lines present in the population at the end of W→S phase. The sampling after S→W phase is identical in both the mixed and non-mixed regimes (Figs. 4.2 and 4.3, step 4). After S→W phase, a single W-morphotype cell line was sampled from each collective to inoculate collectives at the next phase. The probability of a cell line being selected is proportional to the number of cells in this line (N_i) by the end of S→W phase.

Collectives that do not produce any cell line of a novel morphotype by the end of S→W or W→S phases were considered extinct. At the next phase, these collectives were inoculated by a randomly chosen sample. Thus, the total number of collectives remained constant.

The mechanism of extinctions used in the model is a simplified representation of extinction as it occurred in the experiment. In the experiment, the collapsed mat also caused the extinction of the collective. The concept of mat collapse is ignored in the developed model for two reasons. First, the number of extinctions caused by collapsed mats was much smaller

than the number of extinctions caused by absence of novel morphotype, so mat collapse was not the main source of selection pressure. Second, the rate of mat collapse did not change significantly in the course of evolution, therefore, the selection did not improve the robustness of mats in the modelled experiment. As such, mat collapse events were not included in the model.

The population in each run of the simulation contained ten collectives. At the beginning of each simulation run, all collectives in the population were inoculated with a single cell with traits $k_0 = 10.3$ and $p_0 = 3 \cdot 10^{-7}$. There were 500 independent simulation runs for each selection regime and each lasted 30 life cycle generations or 60 phases. The summary of the calculation parameters is presented in Table 4.1.

The results of a simulation run is a collection of growth (k) and transition (p) rates of the cell lines in each collective in each generation. Traits of the samples taken after S→W phase have been recorded, so each collective is represented by a single cell line. Inferred data have been used to measure FCM as described in section 4.5.2.

4.5.2 Measurement of the FCM in the simulative model

The FCM for each selection regime was calculated from traits, in three steps: 1) calculation of particle fitness for each cell line present in a population at the end of the simulation (Section 4.5.2.1); 2) calculation of collective fitness for each collective present in a population at the end of the simulation (Section 4.5.2.2); and 3) calculation of the average correlation coefficient between particle and collective fitnesses across 500 independent simulation runs (Section 4.5.2.3). Details of each step are described in the subsections below.

4.5.2.1 Calculation of particle fitness in the simulative model

Selection at the particle level operates amongst cell lines located in the same collective. The life cycle requires the collective to produce novel morphotype by the end of each phase. Within each collective, multiple cell lines of novel morphotype may emerge. To pass to the next phase, the cell line should be sampled (Figs. 4.2 and 4.3, steps 2 and 4). Therefore,

the particle fitness of a cell line characterises how well the cell line passes to the sample in comparison to other cell lines in the same collective.

The sampling rules differ between phases. A sample taken after the W→S phase contains all S-morphotype cell lines present in a collective in amounts proportional to the number of cells in this cell line by the end of the W→S phase. By contrast, a sample taken after S→W phase contains only one W-morphotype cell line; the probability of the cell line being sampled is also proportional to the number of cells in this cell line by the end of W→S phase. Despite the differences, sampling rules after W→S and S→W phases similarly favour cell lines that contain a higher number of cells than other cell lines within the same collective. Hence, particle fitness has been characterised as the capability of the cell line to grow in numbers in the presence of competitor cell lines.

The particle fitness of the cell line (later referred to as *tested* cell line) has been measured in a growth competition with the constructed *reference* cell line. The reference cell line represented an average cell line in the evolved population. The traits of the reference cell line were chosen as the average values across all cell lines that exist in the population. Tested and reference cell lines were inoculated in the same ecological niche with one cell in each line and grew until the niche reached saturation ($N_{\text{Tested}} + N_{\text{Reference}} = N_{\text{MAX}}$). Emergence of new cell lines was suppressed in this test, so only two lines were present. Then the number of cells in each cell line was calculated. The particle fitness of the tested cell line was calculated as a ratio of the cell number produced by the tested and reference cell lines:

$$F_P(\text{Tested}) = \frac{N_{\text{Tested}}}{N_{\text{Reference}}} \tag{4.7}$$

Here, F_P is the particle fitness of the tested cell line; N_{Tested} and $N_{\text{Reference}}$ are the numbers of cells in the tested and reference cell lines, respectively.

Particle fitness calculated by Eq. 4.7 approximates the chances of the cell line being sampled after the phase of life cycle. However, particle fitness in S→W phase also depends on the transition rate. In S→W phase, the collective is inoculated with a sample containing several S-morphotype cell lines. Therefore, an S-morphotype cell line with a high transition rate

would produce W-morphotype cell lines earlier – so its offspring cell lines would have the advantage of exploiting the mat niche.

To investigate the influence of transition rate on the number of W-morphotype cell lines produced in S→W phase, I conducted a series of preliminary simulations. In a competition between two S-morphotype cell lines with 10% difference in growth rate[1] and equal transition rates, the faster growing line produced on average 6.9 times more W-morphotype cells than the slower growing line. In a competition between two S-morphotype cell lines with a 10 % difference in transition rate[2] and equal growth rates, the cell line with the higher transition rate produced on average only 5% more W-morphotype cells than the cell line with the lower transition rate. Thus, I concluded that in S→W phase the growth rate has a stronger impact on particle fitness than transition rate and that the influence of transition rate on particle fitness can be disregarded.

By contrast, in W→S phase the suggested measurement of particle fitness adequately represents the survival chances of the cell line. In this phase, the competition occurs between S-morphotype lines; all of them are descendants of a single W-morphotype line used to inoculate the collective at the start of W→S phase. The only trait affecting the success in this competition is the growth rate of S-morphotype cell lines. Therefore, Eq. 4.7 is an accurate characterisation of particle fitness in both W→S and S→W phases of the life cycle.

4.5.2.2 Calculation of collective fitness in the simulative model

Collective fitness is determined by the chance of the collective passing its cell lines to the next generation of the life cycle (Figs. 4.2 and 4.3). In the non-mixed regime, this chance can be estimated by the likelihood of the collective avoiding extinction by producing a novel phenotype in each phase. However, in the mixed regime, the number of offspring collectives also depends on the performance of sampled cell lines in the mixed sample. The result of competition of cell lines in the mixed sample depends of both traits of the cell lines sampled from the collective whose fitness was assessed and of traits of cell lines from competing

[1] Specifically, one cell line had trait values (k_0, p_0) and another line had $(k_0 + v_k, p_0)$

[2] One cell line had trait values (k_0, p_0) and another line had $(k_0, p_0 + v_p)$

collectives. Therefore, the fitness of collectives in the simulative model is assessed as the number of offspring produced in the presence of competitors.

The collective fitness of a particular collective (later referred to as the *tested* collective) was measured by a competition with the *reference* collective – which was inoculated with the reference cell line used in the calculation of particle fitness. The population was initiated with five tested and five reference collectives. The average number of collectives descended from the tested collective after one generation of the life cycle (W→S→W) was calculated. Similarly, the average number of collectives descended from the reference collective after one generation of the life cycle was calculated. To prevent the impact of the particle-level selection on the measurement of collective fitness, all emerged cell lines had the same growth and transition rates as the parent cell lines. The collective fitness of the tested collective was calculated as the ratio of the expected number of collectives descended from the tested collective to the expected number of collectives descended from the reference collective:

$$F_C(\text{Tested}) = \left(\frac{\text{Number of tested collectives}}{\text{Number of reference collectives}} \right)_{\text{after one generation}} \tag{4.8}$$

Here, F_C is collective fitness of the tested collective and the ordering of phases in the life cycle is W→S→W.

4.5.2.3 Calculation of FCM in the simulative model

Particle and collective fitnesses were calculated for each collective in the population. The FCM was calculated as a correlation coefficient of the particle and the collective fitness as defined in Chapter three:

$$\text{FCM} = \frac{\langle (F_P - \langle F_P \rangle)(F_C - \langle F_C \rangle) \rangle}{\sqrt{\langle (F_P - \langle F_P \rangle)^2 \rangle} \sqrt{\langle (F_C - \langle F_C \rangle)^2 \rangle}} \tag{4.9}$$

Here, F_P is the particle fitness averaged within collectives; F_C is the collective fitness; $\langle x \rangle$ is the mean value of x where averaging is performed across all collectives in a population.

The FCM values have been calculated for each of the 500 runs in the mixed and non-

mixed selection regimes. The overall FCM for a selection regime was calculated as the average of all 500 of the resultant FCM values.

4.5.3 A detailed description of the predictive model

The predictive model determines FCM from the rules of selection at the particle and collective levels without the simulation of evolution. In Chapter three I investigated a model population in which trait-to-fitness functions are linear:

$$\begin{aligned} F_P &= \alpha_{Pk}k + \alpha_{Pp}p \\ F_C &= \alpha_{Ck}k + \alpha_{Cp}p \end{aligned} \tag{4.10}$$

Here, F_P and F_C are particle and collective fitnesses; k and p are traits (growth and transition rates in current model); α_{Pk}, α_{Pp}, α_{Ck} and α_{Cp} are impacts of traits on fitnesses, determined by rules of selection.

In Chapter three, I showed that in such a model the FCM can be calculated as:

$$\text{FCM} = \frac{\alpha_{Pk}\alpha_{Ck}\sigma_k^2 + \alpha_{Pp}\alpha_{Cp}\sigma_p^2 + \rho_T\sigma_k\sigma_p(\alpha_{Pk}\alpha_{Cp} + \alpha_{Pp}\alpha_{Ck})}{\sqrt{\alpha_{Pk}^2\sigma_k^2 + \alpha_{Pp}^2\sigma_p^2 + 2\rho_T\sigma_k\sigma_p\alpha_{Pk}\alpha_{Pp}}\sqrt{\alpha_{Ck}^2\sigma_k^2 + \alpha_{Cp}^2\sigma_p^2 + 2\rho_T\sigma_k\sigma_p\alpha_{Ck}\alpha_{Cp}}} \tag{4.11}$$

Here, α_{Pk}, α_{Pp}, α_{Ck} and α_{Cp} are impacts of traits on fitnesses; σ_k and σ_p are variations of growth and transition rates in the population; ρ_T is a covariation of traits.

In the non-linear model, the impacts of traits on fitnesses can be replaced with fitness gradients.

$$\begin{aligned} \alpha_{Pk} &= \frac{\partial F_P}{\partial k}, \quad \alpha_{Pp} = \frac{\partial F_P}{\partial p} \\ \alpha_{Ck} &= \frac{\partial F_C}{\partial k}, \quad \alpha_{Cp} = \frac{\partial F_C}{\partial p} \end{aligned} \tag{4.12}$$

Here, α_{Pk}, α_{Pp}, α_{Ck} and α_{Cp} are components of fitness gradients determined by rules of selection; F_P and F_C are particle and collective fitnesses; k and p are growth and transition

rates.

Biological mechanisms responsible for expression of traits used in my model (growth and transition rates) are very different. The growth rate depends on rates of resource uptake and processing, while the transition rate depends on the performance of the replication machinery. Thus, it is unlikely that the growth and transition rates are causally connected in the experimental population, therefore, the model assumes that these traits are non-correlated $(\rho_T = 0)$.

Variations of traits in the evolved population are not available in the predictive model, so they were estimated based on the selection rules (see Section 4.5.1). The only source of trait variation in the models are transitions between W- and S-morphotypes. Hence, variations of traits within the population (σ_k and σ_p) are proportional to the standard deviation of traits' changes at mutation (v_k and v_p). In Chapter three, I showed that Eq. 4.11 had a more intuitive form if fitness gradients were calculated in the space of normalised traits:

$$\begin{aligned} k' &= \frac{k}{v_k} \\ p' &= \frac{p}{v_p} \end{aligned} \tag{4.13}$$

Here, k and p are the growth and transition rate; k' and p' are normalised traits; and v_k, v_p are standard deviations of traits at mutation.

If fitness gradients are calculated for the normalised traits and traits are non-correlated $(\rho_T = 0)$, then Eq. 4.11 transforms into:

$$\text{FCM} = \frac{\alpha_{Pk}\alpha_{Ck} + \alpha_{Pp}\alpha_{Cp}}{\sqrt{\alpha_{Pk}^2 + \alpha_{Pp}^2}\sqrt{\alpha_{Ck}^2 + \alpha_{Cp}^2}} = \cos(\theta_{\overline{\alpha}_P\overline{\alpha}_C}) \tag{4.14}$$

Here, α_{Pk} and α_{Pp} are the components of the particle fitness gradient calculated in the space of normalised traits (k', p'); α_{Ck} and α_{Cp} are the components of the collective fitness gradient; and $\theta_{\overline{\alpha}_P\overline{\alpha}_C}$ is the angle between the directions of the optimal increase in particle- and collective-level fitnesses.

Eq. 4.14 is used in the predictive model. The scheme of the calculation of the FCM is

presented in Fig. 4.4.

Fitness gradients are calculated as directions of the optimal particle or collective fitness increase for the initial cell line with the traits (k'_0, p'_0). To calculate the fitness gradients, 100 cell lines were created whose traits were evenly distributed on a circle with a radius of one and the centre in the initial cell line: $(k' - k'_0)^2 + (p' - p'_0)^2 = 1$. Then the collective and particle fitness for each of these cell lines were calculated using methods described in sections 4.5.2.1 and 4.5.2.2 where the initial cell line (k_0, p_0) was used as the reference line. The line that had the highest particle (collective) fitness determined the direction of the particle (collective) level fitness gradient. The components of the fitness gradients are calculated as:

$$\begin{aligned} \alpha_{Pk} &= k'_{\text{Highest } F_P} - k'_0 \\ \alpha_{Pp} &= p'_{\text{Highest } F_P} - p'_0 \\ \alpha_{Ck} &= k'_{\text{Highest } F_C} - k'_0 \\ \alpha_{Cp} &= p'_{\text{Highest } F_C} - p'_0 \end{aligned} \tag{4.15}$$

Here, α_{Pk} and α_{Pp} are the components of the particle fitness gradient; α_{Ck}, α_{Cp} are the components of the collective fitness gradient; k'_0 and p'_0 are the normalised initial growth and transition rates; $k'_{\text{Highest } F_P}$ and $p'_{\text{Highest } F_P}$ are normalised growth and transition rates of the cell line with the highest particle fitness; and $k'_{\text{Highest } F_C}$ and $p'_{\text{Highest } F_C}$ are normalised growth and transition rates of the cell line with the highest collective fitness.

Note, this method of calculation of the fitness gradients recover only directions of fitness gradients, which is enough to calculate the predicted FCM, as Eq. 4.14 is scale free.

Components of the fitness gradients, as obtained from the predictive model according to Eq. 4.15, have been used in Eq. 4.14 to calculate the predicted value of FCM.

4.5.4 Measurement of the FCM from experimental data

To calculate FCM in experimental populations, data from the life history analysis experiment of Hammerschmidt et al. (2014, data) were used. The experimental dataset contains cell counts of S- and W-morphotypes present in collectives a certain number of days after

inoculation. For each experimental population, three independent replicates of the cell count measurements have been done once a day. The experimental data were available for days one to six of S→W phase and for days one to twelve of W→S phase. The experimental data do not allow for an identical measurement of particle and collective fitness to that of the procedure used in the simulative model (Section 4.5.2). Therefore, a separate procedure has been developed so as to be compatible with available data and remain close to the fitness measurement used in the simulative model – this was used to calculate particle and collective fitness and to infer the experimental FCM according to Eq. 4.3.

The experimental dataset has been filtered. Before day three, the population was in an exponential phase of growth – the cell counts and morphotype composition of collectives changed rapidly. Therefore, data from the first two days were not included when calculating fitnesses. Similarly, after day nine the population started to decay due to the depletion of nutrients in the environment, so data after this period were not used. In between these days, the cell counts and morphotype composition of the population were stable. Thus, the fitnesses were calculated based on the cell counts observed between days three and six of S→W phase, and days three and nine of W→S phase.

The particle fitness in mixed and non-mixed regimes characterises the cell growth (see Section 4.5.2.1) and was calculated as:

$$F_P^{\text{experiment}} = \langle N_{\text{S in } S\to W \text{ phase}} \rangle \cdot \langle N_{\text{W in } W\to S \text{ phase}} \rangle \tag{4.16}$$

Here, $F_P^{\text{experiment}}$ is the particle fitness obtained from experimental data; $\langle N_{\text{S in } S\to W \text{ phase}} \rangle$ is the average number of S-morphotype cells observed in S $\to$ W phase; $\langle N_{\text{W in } W\to S \text{ phase}} \rangle$ is the average number of W-morphotype cells observed in W $\to$ S phase. The averaging is performed across the chosen time range and measurement replicas.

Selection applied at the collective level differs between mixed and non-mixed regimes.

In the non-mixed regime, the collective fitness represents the ability of the collective to produce novel morphotypes. Therefore, collective fitness in the non-mixed regime is calcu-

lated as:

$$F_C^{\text{non-mixed}} = \left(\frac{\#W^+\text{collectives}}{\#\text{all collectives}}\right)_{\text{in } S\to W \text{ phase}} \cdot \left(\frac{\#S^+\text{collectives}}{\#\text{ all collectives}}\right)_{\text{in } W\to S \text{ phase}} \tag{4.17}$$

Here, $F_C^{\text{non-mixed}}$ is collective fitness in the non-mixed regime, obtained from experimental data; $\#W^+$ and $\#S^+$ are numbers of collectives containing W- and S- morphotypes cells, respectively. The collective fitness is a product of the fraction of the collectives containing W-morphotype cells in S→W phase by the fraction of the collectives containing S-morphotype cells in W→S phase.

In the mixed regime, the evolutionary success of the collective depends on both the chance of creating a novel morphotype and the growth rate of cells after the mixing step. Therefore, collective fitness in the mixed selection regime is calculated as:

$$F_C^{\text{mixed}} = \left(\frac{\#W^+\text{collectives}}{\#\text{all collectives}}\right)_{\text{in } S\to W \text{ phase}} \cdot \left(\frac{\#S^+\text{collectives}}{\#\text{ all collectives}}\right)_{\text{in } W\to S \text{ phase}} \cdot \\ \cdot \langle N_{\text{S in } S\to W \text{ phase}}\rangle \cdot \langle N_{\text{W in } W\to S \text{ phase}}\rangle \tag{4.18}$$

Here, F_C^{mixed} is collective fitness in the mixed regime, obtained from experimental data; $\#W^+$ and $\#S^+$ are numbers of collectives containing W- and S-morphotypes cells, respectively; $\langle N_{\text{S in } S\to W \text{ phase}}\rangle$ is the average number of S-morphotype cells in S → W phase; $\langle N_{\text{W in } W\to S \text{ phase}}\rangle$ is the average number of W-morphotype cells in W → S phase. The averaging is performed across the chosen time range and measurement replicas. Collective fitness is a product of particle fitness (Eq. 4.16) and the capability to produce novel morphotypes (Eq. 4.17).

The FCM is calculated from the set of particle-level and collective-level fitnesses according to Eq. 4.3. The experimental dataset was available for 12 independent populations evolved under the non-mixed regime and for nine independent populations evolved under the mixed regime. Particle- and collective-level fitnesses were calculated for each population.

So, the FCM was measured across a set of independent populations.

4.5.5 Estimation of uncertainty of FCM

In experimental data, the uncertainty of the FCM measurement is affected by the uncertainty in the measurement of fitness and the limited size of the data sample. The uncertainty caused by the limited size of data sample was estimated as 95% confidence interval of correlation coefficient under the assumption that the fitness distribution is a two-dimensional normal distribution.

In the predictive model, the uncertainty of the FCM measurement is determined by the angular resolution of the fitness gradients' calculation. The predictive model (Section 4.2.2) operates with 100 directions in the traits space; therefore, the uncertainty of directions of the fitness gradients is equal to $\pi/100$ radians (half of the angle between two neighbouring directions). Thus, the angle between fitness gradients is determined with a uncertainty equal to $\pi/50$ radians. The uncertainty of the FCM obtained in the predictive model is estimated as the change in the FCM caused by the change in the angle between the fitness gradients by $\pi/50$ radians.

In the simulative model, the uncertainty of the measurement of the FCM is determined by the limited sample size (500 independent runs), small number of collectives within each run (ten collectives) and the stochastic nature of the model. The variation in the measured FCM is characterised by the 95% sample confidence intervals calculated from the set of 500 independent runs. The uncertainty of the average value is determined by the standard error of mean (SEM).

4.5.6 A detailed description of additional selection regimes

A series of additional selection regimes has been developed to extend the set of investigated selection conditions beyond the two experimentally studied regimes. So, the mixed and non-mixed life cycles described in section 4.5.1.2 have been modified. The *guiding selective events* were imposed at the particle and collective levels to influence the directions of

selection operating in a population. Each additional selection regime features a unique combination of guiding events at the particle and collective levels, so the whole set of regimes covered a wide range of selective conditions.

At the particle level, the guiding selective event replaced the procedures of cell line sampling used in the experimentally investigated selection regimes (Fig. 4.2 and 4.3, steps 2 and 4). The particle-level guiding selective event samples the single cell line after both W→S and S→W phases of the life cycle (Fig. 4.5, steps 2 and 4). The probability of the cell line being sampled is proportional to the value of the particle scoring function $S_P(k,p)$. The particle-level scoring function is chosen independently for each additional regime from a list of eight functions: $S_P(k,p) \in \{k, kp, p, \frac{p}{k}, \frac{1}{k}, \frac{1}{kp}, \frac{1}{p}, \frac{k}{p}\}$. Thus, the set of particle scoring functions covers eight major directions of the particle-level selection in the space of traits (see Fig. 4.6 and Table 4.2).

At the collective level, the guiding selective event is introduced after the replacement of the extinct collectives (Fig. 4.5). A single collective is chosen to become extinct and another collective is chosen to replace the extinct collective. The probability of being chosen to replace is proportional to the collective scoring function $S_C(k,p)$. The probability of going extinct is inversely proportional to the same scoring function. The collective-level scoring function used in the guiding event is independently chosen for each regime from the same list of functions as used at the particle level: $S_C(k,p) \in \{k, kp, p, \frac{p}{k}, \frac{1}{k}, \frac{1}{kp}, \frac{1}{p}, \frac{k}{p}\}$.

Thus, each selection regime is determined by three components: selection pressure imposed at the particle level (eight variants of S_P), selection pressure imposed at the collective level (eight variants of S_C), and the organisation of the life cycle (two variants: mixed and non-mixed). Thus, $8 \cdot 8 \cdot 2 = 128$ different additional selection regimes have been investigated, in addition to the two selection regimes for which experimental data have been available.

The calculation of particle and collective fitnesses was changed to reflect the changes in selection introduced by the guiding selective events. In additional selection regimes, the chance of the cell line being sampled after the phase is determined by the particle scoring

function. Therefore, particle fitness is calculated as (c.f. Eq. 4.7):

$$F_P(\text{Tested}) = \frac{S_P(k_{\text{Tested}}, p_{\text{Tested}})}{S_P(k_{\text{Reference}}, p_{\text{Reference}})} \tag{4.19}$$

Here, $F_P(\text{Tested})$ is a particle fitness of the tested cell line; k_{Tested} and p_{Tested} are the growth and transition rates of the tested cell line; $k_{\text{Reference}}$ and $p_{\text{Reference}}$ are the growth and transition rates of the reference cell line, which are equal to the average traits in the population; $S_P(k, p)$ is the particle scoring function in the given additional selection regime.

Collective fitness in the additional regimes is calculated in the same way as in the experimentally studied regimes, as described in section 4.5.2.2. Collective-level fitness is equal to the ratio between the average number of the tested and reference collectives collectives, after a single generation of the life cycle in a population that initially contained five collectives of each type.

In the simulative model, 500 independent runs have been computed for each additional regime. Each run lasted for 30 generations. FCM have been calculated for the populations in the final generation.

The set of additional selective regimes significantly increased the number of selective conditions for which the accuracy of FCM prediction has been tested.

4.5.7 A calculation of the effect of guiding selective events on the evolution of the modelled population

The directions of fitness gradients obtained by the predictive model (Eq. 4.15) may differ from the directions imposed by guiding selective events (Table 4.2). This is due to the fact that guiding selective events are one of several factors that influence fitness gradients. Other factors are imposed by the life cycle: selection occurring during the mixing procedure and the requirement of the life cycle to produce novel morphotypes at each phase of the life cycle. The mixing procedure pools together cell lines from different collectives, thus, in mixed selection regimes, the number of offspring collectives depends on the competition

of cell lines at the particle level. Therefore, the fitness gradient at the collective level is dependent on the choice of scoring function at the particle level. The requirement to produce novel morphotypes applies constant selection pressure, independent of the choice of scoring function at the collective level. The fitness gradients ($\overline{\alpha}_P$ and $\overline{\alpha}_C$) obtained by the predictive model are combinations of these factors. However, relative contributions of the life cycle and guiding events to selection operating in additional regimes are unknown.

To find the relative contributions of the life cycle and guiding events, fitting of the directions of selection ($\overline{\alpha}_P$ and $\overline{\alpha}_C$) was performed by the predictive model by linear combination of selection pressures imposed by the life cycle and guiding events:

$$\begin{aligned}
&\measuredangle(\overline{\alpha}_P, \overline{\beta}_P) = \epsilon_P \to 0 \\
&\measuredangle(\overline{\alpha}_C, \overline{\beta}_C) = \epsilon_C \to 0 \\
&\overline{\beta}_P = X_P \cdot grad(S_P) + Y_P \cdot grad(S_C) + \overline{Z}_P \\
&\overline{\beta}_C = X_C \cdot grad(S_P) + Y_C \cdot grad(S_C) + \overline{Z}_C
\end{aligned} \tag{4.20}$$

Here, $\measuredangle(\overline{\alpha}, \overline{\beta})$ is an angle between vectors $\overline{\alpha}$ and $\overline{\beta}$; $\overline{\alpha}_P$ and $\overline{\alpha}_C$ are vectors of fitness gradients calculated by the predictive model; $\overline{\beta}_P$ and $\overline{\beta}_C$ are vectors of the fitted directions of selection at the particle and collective levels; $grad(S_P)$ and $grad(S_C)$ are gradients of scoring functions that represent the component of selection imposed by guiding selective events at particle and collective levels, respectively; X_P and X_C are the impacts of the particle-level guiding event on selection operating at particle and collective levels, respectively; Y_P and Y_C are the impacts of the collective-level guiding event on selection operating at particle and collective levels, respectively; $\overline{Z}_P = (Z_{Pk}, Z_{Pp})$ and $\overline{Z}_C = (Z_{Ck}, Z_{Cp})$ are the impacts of selection imposed by the life cycle (mixed or non-mixed); ϵ_P and ϵ_C are residual errors, which were minimised in the fitting.

The fitting procedure presented in Eq. 4.20 takes into account the directions of fitness gradient vectors but not their magnitude. Thus, the proportional scaling of the fitting parameters X, Y, $\overline{Z}$ does not change the residual errors. To encompass this, the impact of the scoring function gradient on the fitness gradient at the same level was set equal to 1: $X_P = 1$

and $Y_C = 1$. Therefore, only six parameters were fitted: Y_P, X_C, $\overline{Z}_P = (Z_{Pk}, Z_{Pp})$ and $\overline{Z}_C = (Z_{Ck}, Z_{Cp})$.

Chapter 5

Concluding discussion

5.1 Summary of main results

The search for a single underlying reason behind the various events is a major motivation of the scientific progress. Investigation into the origins of multicellularity is no exception. There is a record of multiple independent events of emergence of multicellularity in the history of life (Grosberg and Strassmann 2007) and multiple scenarios have been considered theoretically (Maynard Smith and Szathmáry 1995, Okasha 2006, Godfrey-Smith 2009). However, no unifying framework has been proposed yet. In this thesis, I focused on two aspects of the evolution of multicellularity: emergence of cooperation in early multicellular collectives and fitness decoupling that occurs in the course of the transition in individuality.

The evolution of multicellularity starts from the emergence of collectives of cells that have a selective advantage over solitary cells. This selective advantage can be achieved by means of cooperation between members of a given collective. The cooperative behaviour is costly and the cooperation benefit offsets this cost. Non-cooperative members of a given collective do not pay a cost of cooperation but receive the benefit, and therefore, have a selective advantage over cooperators residing in this collective. Among early collectives, the evolution of cooperation is further complicated by limited capability of cells to coordinate their actions. Therefore, I investigated how cooperation may evolve if cells act independently

of each other and how the coordination of cell actions helps the evolution of cooperation. As a result, I found that evolution of cooperation is possible in the absence of coordinated actions of cells, but only in a form of weak altruism, while strong altruism requires the coordination of actions.

As soon as collectives formed, the next step in evolution of multicellularity is the evolution of Darwinian individuality (Lewontin 1970) at collective level. Prior to the evolution of multicellularity, cells (or particles as they referred in this study) inside collectives were Darwinian individuals, but the collectives themselves were not. In the course of evolution, Darwinian individuality passes from level of particles to level of collectives, so collectives begin to participate in the natural selection in their own right. While the transition in individuality from particles to collectives is a crucial step for the evolution of multicellularity, its manifestations are not as apparent as manifestations of cooperation. This complicates the investigation of the transition in individuality. In my thesis, I proposed a method to detect the transition in individuality based on the concept of the fitness decoupling (Michod and Roze 1999) – the fitness correlation metric (FCM). This metric allowed me to formulate a criterion for selection to promote a transition in individuality in a form of simple mathematical expression: directions of particle and collective fitness gradients in the space of traits should be orthogonal to each other. I tested the FCM on the experimental data obtained by Hammerschmidt et al. (2014) and confirmed that this metric reliably indicates selection regimes promoting the transition in individuality.

5.1.1 Cooperation may evolve under limited capability of particles to coordinate their actions

In my thesis, I have asked how cooperation may evolve if cells within collectives act independently of each other and how coordination of cell actions may promote the evolution of cooperation. I built a model of a population in which interactions between collectives were limited to the migration of particles between them. The process of migration in its simplest form is an independent action of a single particle, and as such, no coordinated activity of

particles is necessary for migration to take place.

In addition, I investigated modes of migration with various degrees of coordination of particles' actions. In the propagule migration mode, particles migrate between collectives in pairs, which illustrates the case of coordination among small number of particles at once. In the caravan migration mode, consecutive migrants follow the first one, which illustrates the case of coordination among large number of particles, or even among all particles in collective. Finally, in the differential migration mode, cooperating particles have higher propensity to migrate than non-cooperators, which illustrates the case, where actions of particles are subjugated to a collective. These migration modes along with the case of well-mixed population were tested for a capability to promote cooperation.

Results of modelling shows that cooperation may evolve in a single individual migration mode in which migration is performed by independent particles and collectives serve only as a boundary between them. While a number of models of the evolution of cooperation in a group-structured populations have been previously developed (Wilson 1975, Avilés 2002, Traulsen and Nowak 2006), these models involved the actions affecting the whole collective (such as dissolution of particles into common pool (Wilson 1975), or fragmentation of collectives (Traulsen and Nowak 2006)), which are impossible without coordinated actions of multiple particles within collective. The single individual migration mode does not invoke any coordinated activity of particles, so it is more relevant representation of early multicellular collectives than previously developed models. Thus, upon the emergence of collectives, no further complexity is needed for the evolution of cooperation among particles by means of migration.

My results also shows that the coordination of actions between particles can further promote the evolution of cooperation. In the single individual migration mode, cooperation may evolve only in a form of weak altruism, while the strong altruism is always in disadvantage. In migration modes involving coordinated migration, weakly altruistic cooperation may evolve under lower benefit-to-cost ratios than in the single individual migration mode. Also in these modes, cooperation in a form of strong altruism can have a selective advantage. So, the evo-

lution of strong altruism in these modes is associated with the coordination of player actions, but not with the group structure alone.

5.1.2 Fitness decoupling can be detected by the fitness correlation metric (FCM)

The transition in individuality from particles to collectives is a crucial step for the evolution of multicellularity. One of the main obstacles in the investigation of the transition in individuality is its subtle effects. In other words, it may be difficult to distinguish between a population in which the collectives are merely groups of cells (like in single individual migration mode considered in chapter two) and a population in which collectives are units of selection. So, the most important effect of the transition in individuality is that collectives begin to reproduce by their own means, which are likely to be different from means of reproduction of particles within them. This is known as fitness decoupling (Michod and Roze 1999) and is likely to be a hallmark of the transition in individuality. However, this concept did not have a reliable measure, which could be applied to any populations without specific properties, such as reproductive division of labour.

In chapter three, I suggested a general numerical measure of fitness decoupling – the fitness correlation metric (FCM). The FCM value is equal to the correlation coefficient between collective and average particle fitnesses in a given population. Prior to the transition in individuality, the reproduction of collectives relies on the reproduction of particles within them, so bot particle and collective fitnesses are highly correlated, so the FCM value is about one. When transition in individuality occurs, fitnesses are likely to become decoupled, and in such case the numbers of offspring particles and offspring collectives are no more correlated. Thus, the FCM value decreases and approaches zero as reproduction of collectives becomes independent from reproduction of particles within it. Hence, the measurement of the FCM value makes it possible to determine the fitness (de-)coupling state.

The FCM metric has an advantage over the previously developed metric of the fitness decoupling – MVSHN index (Michod et al. 2006, Bossert et al. 2013). FCM can be measured

for any population with tractable genealogy of particles, while the MVSHN index is limited to populations exhibiting a reproductive division of labour. I have shown that in populations in which both metrics can be applied, both FCM and MVSHN index show similar results.

5.1.3 The fitness (de-)coupling state can be inferred from selective conditions

Natural selection favours traits that improves the fitness of individuals. However, which traits are evolutionary beneficial is dependent on the selective conditions under which a given population evolves. For instance, in experimental evolution studies where selective conditions are under the control of researchers, the properties of evolved populations may be significantly different from the ancestral type (Lenski et al. 1990, Ratcliff et al. 2012, Hammerschmidt et al. 2014), including emergence of new traits (Rainey and Rainey 2003, Beaumont et al. 2009). Selective conditions influence the capability of fitnesses to become decoupled in the course of evolution. Therefore, it is possible to find the relationship between selective conditions and the value of FCM that will be achieved under given selection regime. In chapter three, I showed that in a population with linear traits-to-fitness functions, the FCM value can be expressed through directions of fitness gradients in a space of traits. Thus, fitness decoupling is promoted by the selection regimes, which favour different combination of traits at particle and collective levels.

In chapter four, I showed that FCM values of populations evolved in experimental evolution study performed by Hammerschmidt et al. (2014) are close to values inferred from fitness gradients that were calculated from rules of selection. Additionally, in a model based on the experimental setup of Hammerschmidt et al. (2014) that features non-linear traits-to-fitness functions, the directly FCM values were close to values inferred from fitness gradients for multiple additional selection regimes. Thus, the FCM value can be reliably estimated from the rules of selection applied to population.

The capability to predict the fitness (de-)coupling state before evolution takes place provides insights useful for design of selection regimes involving multilevel selection, such as

works of Ratcliff et al. (2012, 2013a).

5.2 Future directions

Models presented in this study provide the method for detection of fitness decoupling applicable to any population. This opens new opportunities for the investigation of the origins of multicellularity.

1. *Search for a general mechanism of the transition in individuality.* A range of features promoting transitions in individuality are known: reproductive division of labour (Michod et al. 2006, Michod 2007); dispersal of non-cohesive defectors as a prototypical collective reproduction (Rainey and Kerr 2010); two-phase life cycles (Hammerschmidt et al. 2014); recurrence of collectives by "staying together" modes (Tarnita et al. 2013). This variety of features makes difficult to infer a possible underlying mechanism governing the transition in individuality.

   Conditions promoting fitness decoupling suggested in my work indicate that fitness decoupling requires the orthogonality of fitness gradient vectors calculated in the space of traits. All previously indicated mechanisms help to fulfil this requirement. For instance, in populations expressing a reproductive division of labour, there are two traits that differently affect particle and collective fitnesses: the level and the asymmetry of division of labour (see Section 3.3.1 for details). Two-phase life cycles make it possible to separate in time, selection at particle and collective levels (Hammerschmidt et al. 2014), so they can be performed by different processes. These phenomenologic similarities establish a base for a search for a unified causal principle of the evolution of multicellularity.

2. *Controlled experimental evolution of transition in individuality.* Theory developed in my thesis predicts that directions of fitness gradients are responsible for fitness decoupling. Experimental data obtained for a non-mixed selection regime used in the

experimental evolution study of Hammerschmidt et al. (2014) supports this prediction. An additional experimental evidence covering multiple selection regimes would further test this prediction.

A simple experimental setup, which could be used for this test can be constructed using a bacterial population carrying two genes coding different fluorescent proteins, such as their fluorescence levels can be measured independently. In the experiment, these expression levels pose as two numerical traits establishing a two-dimensional space of traits. The group structure could be imposed by a well plate, or by a set of Petri dishes and then, selection at the particle and collective level can be performed based on the fluorescence levels. Selection at the collective level can be performed by automatic sampling and reinoculation, while selection at the particle level can be performed by a cytometer with a sorter. This setup makes it possible to control the directions of fitness gradients by the choice of criteria used for sorting (sampling) of cells (collectives) in a given selection regime. Therefore, multiple combinations of fitness gradients could be experimentally tested for an ability to promote fitness decoupling.

3. *Investigation of fitness decoupling in populations with complex traits-to-fitness functions.* In my thesis, I used linear trait-to-fitness functions to investigate relation between the choice of this function and FCM that evolves in the course of selection. Linear functions are the simplest class of traits-to-fitness functions. The investigation of more complex traits-to-fitness functions, such as non-linear, or context-dependent (i.e. when fitness of particle also depends on the traits of other particles) may provide an additional insights into the fitness decoupling. For instance, population with complex traits-to-fitness function may exhibit fitness decoupling under conditions that would prevented fitness decoupling if traits-to-fitness functions were linear. Another application of complex traits-to-fitness function will be models that predict FCM in experimental and natural populations with higher accuracy than models utilizing linear functions.

Bibliography

Abou Chakra, M. and Traulsen, A. (2014). Under high stakes and uncertainty the rich should lend the poor a helping hand. *Journal of Theoretical Biology*, 341:123 –130.

Aledo, J. C. (2008). An early and anaerobic scenario for the transition to undifferentiated multicellularity. *Journal of Molecular Evolution*, 67(2):145–153.

Antal, T., Nowak, M. A., and Traulsen, A. (2009). Strategy abundance in 2×2 games for arbitrary mutation rates. *Journal of Theoretical Biology*, 257:340–344.

Archetti, M. and Scheuring, I. (2012). Review: Evolution of cooperation in one-shot social dilemmas without assortment. *Journal of Theoretical Biology*, 299:9–20.

Avilés, L. (2002). Solving the freeloaders paradox: genetic associations and frequency-dependent selection in the evolution of cooperation among nonrelatives. *Proceedings of the National Academy of Sciences of the United States of America*, 99(22):14268–14273.

Avital, E. and Jablonka, E. (2000). *Animal Traditions: Behavioural Inheritance in Evolution*. Cambridge University Press, Cambridge.

Axelrod, R. and Hamilton, W. D. (1981). The evolution of cooperation. *Science*, 211(4489):1390–1396.

Bach, L. A., Helvik, T., and Christiansen, F. B. (2006). The evolution of n-player cooperation - threshold games and ESS bifurcations. *Journal of Theoretical Biology*, 238:426–434.

Baldauf, S. L. and Doolittle, W. F. (1997). Origin and evolution of the slime molds (mycetozoa). *Proceedings of the National Academy of Sciences of the United States of America*, 94(22):12007–12012.

Bardele, C. F. and Margulis, L. (1981). *Symbiosis in Cell Evolution: Life and its Environment on the Early Earth.* W.H. Freeman & Company, San Francisco.

Beaumont, H. J. E., Gallie, J., Kost, C., Ferguson, G. C., and Rainey, P. B. (2009). Experimental evolution of bet hedging. *Nature*, 462(7269):90–93.

Bonner, J. (1959). *The Cellular Slime Molds*. Princeton University Press, Princeton, NJ.

Bonner, J. T. (1998). The origins of multicellularity. *Integrative Biology*, 1:27–36.

Bonner, J. T. (2000). *First Signals: The Evolution of Multicellular Development*. Princeton University Press, Princeton, NJ.

Bossert, W., Qi, C. X., and Weymark, J. A. (2013). Extensive social choice and the measurement of group fitness in biological hierarchies. *Biology and Philosophy*, 28(1):75–98.

Bourrat, P. (2015). Levels, time and fitness in evolutionary transitions in individuality. *Philosophy and Theory in Biology*, 7.

Boyd, R. and Richerson, P. J. (1985). *Culture and the Evolutionary Process*. University of Chicago Press.

Boyd, R. and Richerson, P. J. (1992). Punishment allows the evolution of cooperation (or anything else) in sizable groups. *Ethology and Sociobiology*, 13(3):171–195.

Brown, J. S. and Vincent, T. L. (1992). Organization of predator-prey communities as an evolutionary game. *Evolution*, 46(5):1269–1283.

Buss, L. W. (1982). Somatic cell parasitism and the evolution of somatic tissue compatibility. *Proceedings of the National Academy of Sciences of the United States of America*, 79(17):5337–5341.

3086 Buss, L. W. (1987). *The Evolution of Individuality*. Princeton University Press, Princeton,
3087 NJ.

3088 Charnov, E. L. and Krebs, J. R. (1975). The evolution of alarm calls: altruism or manipula-
3089 tion? *American Naturalist*, 109(965):107–112.

3090 Christiansen, F. B. (1975). Hard and soft selection in a subdivided population. *American*
3091 *Naturalist*, 109:11–16.

3092 Clements, K. C. and Stephens, D. W. (1995). Testing models of non-kin cooperation: mutu-
3093 alism and the prisoner's dilemma. *Animal Behaviour*, 50(2):527–535.

3094 Crespi, B. J. (2001). The evolution of social behavior in microorganisms. *Trends in Ecology*
3095 *and Evolution*, 16(4):178–183.

3096 Damuth, J. and Heisler, I. L. (1988). Alternative formulations of multilevel selection. *Biology*
3097 *and Philosophy*, 3(4):407–430.

3098 Darwin, C. (1859). *On the Origin of Species by Means of Natural Selection*. John Murray,
3099 London.

3100 Dawes, R. M. (1980). Social dilemmas. *Annual Review of Psychology*, 31:169–193.

3101 Dawkins, R. (1976). *The Selfish Gene*. Oxford University Press, Oxford.

3102 De Monte, S. and Rainey, P. B. (2014). Nascent multicellular life and the emergence of
3103 individuality. *Journal of Biosciences*, 39(2):237–248.

3104 De Silva, H., Hauert, C., Traulsen, A., and Sigmund, K. (2010). Freedom, enforcement, and
3105 the social dilemma of strong altruism. *Journal of Evolutionary Economics*, 20(2):203 –
3106 217.

3107 Delwart, E. L., Sheppard, H. W., Walker, B. D., Goudsmit, J., and Mullins, J. I. (1994).
3108 Human immunodeficiency virus type 1 evolution in vivo tracked by DNA heteroduplex
3109 mobility assays. *Journal of Virology*, 68(10):6672–6683.

Doebeli, M., Fletcher, J. A., Wilson, D. S., and Zwick, M. (2006). What's wrong with inclusive fitness? *Trends in Ecology and Evolution*, 21(11):597–598.

Dugatkin, L. A. (1997). *Cooperation Among Animals: An Evolutionary Perspective (Oxford Series in Ecology and Evolution)*. Oxford University Press, Oxford.

Dugatkin, L. A., Mesterton-Gibbons, M., and Alasdair, I. H. (1992). Beyond the prisoner's dilemma: Toward models to discriminate among mechanisms of cooperation in nature. *Trends in Ecology and Evolution*, 7(6):202–205.

Eshel, I. (1972). On the neighbor effect and the evolution of altruistic traits. *Theoretical Population Biology*, 3:258–277.

Eshel, I. and Motro, U. (1988). The three brothers' problem: kin selection with more than one potential helper. 1. The case of immediate help. *American Naturalist*, 132(4):550–566.

Fisher, R. A. (1958). *The genetical theory of natural selection*. At The Clarendon Press.

Fletcher, J. A. and Doebeli, M. (2009). A simple and general explanation for the evolution of altruism. *Proceedings of the Royal Society B*, 276:13–19.

Frank, S. A. (1998). *Foundations of Social Evolution*. Princeton University Press, Princeton, NJ.

Fudenberg, D., Nowak, M. A., Taylor, C., and Imhof, L. A. (2006). Evolutionary game dynamics in finite populations with strong selection and weak mutation. *Theoretical Population Biology*, 70:352–363.

Garcia, T. and De Monte, S. (2013). Group formation and the evolution of sociality. *Evolution*, 67(1):131–141.

Gavrilets, S. (2010). Rapid transition towards the division of labor via evolution of developmental plasticity. *PLoS Computational Biology*, 6(6):e1000805.

Gilbert, O. M., Queller, D. C., and Strassmann, J. E. (2009). Discovery of a large clonal patch of a social amoeba: implications for social evolution. *Molecular Ecology*, 18(6):1273–1281.

Godfrey-Smith, P. (2009). *Darwinian Populations and Natural Selection*. Oxford University Press, Oxford.

Goel, N. S. and Richter-Dyn, N. (1974). *Stochastic Models in Biology*. Academic Press, New York.

Gokhale, C. S. and Traulsen, A. (2010). Evolutionary games in the multiverse. *Proceedings of the National Academy of Sciences of the United States of America*, 107:5500–5504.

Gokhale, C. S. and Traulsen, A. (2014). Evolutionary multiplayer games. *Dynamic Games and Applications*.

Gray, M. W. (1989). The evolutionary origins of organelles. *Trends in Genetics*, 5:294–299.

Grosberg, R. K. and Strassmann, J. E. (2007). The evolution of multicellularity: A minor major transition? *Annual Review of Ecology, Evolution, and Systematics*, 38:621–54.

Hamilton, W. D. (1963). The evolution of altruistic behavior. *American Naturalist*, 97(896):354–356.

Hamilton, W. D. (1964). The genetical evolution of social behavior I and II. *Journal of Theoretical Biology*, 7:1–16 + 17–52.

Hammerschmidt, K., Rose, C., Kerr, B., and Rainey, P. (unpublished data). Evolution of group-structured bacterial population in mixed and non-mixed regimes.

Hammerschmidt, K., Rose, C., Kerr, B., and Rainey, P. B. (2014). Life cycles, fitness decoupling and the evolution of multicellularity. *Nature*, 515(7525):75–79.

Hardin, G. (1968). The tragedy of the commons. *Science*, 162(3859):1243–1248.

3156 Hauert, C. and Imhof, L. A. (2012). Evolutionary games in deme structured, finite popula-
3157 tions. *Journal of Theoretical Biology*, 299:106–112.

3158 Hauert, C., Imhof, L. A., and Chen, Y. T. (2014). Fixation times in deme structured, finite
3159 populations with rare migration. *Journal of Statistical Physics*, 156(4):739–759.

3160 Hauert, C., Michor, F., Nowak, M. A., and Doebeli, M. (2006). Synergy and discounting of
3161 cooperation in social dilemmas. *Journal of Theoretical Biology*, 239:195–202.

3162 Heisler, I. L. and Damuth, J. (1987). A method for analysing selection in hierarchically
3163 structured populations. *American Naturalist*, 130:582–602.

3164 Herron, M. D., Hackett, J. D., Aylward, F. O., and Michod, R. E. (2009). Triassic origin and
3165 early radiation of multicellular volvocine algae. *Proceedings of the National Academy of*
3166 *Sciences of the United States of America*, 106(9):3254–3258.

3167 Hölldobler, B. and Wilson, E. O. (1990). *The Ants*. Belknap Press.

3168 Hui, C. and McGeoch, M. A. (2007). Spatial patterns of prisoner's dilemma game in
3169 metapopulations. *Bulletin of Mathematical Biology*, 69(2):659–676.

3170 Huse, H. K., Kwon, T., Zlosnik, J. E. A., Speert, D. P., Marcotte, E. M., and Whiteley, M.
3171 (2010). Parallel evolution in Pseudomonas aeruginosa over 39,000 generations in vivo.
3172 *mBio*, 1(4):e00199–10.

3173 Inouye, K. and Takeuchi, I. (1979). Analytical studies on migrating movement of the pseudo-
3174 plasmodium of Dictyostelium discoideum. *Protoplasma*, 99(4):289–304.

3175 Kaiser, D. (2001). Building a multicellular organism. *Annual Review of Genetics*, 35(1):103–
3176 123.

3177 Kandori, M., Mailath, G. J., and Rob, R. (1993). Learning, mutation, and long run equilibria
3178 in games. *Econometrica*, 61:29–56.

3179 Karlin, S. and Taylor, H. M. A. (1975). *A First Course in Stochastic Processes*. Academic,
3180 London, 2nd edition edition.

3181 Kaushik, S. and Nanjundiah, V. (2003). Evolutionary questions raised by cellular slime mould
3182 development. *Proceedings of the Indian National Science Academy-Part B: Biological*
3183 *Sciences*, 69(5):825–852.

3184 Kelly, J. K. (1992). Restricted migration and the evolution of altruism. *Evolution*, 46:1492 –
3185 1495.

3186 Kerr, B., Godfrey-Smith, P., and Feldman, M. W. (2004). What is altruism? *Trends in*
3187 *Ecology and Evolution*, 19(3):135–140.

3188 Kirk, D. L. (2005). A twelve step program for evolving multicellularity and a division of
3189 labor. *BioEssays*, 27(3):299–310.

3190 Koschwanez, J. H., Foster, K. R., and Murray, A. W. (2013). Improved use of a public good
3191 selects for the evolution of undifferentiated multicellularity. *Elife*, 2:e00367.

3192 Krebs, J. R. and Davies, N. B. (2009). *Behavioural Ecology: An Evolutionary Approach.*
3193 John Wiley and Sons.

3194 Kurokawa, S. and Ihara, Y. (2009). Emergence of cooperation in public goods games. *Pro-*
3195 *ceedings of the Royal Society B*, 276:1379–1384.

3196 Lenski, R. E., Rose, M. R., Simpson, S. C., and Tadler, S. C. (1990). Long-term experimen-
3197 tal evolution in Escherichia coli. I. Adaptation and divergence during 2,000 generations.
3198 *American Naturalist*, 138(6):1315–1341.

3199 Lewontin, R. C. (1970). The units of selection. *Annual Review of Ecology and Systematics*,
3200 1:1–18.

3201 Libby, E. and Rainey, P. B. (2013). A conceptual framework for the evolutionary origins of
3202 multicellularity. *Physical Biology*, 10(3):035001.

Libby, E., Ratcliff, W. C., Travisano, M., and Kerr, B. (2014). Geometry shapes evolution of early multicellularity. *PLoS Computational Biology*, 10(9):e1003803.

Margulis, L. (1970). *Origin of Eukaryotic Cells: Evidence and Research Implications for a Theory of the Origin and Evolution of Microbial, Plant, and Animal Cells on the Precambrian Earth.* New Haven: Yale University Press.

Maynard Smith, J. (1987). How to model evolution. In Dupre, J., editor, *The latest on the Best: Essays on Evolution and Optimality*. MIT Press, Cambridge, MA.

Maynard Smith, J. and Szathmáry, E. (1993). The origin of chromosomes I. Selection for linkage. *Journal of Theoretical Biology*, 164(4):437–446.

Maynard Smith, J. and Szathmáry, E. (1995). *The Major Transitions in Evolution*. Freeman.

Mesterton-Gibbons, M. and Dugatkin, L. A. (1992). Cooperation among unrelated individuals: evolutionary factors. *Quarterly Review of Biology*, 67(3):267–281.

Michod, R. E. (2007). Evolution of individuality during the transition from unicellular to multicellular life. *Proceedings of the National Academy of Sciences of the United States of America*, 104:8613–8618.

Michod, R. E. and Roze, D. (1999). Cooperation and conflict in the evolution of individuality III. In Nehaniv, C., editor, *Mathematical and Computational Biology: Computational Morphogenesis, Hierarchical Complexity, and Digital Evolution*, volume 26, pages 47–92. American Mathematical Society.

Michod, R. E. and Roze, D. (2001). Cooperation and conflict in the evolution of multicellularity. *Heredity*, 86(1):1–7.

Michod, R. E., Viossat, Y., Solari, C. A., Hurand, M., and Nedelcu, A. M. (2006). Life-history evolution and the origin of multicellularity. *Journal of Theoretical Biology*, 239(2):257–272.

3227 Milinski, M. (1987). Tit for tat in sticklebacks and the evolution of cooperation. *Nature*,
3228 325(6103):433–435.

3229 Moran, P. A. P. (1953). The estimation of the parameters of a birth and death process. *Journal*
3230 *of the Royal Statistical Society: Series B*, 15(2):241–245.

3231 Mwangi, M. M., Wu, S. W., Zhou, Y., Sieradzki, K., de Lencastre, H., Richardson, P., Bruce,
3232 D., Rubin, E., Myers, E., Siggia, E. D., and Tomasz, A. (2007). Tracking the in vivo
3233 evolution of multidrug resistance in Staphylococcus aureus by whole-genome sequenc-
3234 ing. *Proceedings of the National Academy of Sciences of the United States of America*,
3235 104(22):9451–9456.

3236 Nakagaki, T. (2001). Smart behavior of true slime mold in a labyrinth. *Research in Microbi-*
3237 *ology*, 152(9):767–770.

3238 Nowak, M. A. (2006a). *Evolutionary Dynamics*. Harvard University Press, Cambridge MA.

3239 Nowak, M. A. (2006b). Five rules for the evolution of cooperation. *Science*, 314(5805):1560–
3240 1563.

3241 Nowak, M. A., Sasaki, A., Taylor, C., and Fudenberg, D. (2004). Emergence of cooperation
3242 and evolutionary stability in finite populations. *Nature*, 428:646–650.

3243 Nowak, M. A., Tarnita, C. E., and Wilson, E. O. (2010). The evolution of eusociality. *Nature*,
3244 466(7310):1057–1062.

3245 Ohtsuki, H. (2012). Does synergy rescue the evolution of cooperation? an analysis for ho-
3246 mogeneous populations with non-overlapping generations. *Journal of Theoretical Biology*,
3247 307:20–28.

3248 Okasha, S. (2006). *Evolution and the levels of selection*. Oxford University Press, Oxford.

3249 Pacheco, J. M., Santos, F. C., Souza, M. O., and Skyrms, B. (2009). Evolutionary dynamics
3250 of collective action in n-person stag hunt dilemmas. *Proceedings of the Royal Society B*,
3251 276:315–321.

Peña, J. (2012). Group size diversity in public goods games. *Evolution*, 66:623–636.

Pfeiffer, T. and Bonhoeffer, S. (2003). An evolutionary scenario for the transition to undifferentiated multicellularity. *Proceedings of the National Academy of Sciences of the United States of America*, 100(3):1095–1098.

Porat, D. and Chadwick-Furman, N. E. (2004). Effects of anemonefish on giant sea anemones: expansion behavior, growth, and survival. *Hydrobiologia*, 530(1–3):513–520.

Powers, S., Penn, A. S., and Watson, R. A. (2011). The concurrent evolution of cooperation and the population structures that support it. *Evolution*, 65(6):1527–1543.

Price, G. (1970). Selection and covariance. *Nature*, 227:520–521.

Price, G. (1972). Extension of covariance selection mathematics. *Annals of Human Genetics*, 35(4):485–490.

Price, G. (1995). The nature of selection. *Journal of Theoretical Biology*, 175(3):389–296.

Purcell, J., Brelsford, A., and Avilés, L. (2012). Co-evolution between sociality and dispersal: The role of synergistic cooperative benefits. *Journal of Theoretical Biology*, 312C:44–54.

Queller, D. C. (1992). Quantitative genetics, inclusive fitness, and group selection. *American Naturalist*, 139(3):540–558.

Rainey, P. B. and Kerr, B. (2010). Cheats as first propagules: A new hypothesis for the evolution of individuality during the transition from single cells to multicellularity. *BioEssays*, 32(10):872–880.

Rainey, P. B. and Rainey, K. (2003). Evolution of cooperation and conflict in experimental bacterial populations. *Nature*, 425(6953):72–74.

Rainey, P. B. and Travisano, M. (1998). Adaptive radiation in a heterogeneous environment. *Nature*, 394(6688):69–72.

Ratcliff, W. C., Denison, R. F., Borrello, M., and Travisano, M. (2012). Experimental evolution of multicellularity. *Proceedings of the National Academy of Sciences of the United States of America*, 109(5):1595–1600.

Ratcliff, W. C., Herron, M. D., Howell, K., Pentz, J. T., Rosenzweig, F., and Travisano, M. (2013a). Experimental evolution of an alternating uni-and multicellular life cycle in Chlamydomonas reinhardtii. *Nature Communications*, 4.

Ratcliff, W. C., Pentz, J. T., and Travisano, M. (2013b). Tempo and mode of multicellular adaptation in experimentally evolved Saccharomyces cerevisiae. *Evolution*, 67(6):1573–1581.

Rausch, H., Larsen, N., and Schmitt, R. (1989). Phylogenetic relationships of the green alge Volvox carteri deduced from small-subunit ribosomal RNA comparisons. *Journal of Molecular Evolution*, 29(3):255–265.

Renaud, F. and De Meeus, T. (1991). A simple model of host-parasite evolutionary relationships. Parasitism: compromise or conflict? *Journal of Theoretical Biology*, 152(3):319–327.

Rice, S. H. (2004). *Evolutionary theory: mathematical and conceptual foundations.* Sunderland MA: Sinauer.

Rodrigues, J. F. M., Rankin, D. J., Rossetti, V., Wagner, A., and Bagheri, H. C. (2012). Differences in cell division rates drive the evolution of terminal differentiation in microbes. *PLoS Computational Biology*, 8(4):e1002468.

Sathe, S., Kaushik, S., Lalremruata, A., Aggarwal, R. K., Cavender, J. C., and Nanjundiah, V. (2010). Genetic heterogeneity in wild isolates of cellular slime mold social groups. *Microbial Ecology*, 60(1):137–148.

Schierwater, B. (2005). My favorite animal, Trichoplax adhaerens. *BioEssays*, 27(12):1294–1302.

Schirrmeister, B. E., Antonelli, A., and Bagheri, H. C. (2011). The origin of multicellularity in cyanobacteria. *BMC Evolutionary Biology*, 11(1):45.

Shapiro, J. A. (1998). Thinking about bacterial populations as multicellular organisms. *Annual Review of Microbiology*, 52:81–104.

Shelton, D. E. and Michod, R. E. (2014). Group selection and group adaptation during a major evolutionary transition: insights from the evolution of multicellularity in the volvocine algae. *Biological Theory*, 9(4):1–18.

Sigmund, K. (2010). *The calculus of selfishness*. Princeton Univ. Press.

Simon, B., Fletcher, J. A., and Doebeli, M. (2013). Towards a general theory of group selection. *Evolution*, 67(6):1561–1572.

Smith, N. G. C. and Eyre-Walker, A. (2002). Adaptive protein evolution in Drosophila. *Nature*, 415(6875):1022–1024.

Sober, E. (1993). *The nature of selection: evolutionary theory in philosophical focus*. University of Chicago Press.

Solari, C. A., Kessler, J. O., and Goldstein, R. E. (2007). Motility, mixing, and multicellularity. *Genetic Programming and Evolvable Machines*, 8(2):115–129.

Spiers, A. J., Bohannon, J., Gehrig, S. M., and Rainey, P. B. (2003). Biofilm formation at the air–liquid interface by the Pseudomonas fluorescens sbw25 wrinkly spreader requires an acetylated form of cellulose. *Molecular Microbiology*, 50(1):15–27.

Stein, J. R. (1958). A morphologic and genetic study of Gonium pectorale. *American Journal of Botany*, 45:664–672.

Stephens, D. W. and Anderson, J. P. (1997). Reply to roberts: cooperation is an outcome, not a mechanism. *Animal Behaviour*, 53(6):1363–1364.

Strassmann, J. E., Zhu, Y., and Queller, D. C. (2000). Altruism and social cheating in the social amoeba Dictyostelium discoideum. *Nature*, 408:965–967.

Szathmáry, E. and Maynard Smith, J. (1993). The evolution of chromosomes II. Molecular mechanisms. *Journal of Theoretical Biology*, 164(4):447–454.

Szathmáry, E. and Maynard Smith, J. (1995). The major evolutionary transitions. *Nature*, 374(6519):227–232.

Tarnita, C. E., Taubes, C. H., and Nowak, M. A. (2013). Evolutionary construction by staying together and coming together. *Journal of Theoretical Biology*, 320:10–22.

Tomitani, A., Knoll, A. H., Cavanaugh, C. M., and Ohno, T. (2006). The evolutionary diversification of cyanobacteria: Molecular-phylogenic and paleontological perspectives. *Proceedings of the National Academy of Sciences of the United States of America*, 103(14):5442–5447.

Traulsen, A. and Hauert, C. (2009). Stochastic evolutionary game dynamics. In Schuster, H. G., editor, *Reviews of Nonlinear Dynamics and Complexity*, volume 2, pages 25–61. Wiley-VCH, Weinheim.

Traulsen, A. and Nowak, M. A. (2006). Evolution of cooperation by multi-level selection. *Proceedings of the National Academy of Sciences of the United States of America*, 103:10952–10955.

Traulsen, A., Shoresh, N., and Nowak, M. A. (2008). Analytical results for individual and group selection of any intensity. *Bulletin of Mathematical Biology*, 70:1410–1424.

van Veelen, M. (2009). Group selection, kin selection, altruism and cooperation: when inclusive fitness is right and when it can be wrong. *Journal of Theoretical Biology*, 259(3):589–600.

Velicer, G. J. and Yuen-tsu, N. Y. (2003). Evolution of novel cooperative swarming in the bacterium myxococcus xanthus. *Nature*, 425(6953):75–78.

Vincent, T. L. and Brown, J. S. (2005). *Evolutionary game theory, natural selection, and Darwinian dynamics*, volume 382. Cambridge University Press, Cambridge.

Wade, M. J. (1985). Soft selection, hard selection, kin selection, and group selection. *American Naturalist*, pages 61–73.

Wahl, L. M. (2002). Evolving the division of labour: generalists, specialists and task allocation. *Journal of Theoretical Biology*, 219(3):371–388.

Wakano, J. Y. and Hauert, C. (2011). Pattern formation and chaos in spatial ecological public goods games. *Journal of Theoretical Biology*, 268(1):30–38.

Wakano, J. Y., Nowak, M. A., and Hauert, C. (2009). Spatial dynamics of ecological public goods. *Proceedings of the National Academy of Sciences of the United States of America*, 106:7910–7914.

Wallace, B. (1968). Polymorphism, population size, and genetic load. *Population Biology and Evolution*, pages 87–108.

Weibull, J. W. (1997). *Evolutionary game theory*. MIT Press, Cambridge, MA.

Williams, G. C. (1966). *Adaptation and natural selection*. Princeton University Press, Princeton, NJ.

Wilson, D. S. (1975). A theory of group selection. *Proceedings of the National Academy of Sciences of the United States of America*, 72(1):143–146.

Wilson, D. S. (1977). Structured demes and the evolution of group-advantageous traits. *American Naturalist*, 111(977):157–185.

Wilson, D. S. (1980). *The natural selection of populations and communities*. Benjamin/Cummings, Menlo Park, CA.

Wilson, D. S. and Wilson, E. O. (2007). Rethinking the theoretical foundation of sociobiology. *The Quarterly Review of Biology*, 82(4):327 – 348.

Wingreen, N. S. and Levin, S. A. (2006). Cooperation among microorganisms. *PLoS Biology*, 4(9):e299.

Wu, B., Altrock, P. M., Wang, L., and Traulsen, A. (2010). Universality of weak selection. *Physical Review E*, 82(4):046106.

Wu, B., Bauer, B., Galla, T., and Traulsen, A. (2015). Fitness-based models and pairwise comparison models of evolutionary games are typically different - even in unstructured populations. *New Journal of Physics*, 17(2):023043.